OCS Study
BOEM 2016-039

Modeling At-Sea Occurrence and Abundance of Marine Birds to Support Atlantic Marine Renewable Energy Planning

Phase I Report

US Department of the Interior
Bureau of Ocean Energy Management
Office of Renewable Energy Programs

BOEM
Bureau of Ocean Energy Management

OCS Study
BOEM 2016-039

Modeling At-Sea Occurrence and Abundance of Marine Birds to Support Atlantic Marine Renewable Energy Planning

Phase I Report

Authors

Brian P. Kinlan
Arliss J. Winship
Timothy P. White
John Christensen

Prepared under NCCOS IAA MOA-2013-046-8696, BOEM OCS Study 2016-039, and NCCOS BOEM IAA M13PG00005
by
U.S. Department of Commerce
National Oceanic and Atmospheric Administration
National Ocean Service
National Centers for Coastal Ocean Science
Center for Coastal Monitoring and Assessment
Biogeography Branch
1305 East-West Hwy, SSMC-4, N/SCI-1
Silver Spring, MD 20910

Published by
U.S. Department of the Interior
Bureau of Ocean Energy Management
Office of Renewable Energy Programs
May 2016

DISCLAIMER

This study was funded, in part, by the US Department of the Interior, Bureau of Ocean Energy Management (BOEM), Environmental Studies Program, Washington, DC, through Inter-Agency Agreement Number M13PG00005 with the US Department of Commerce, National Oceanic and Atmospheric Administration, National Ocean Service, National Centers for Coastal Ocean Science, Silver Spring, MD. This report has been technically reviewed by BOEM and it has been approved for publication. The views and conclusions contained in this document are those of the authors and should not be interpreted as representing the opinions or policies of the US Government, nor does mention of trade names or commercial products constitute endorsement or recommendation for use.

REPORT AVAILABILITY

To download a PDF file of this Environmental Studies Program report, go to the US Department of the Interior, Bureau of Ocean Energy Management, Environmental Studies Program Information System website and search on OCS Study BOEM 2016-039. You may request the report from the BOEM Office of Renewable Energy Programs. The contact information is:

U.S. Department of the Interior
Bureau of Ocean Energy Management
Office of Renewable Energy Programs
45600 Woodland Road, VAM-OREP
Sterling, VA 20166

CITATION

Kinlan, B.P., A.J. Winship, T.P. White, and J. Christensen. 2016. Modeling At-Sea Occurrence and Abundance of Marine Birds to Support Atlantic Marine Renewable Energy Planning: Phase I Report. U.S. Department of the Interior, Bureau of Ocean Energy Management, Office of Renewable Energy Programs, Sterling, VA. OCS Study BOEM 2016-039. xvii+113 pp.

ACKNOWLEDGEMENTS

We thank the many scientists who collected and contributed the survey data analyzed in this study. We are grateful to Mark Wimer (USGS) and Allison Sussman (USGS) for processing the data in the Avian Compendium database and providing those data to us. We thank Peter Cornillon, Peter Miller, Matt Poti, and Tim Wynne for providing and helping with the processing of some of the environmental predictor data. This project was funded by the Bureau of Ocean Energy Management (BOEM) through Intra-agency Agreement M11PG00059 with the United States Geological Survey (USGS) and Inter-agency Agreement M13PG00005 with the U.S. Department of Commerce, National Oceanic and Atmospheric Administration, National Ocean Service, National Centers for Coastal Ocean Science (NCCOS), and by the United States Geological Survey through Inter-agency Agreement G13PG00008 with NCCOS. Brian Kinlan, Arliss Winship, and Tim White were supported by NOAA Contracts No. DG133C07NC0616 and EA-133C-14-NC-1384 with CSS-Dynamac.

ABOUT THE COVER

Cover photo (Great Shearwater) courtesy of David Pereksta (BOEM). Used with permission.

Executive Summary

Marine birds have the potential to be affected by human activities in the marine environment such as offshore wind energy development. This report describes the first phase of a project aimed at producing maps of the spatial distributions of marine bird species in U.S. Atlantic Outer Continental Shelf (OCS) waters that can be used to inform marine spatial planning in the region.

Visual sighting survey data from over three decades, contained in the 'Compendium of Avian Occurrence Information for the Continental Shelf waters along the Atlantic Coast of the U.S.' database, were analyzed to derive seasonal and annual maps of the spatial distributions of 40 marine bird species in U.S. Atlantic OCS waters from Florida to Maine.

Spatial predictive modeling was applied to the survey data to account for spatial and temporal heterogeneity in survey effort, platform, and protocol. An ensemble machine-learning technique, component-wise boosting of hierarchical zero-inflated count models, was used to relate the relative occurrence and abundance of each species to multiple spatial and temporal environmental predictor variables while accounting for survey heterogeneity and the aggregated nature of sightings. Dynamic spatial environmental predictor variables were formulated as long-term climatologies. The modeling technique allowed for complex non-linear relationships between response and predictor variables and interacting effects among predictors. Bootstrapping was used to derive estimates of the uncertainty in model predictions.

Model predictions are presented as seasonal and annual maps of the relative probability of occurrence and relative abundance of study species throughout the U.S. Atlantic OCS. These maps indicate where species are more or less likely to occur and where species are likely to be more or less abundant. The analysis was not designed to estimate the absolute probability of occurrence or the absolute number/density of individuals of a given species that would be expected in any location, so the maps should not be interpreted that way. Also, the maps represent the spatial distributions of birds averaged over time (e.g., across days within a season and across years for a given season). The analysis was not designed to provide predictions of the number of birds that would be expected in a specific location at a specific date or time, so the maps should also not be interpreted that way. Furthermore, large variations in predicted long-term relative occurrence and abundance at the 2-km spatial resolution of the study grid are not necessarily realistic. Interpretation of the maps is probably more reliable at the regional scale (i.e., 10-100 km). The maps presented here provide preliminary broad-scale spatial information that can be used to guide future data collection efforts and aid marine spatial planning in the region.

Four types of supplementary information are provided along with the maps of predicted relative occurrence and abundance to indicate the quality of those predictions. First, the distribution of survey effort is presented as a series of isopleths to indicate where the majority of the survey data were collected. Model predictions in areas with few or no data should be interpreted with caution. Second, for each species-season combination a 'badge' is included on the maps, representing the statistical fit of the model to the data in terms of several performance metrics. The badge indicates the quality of model predictions in areas with survey data but not in areas without survey data. Third, estimates of the precision of model predictions are presented as maps of the variability, quantiles, and confidence interval width of the

bootstrapped distributions of model predictions. Less precise predictions should be interpreted with more caution. Fourth, we present an expert assessment of how well the predictions for each species match what is known about the species' distribution. These four supplementary sources of information should be considered in conjunction with the maps of predicted relative occurrence and abundance.

The relative importance of different predictor variables is presented, indicating which variables most influenced the predicted distributions for each species in each season. While the primary objective of this study was not to determine the ecological drivers and mechanisms behind the spatial distributions of marine bird species in the study area, our model results may provide useful hypotheses for future studies aimed more at ecological inference.

A second phase of this project is currently underway that will expand, refine, and improve the modeling and results presented here. The second phase is projected to be completed by the fall of 2017.

Modeling At-Sea Occurrence and Abundance of Marine Birds to Support Atlantic Marine Renewable Energy Planning: Phase I Report

Contents

List of Figures

List of Tables

List of Appendices (digital)

Appendix A. Descriptions of individual survey datasets analyzed.

Appendix B. Maps of spatial environmental predictor variables used in spatial predictive modeling.

Appendix C. Diagnostic boosting performance plots for the best model for each species and season. Plots show the values of 6 performance metrics (CRPS_0_CV, CRPS_Zinf_CV, MedianAE_nz_CV, MedianBias_nz_CV, risk, and RMSE_CV) by boosting iteration, for each of 20 cross-validation replicates during tuning of the number of boosting iterations. Vertical red lines indicate the optimal number of boosting iterations determined through cross-validation.

Appendix D. Supplemental model fit tables. Supplementary information presented includes shrinkage (learning) rates, boosting offsets, log-likelihoods, and risk (calculated during cross-validation) for the best model for each species and season.

Appendix E. Best model comparison plots. Performance metrics for the best model for each species and season.

Appendix F. Receiver operating characteristic (ROC) curve plots for the best model for each species and season. Two plots are presented for each model: 1) ROC curve for prediction of presence/absence ('occupancy'), and 2) ROC curve for prediction of non-zero data above/below median observed non-zero value ('abundance_nz').

Appendix G. Brier score plots for the best model for each species and season. Plots show Brier score calculated at quantile thresholds of non-zero data.

Appendix H. Variable importance plots for each component of the best model for each species and season.

Appendix I. Plots of the bootstrapped marginal effects of each predictor variable in each component of the best model for each species and season. The solid line represents the mean effect and grey shading indicates +/- 1 bootstrapped standard deviation.

Appendix J. Plots of two-way interactions between the effects of predictor variables in each component of the best model for each species and season.

Appendix K. Maps of seasonal predicted relative occupancy and abundance (and their uncertainty) for each species and season modeled.

Appendix L. Maps of average annual predicted relative occupancy and abundance (and their CVs) for each species modeled.

Appendix M. Maps of average annual predicted relative occupancy and abundance for three species groups (Table 12).

Appendix N. Description (manifest) of the digital data deliverable accompanying this report.

Abbreviations and Acronyms

AE	absolute error
AUC	area under the ROC curve
BOEM	Bureau of Ocean Energy Management
COTE	Common Tern
CRPS	continuous rank probability score
CV	cross-validation
GLM	generalized linear model
NOGA	Northern Gannet
OCS	Outer Continental Shelf
PDE	percent deviance explained
RAZO	Razorbill
RMSE	root mean square error
ROC	receiver operating characteristic
USGS	United States Geological Survey
USFWS	United States Fish and Wildlife Service
WWSC	White-winged Scoter
ZINB	zero-inflated negative binomial
ZIP	zero-inflated Poisson

* Please see Table 2 for full list of species codes and Table 6 for full list of model performance metric codes

1. Introduction

Marine birds spend much of their time in coastal waters and on the open ocean. As a result, these species have the potential to be affected by human activities in the marine environment such as offshore wind energy development. A prerequisite for quantifying that potential is knowledge of the spatial distributions of marine birds at sea. This report describes the first phase of a project aimed at producing maps of the spatial distributions of marine bird species in U.S. Atlantic Outer Continental Shelf waters (Fig. 1) that can be used to inform marine spatial planning in the region.

Some of the best available information about the at-sea distributions of marine birds comes from visual sighting surveys conducted aboard boats and aircraft. For U.S. Atlantic Outer Continental Shelf waters many data from past sighting surveys have been compiled in the 'Compendium of Avian Occurrence Information for the Continental Shelf waters along the Atlantic Coast of the U.S.', hereinafter referred to as the 'Avian Compendium' (O'Connell et al. 2009). The Avian Compendium database was developed by the U.S. Geological Survey (USGS) Patuxent Wildlife Research Center and is currently maintained by the U.S. Fish and Wildlife Service (USFWS). The project described here analyzed sighting data from the Avian Compendium to derive maps of the spatial distributions of 40 marine bird species in U.S. Atlantic Outer Continental Shelf waters from Florida to Maine.

The data in the Avian Compendium represent numerous surveys over more than three decades. Survey coverage and intensity is highly variable geographically (Fig. 2) and temporally, especially between individual datasets. Furthermore, a wide range of survey platforms, observers, and protocols were used. This heterogeneity complicates the quantification of the at-sea distribution of marine birds from these data, and biases simple data summary approaches. To deal with this heterogeneity, the project described here employed spatial predictive modeling. An ensemble machine-learning technique was used to model counts of each species as a function of multiple predictor variables while accounting for heterogeneous survey effort. The fitted models were then used to predict the spatial distribution of relative occurrence and abundance of each species throughout the study area.

The distributions of marine birds at sea are a result of interactions between their behavior (e.g., foraging) and the environment. Atmospheric and oceanographic features and processes across a range of spatial and temporal scales influence the environmental conditions and prey availability experienced by marine birds, and thus ultimately determine their at-sea distributions. The spatial predictive modeling framework employed here relied on a wide suite of spatial and temporal environmental predictor variables to explain and predict the distributions of marine birds. In particular, static environmental variables (e.g., bathymetry) and long-term climatologies of dynamic environmental variables (e.g., sea surface temperature) were considered to explain spatial patterns of relative occurrence and abundance.

The project described here is designed to provide broad-scale spatial information that can be used to guide future data collection efforts and aid marine spatial planning in the region. This report describes preliminary results from the first phase of the project. A second phase of the project is currently underway that will expand, refine, and improve the modeling and results presented here. It is important to note that the results presented in this report represent the spatial distributions of birds averaged over time. The project was not designed to provide precise predictions of the absolute number of individuals of a given species that would be expected in a specific location at a specific time. The project was also not designed to determine the ecological drivers of marine bird distributions, although the results provide related hypotheses for future research.

2. Methods

2.1 Overview

A statistical modeling framework was used to relate bird sighting data from historical surveys to a range of temporal and spatial environmental predictor variables. The estimated relationships between the relative occurrence and abundance of birds and the predictor variables were then used to predict the spatial distributions of birds across the entire study area. Separate models were developed for each combination of species and season for which there were sufficient data. Seasons reflected major transitions in environmental conditions in the study region: spring (March-May), summer (June-August), fall (September-November), and winter (December-February).

2.2 Survey data

Bird sighting data were derived from a large relational database (hereinafter referred to as the 'Avian Compendium') containing observational datasets on marine birds along the Atlantic Coast of the United States (see O'Connell et al. 2009 for more details). These datasets were collected by a range of entities including government agencies, non-governmental organizations, academic researchers, and other individuals. Developed and previously maintained by USGS Patuxent Wildlife Research Center, the Avian Compendium is now maintained by USFWS through an intra-agency agreement with BOEM (M14PG00014).

We analyzed science-quality, geographically-referenced, visual sighting data from the Avian Compendium. The original data took the form of species-specific counts of birds along boat-based or aerial strip transects. Counts were sometimes recorded continuously, and other times were aggregated into recording bins of mostly 10 or 15 minute duration, with the majority (79%) being 15 minutes. Binned data were only from boat surveys. To standardize effort across datasets, continuously recorded data were discretized into transect segments 4.63 km long corresponding to the distance that would be covered in 15 minutes at a speed of 10 knots, which is a typical survey speed. Counts for each species were summed within each transect segment. We excluded data from discrete recording bins with duration <10 minutes, and we excluded transect segments <3.086 km that arose from the discretization of continuous data. Thus, our unit of analysis was a transect segment, the majority of which represented 15 minutes or 4.63 km of survey effort, and no less than 10 minutes or 3.086 km of effort. The response data were the numbers of individual birds of each species counted on each transect segment.

We analyzed 75 datasets from the Avian Compendium representing 111,776 transect segments that had survey effort within our study area (Table 1, Fig. 2, Appendix A). The datasets spanned 1978-2014 with most survey effort occurring from 1978-1988 and from 2002 onward. The datasets with the largest combined sample size and widest geographic coverage were collected by Manomet Bird Observatory in coordination with the National Marine Fisheries Service and other cruises between 1978 and 1988 (datasets CSAP and NOAAMBO7880). More recent surveys by USFWS as part of the Atlantic Marine Assessment Program for Protected Species also covered the entire U.S. Atlantic Coast (datasets AMAPPS_FWS). Other multi-year survey efforts covered large sections of the coast including NOAA ecosystem monitoring cruises from North Carolina to the Gulf of Maine (datasets EcoMon) and pelagic surveys off Georgia, South Carolina, and Florida (dataset GeorgiaPelagic). The remaining datasets were more localized, often from New England and the Gulf of Maine, but sometimes had large sample sizes over multiple years (e.g., datasets CapeWind, HerringAcoustic, and MassAudNanAerial).

For analysis we considered species-season combinations that had ≥50 transect segments with sightings of ≥1 individual. By this criterion 53 species and 144 species-season combinations were amenable to analysis representing sightings of 2,622,023 individual birds. The five species with the greatest numbers of transect segments with sightings in individual seasons were Wilson's Storm-Petrel in summer, Herring Gull in fall, Northern Gannet in winter, Great Shearwater in fall, and Great Black-backed Gull in fall. For this first phase of the project, not all 144 species-season combinations could be modeled in the allotted time, so a prioritized subset of 40 species (118 species-season combinations) were analyzed (Table 2). Prioritization considered Atlantic Marine Bird Conservation Cooperative Species of Concern, US Endangered Species Act listings, USFWS Birds of Conservation Concern (Florida, Southeast, Mid-Atlantic/New England, and Gulf of Maine regions), state endangered species legislation listings, species included in state Ocean Plans (NY, MA, or RI), Northeast Regional Ocean Planning Expert Working Group input (NROC 2016), and relative vulnerability to offshore wind energy projects (Robinson Willmott et al. 2013). For 5 of the modeled lower-priority species (Bonaparte's Gull, Royal Tern, Manx Shearwater, Common Murre, and Band-rumped Storm-Petrel) there was insufficient time to conduct bootstrapping (see Section 2.4.9), so uncertainty estimates are not presented for those models. Also, some seasonal models failed for 3 species (Common Eider – spring, summer, fall; Red-necked Phalarope – spring; and Red Phalarope – fall). These errors will be investigated further in Phase II of this project. Nevertheless, the models for the seasons with the greatest numbers of sightings of these 3 species were successful.

2.3 Predictor variables

A wide range of predictor variables were used to model variation in the number of birds sighted per transect segment and to predict the spatial distributions of birds throughout the study area (Table 3, Fig. 3, Appendix B). Predictor variables fell into one of six categories: survey, temporal, geographic, terrain, physical oceanographic and atmospheric, and biological.

Survey predictor variables were designed to account for variation in counts arising from heterogeneity in the type of survey platform, characteristics of the survey platform (e.g., observation height), observer identity and expertise, species focus, and sighting conditions. These factors influence the probability that individual birds will be detected and correctly identified to the species level. Of these factors, only the type of survey platform (boat or plane) was consistently recorded in all datasets, and thus was directly usable as a predictor variable. We attempted to account for the effects of the remaining factors through two random-effect predictor variables representing survey identity (ID) and transect ID, respectively. The exact definition of transect ID differed somewhat between datasets, but unique transect identities generally represented pre-defined survey transects or individual days of effort. The transect ID predictor variable also allowed for an accounting of some of the variation in counts arising from variation in survey effort (distance and strip width) among transect segments.

Temporal predictor variables were designed to account for variation in counts over time. Day of the year was used to account for changes in the numbers of birds in the study area over time within a season, for example arising from migratory movements in and out of the study area. Year was used to account for changes in the number of birds in the study area across years, for example arising from changes in population abundance or distributional shifts. Effects of day of the year and year were modelled as smooth continuous changes over time. Four climate indices (Table 3) were also included as temporal predictor variables to account for variation in counts across years arising from linkages between the environment and population abundance and distribution. For each climate index two values were included

as predictor variables: the value for the month and year of a given transect segment and the value for the same month one year previous.

Geographic predictor variables were designed to account for variation in counts arising from spatial location per se. Projected longitude and latitude were included as predictor variables and their effects were modeled two ways. The first longitude-latitude predictor term allowed for smooth changes in numbers across the study area arising from spatial factors not captured by the other predictor variables (e.g., colonization history). The second longitude-latitude predictor term was formulated using radial basis functions with the intent of capturing some of the spatial autocorrelation in the data after accounting for the effects of other predictor variables. Distance to land and absolute distance to shelf break (200 m isobath) were also included as geographic predictor variables.

Terrain variables were designed to account for variation in counts arising from the direct and indirect effects of bathymetry on bird distributions. A depth predictor variable was developed by combining information from four different bathymetric datasets (Table 3). Other terrain variables were derived from depth including slope, slope of slope, and planform and profile curvature.

Physical oceanographic and atmospheric predictor variables were designed to account for variation in counts arising from the direct and indirect effects of the physical state and dynamics of the ocean and air above the ocean. Sixteen physical oceanographic and atmospheric predictor variables were developed from a range of data sources (Table 3). Remote sensing data were used to characterize sea surface height, temperature, turbidity, and wind stress. Other variables were derived from the remotely sensed variables including sea surface height and temperature variability, probabilities of cyclonic and anticyclonic eddy rings, probability of sea surface temperature fronts, wind divergence, and an index of upwelling. Estimates from a data-assimilating ocean dynamics model were used to characterize water currents, and divergence and vorticity were derived from current velocities.

One biological predictor variable was included to account for variation in counts arising from the direct and indirect effects of ocean productivity. Remote sensing data were used to characterize sea surface chlorophyll-a concentration.

All of the physical oceanographic and atmospheric and biological variables that we considered are dynamic. We formulated these predictor variables to characterize long-term spatial patterns in average values and variability. Long data time series ranging from 11-22 years were used (Table 3). To characterize average values, monthly mean or median climatologies across years were developed and then integrated to create seasonal climatologies. To characterize variability, standard deviations or probabilities (frequencies) were calculated from the native temporal resolution of the corresponding predictor variables.

Geographic, terrain, physical oceanographic and atmospheric, and biological predictor variables were spatially explicit. Each variable was calculated on a standard study grid with a spatial resolution of 2 km and an oblique Mercator projected coordinate system. When the native spatial resolution of a predictor variable was finer than that of the study grid, predictor values were averaged within study grid cells. When the native spatial resolution of a predictor variable was similar to or coarser than that of the study grid, bilinear interpolation was used to derive predictor values at the center of study grid cells. Each survey transect segment was matched to the predictor variable values from the study grid cell that contained the midpoint of that segment.

Some of the spatially explicit predictor variables were highly correlated with each other (Table 4). Predictor variables were chosen to avoid correlations >0.9, although a few pairs still had correlations >0.9. All but one of the correlations >0.9 involved spatial coordinate variables that were a key structural component of our model. The other correlation >0.9 was between the mean and standard deviation of sea surface height during the summer. Because of the high correlations between some predictor variables, inferences regarding relative variable importance should be made with caution. The accuracy of predictions should be less affected by collinearity among predictor variables.

2.4 Statistical modelling framework

A boosted generalized additive modelling framework (Bühlmann and Hothorn 2007; Hofner et al. 2012) was used to estimate relationships between the numbers of birds counted per transect segment and the predictor variables (Fig. 4). Those relationships were then used to predict the relative occurrence and abundance of each species throughout the study area in each season. Our main objective was to provide accurate predictions, so we chose a modelling framework that allowed for flexible relationships and multi-way interactions between predictor variables while accounting for sampling heterogeneity between and within datasets.

2.4.1 Likelihoods and model components

The number of individuals of a given species counted per transect segment was modelled using zero-inflated Poisson (Eq. 1) and zero-inflated negative binomial likelihoods (Eq. 2) to account for the overdispersed nature of the count data. Each component/parameter of the likelihood was modelled as a separate function of the predictor variables (Schmid et al. 2008; Mayr et al. 2012). For the zero-inflated Poisson likelihood, the two model components were the probability of an 'extra' zero (p) and the mean of the Poisson distribution (μ):

[1] $$L(p,\mu;y) = \prod_{i=1}^{n} [p + (1-p)e^{-\mu}]^{I_{y_i=0}} \left[(1-p)\frac{\mu^{y_i}e^{-\mu}}{y_i!}\right]^{I_{y_i>0}}$$

The same components were modelled for the zero-inflated negative binomial likelihood in addition to the dispersion parameter of the negative binomial distribution (θ):

[2] $$L(p,\mu,\theta;y) = \prod_{i=1}^{n} \left[p + (1-p)\left(\frac{\theta}{\theta+\mu}\right)^{\theta}\right]^{I_{y_i=0}} \left[(1-p)\frac{\Gamma(y_i+\theta)}{y_i!\,\Gamma(\theta)}\left(\frac{\theta}{\theta+\mu}\right)^{\theta}\left(\frac{\mu}{\theta+\mu}\right)^{y_i}\right]^{I_{y_i>0}}$$

The probability of an extra zero was modelled on the logit scale (symbolized by np) while the mean of the Poisson/negative binomial distribution and the dispersion parameter of the negative binomial distribution were modelled on the log scale (mu and th, respectively).

In Eqs 1 and 2, yi represents the total count for transect segment i, n represents the total number of segments, and $I_{y_i=0}$ and $I_{y_i>0}$ are indicators of whether yi is equal to or greater than zero, respectively (I=1 when the condition is true and I=0 when the condition is false).

2.4.2 Base-learners

Within the boosting framework, each model component was essentially modelled as a function of an ensemble of 'base-learners'. Each base-learner represented a specific functional relationship between a model component and one or more predictor variables. We utilized a suite of base-learners each

representing different predictor variables, and different sets of base-learners were employed for different model components (Table 5).

All spatially explicit predictor variables except geographic coordinates were included together in a single tree base-learner. The trees for that learner had a maximum depth of 5, which allowed for interacting effects among the spatially explicit predictor variables. Projected longitude and latitude appeared in two base learners, and those variables always entered the model as a pair. The remaining survey and temporal predictor variables entered the model individually, either through their own base-learners or in the case of climate indexes one at a time through a tree base-learner with a maximum depth of 1. Thus, our model structure did not allow for interactions between temporal and spatial predictor variables.

2.4.3 Stochastic gradient boosting

Stochastic gradient boosting was used to fit models whereby a sub-sample of the data was fitted in each boosting iteration (Friedman 2002). Rather than resampling the data for each boosting iteration, a set of 25 or 50 random samples was created before boosting, and one sample was randomly drawn from this set for each boosting iteration. Root mean square error (RMSE) was used to select the base-learner that gave the best fit to the gradient (all data) in each boosting iteration.

2.4.4 Boosting offsets

Model component estimates were initialized ('offset' in boosting terminology; Hofner et al. 2012) by conducting a preliminary generalized linear model (GLM) analysis. For that analysis, predictor variables were first reduced through principal component and cluster analyses to a smaller set of derived predictors. Those new predictors were then discretized into different numbers of classes. For each number of classes a GLM with a zero-inflated negative binomial likelihood was fit, and the mean estimates for each model component were calculated. Model component estimates were then averaged across the fitted models with the different numbers of predictor classes, weighted by the Akaike Information Criterion for those models.

2.4.5 Tuning of shrinkage rate and number of boosting iterations

A stratified (by transect ID) k-fold cross-validation approach was used to determine values for the shrinkage rate (nu) and number of boosting iterations (mstop) that resulted in the best predictive performance. The shrinkage rate was tuned first by fixing the number of boosting iterations and evaluating out-of-bag model performance in terms of the thresholded continuous rank probability score (CRPS_Zinf; Table 6) for different shrinkage rates. The number of boosting iterations was tuned second by fixing the shrinkage rate and evaluating out-of-bag model performance in terms of the negative log-likelihood. The number of boosting iterations at which performance was maximized was averaged across cross-validation samples (excluding the top and bottom 5%) and used as the number of boosting iterations for the final model fitting. If the number of boosting iterations was less than or greater than specified values, the shrinkage rate was decreased or increased, respectively, and the number of boosting iterations was tuned again. We allowed for a maximum of 8000 boosting iterations, so models with that number of boosting iterations should be interpreted with caution as their performance may have improved with additional boosting iterations. A suite of cross-validation performance metrics were calculated during the tuning of mstop (Table 6).

2.4.6 Model selection and performance

The performance of each of the two fitted models for each species-season combination (Table 7) was evaluated from a suite of performance metrics (Table 6). Cross-validation performance during the tuning

of mstop in terms of the thresholded continuous rank probability score (CRPS_Zinf_CV) was used to select either the zero-inflated Poisson or the zero-inflated negative binomial model as the best final model for each species and season.

The final model for each species and season was assigned an overall model performance category on the basis of four of the performance metrics (Table 8). Performance categories were defined for each of these performance metrics and assigned a numeric code (5=highest to 1=lowest; Table 8). The performance of each final model was assigned an overall performance category equal to the average performance across these four performance metrics. Model performance is displayed on each map figure using a 'badge'.

It is important to recognize that the model performance metrics and badge mainly reflect the statistical fit of the models to the data. They reflect only the data that were analyzed, and they do not reflect the quality of model predictions away from the data. For example, the survey data did not cover everywhere within the study area, so some model predictions are essentially interpolations/extrapolations from data in other parts of the study area. The accuracy of those predictions is not necessarily reflected by the model performance metrics. Nevertheless, the performance metrics and badge give an indication of how accurately a model was able to predict the observed data, and good performance provides a measure of confidence in the modelled distributions, especially within the temporal and spatial coverage of the observed survey data.

As a second assessment of overall model quality the maps were reviewed by one of us (TPW), a marine bird ecologist with substantial knowledge of and firsthand experience with the study area and species. For each species and season the correspondence between the modeled distributions of relative occurrence and abundance and independent expectations was assigned a quality class: 'good', 'fair', or 'poor'. This expert evaluation focused on the bootstrap median model predictions.

2.4.7 Spatial prediction

The final fitted model for each species and season was used to predict relative occurrence and abundance throughout the study area. Relative occurrence was defined as the probability of observing ≥1 individuals on a transect segment, and relative abundance was defined as the mean number of individuals per transect segment. Both relative occurrence and abundance integrated the zero-inflated and Poisson/negative binomial components of the likelihood.

Spatially explicit predicted values were calculated for each cell of the study grid from the values of the spatially explicit predictor variables for that cell. Thus, the predicted relative occurrence and abundance in a given grid cell correspond to predictions for a transect segment whose mid-point falls within that grid cell. All other predictor variables except year were set to their mean values. Three different spatial predictions were made with respect to the year predictor: 1) prediction for the mean year, 2) the average of the predictions for each year, and 3) the average of the predictions for each of the last 10 years.

We excluded predictions outside of the observed geographic range of sightings for each species by masking the spatial predictions. First, a 'traveling salesperson' algorithm was used to connect the midpoints of all of the transect segments on which a given species was sighted in a given season (Hahsler and Hornik 2015). The connecting lines were then buffered with a radius of 100 km and predictions outside of the buffer area were omitted. An annual mask was derived for each species from the union of the seasonal buffer areas.

2.4.8 Variable importance

While our primary objective was not to determine the ecological drivers and mechanisms behind the spatial distributions of marine bird species in the study area, our model results do provide some indication of which variables were most useful for predicting those distributions. Those variables may provide useful starting points for future studies aimed more at ecological inference.

We calculated the relative importance of a given predictor variable in the final fitted models by summing the decrease in the negative log-likelihood in each boosting iteration attributable to that predictor variable. Thus, variable importance reflects the frequency with which a given predictor variable occurred in the selected base-learners across boosting iterations and that variable's ability to explain variation in the data when it was selected. When multiple predictor variables occurred in the selected base-learner for a given boosting iteration, the decrease in the negative log-likelihood was divided evenly among those predictor variables. Relative variable importance was re-scaled so that it summed to 1 across predictor variables.

2.4.9 Uncertainty

Uncertainty in model predictions was estimated using a non-parametric bootstrapping framework. For each bootstrap iteration, the set of unique transect IDs was resampled with replacement, and the data for each transect ID were assigned weights proportional to the frequency of that ID in the sample. These data weights were then applied when fitting the model during that bootstrap iteration. Predictor variables that were not included in the final model were excluded from the bootstrap analysis. Two hundred bootstrap iterations were conducted producing a sample of predictions from which we calculated quantiles and confidence intervals to characterize uncertainty in the predictions.

2.4.10 Implementation

The analysis was coded in R (R Core Team 2014) and relied on multiple existing contributed packages (e.g., mboost; Hothorn et al. 2014).

2.5 Map display

Model spatial predictions are displayed as maps (Figs 16-20 and Appendices K-M). A color spectrum is employed to visualize relative occupancy and abundance ranging from blue (lower values) to red (higher values). The number ranges corresponding to each color are indicated in the map legends. The break points between the number ranges were evenly distributed on one of three scales: arithmetic, natural log, or cumulative distribution. The scale chosen for each map depended on the distribution of model predictions across the study area.

2.6 Warning regarding potentially spurious spatial predictions

A bug in the computer code used for the analysis presented here resulted in spurious spatial patterns in some of the predictions. Essentially, one of the spatial coordinate predictors was scaled incorrectly when making spatial predictions, which sometimes distorted spatial patterns. When present, this distortion is evident as a dominant east-west trend in predicted occupancy and abundance (i.e., vertical banding in the maps). It is difficult to quantify the amount of distortion in the predictions for any given model, but model test results suggest that the potential for distortion was greatest in areas with few survey data or sightings and when the relative importance of the spatial coordinate predictor variables in a model was high. Predictions in areas with a lot of survey data and sightings were less impacted by the bug. The calculated model performance metrics (see Section 2.4.6) reflect any distortion in predictions, so good performance indicates that the model predictions more closely matched the observed data in areas with survey effort.

The maps of predicted relative occurrence and abundance for Common Tern (Fig 16.1A-H) illustrate the effect of this bug. Predictions nearshore where most Common Tern were sighted (Fig. 16.1I) were a good representation of the distribution of Common Tern (see Section 3.4.1.1). The model performance metrics reflected this correspondence as did the expert assessment of model quality (Table 11; overall performance category = 4, expert assessment = fair). However, in offshore areas where there were fewer survey data and sightings the predictions of relative occurrence and abundance exhibit a vertical banding pattern with a strong east-west gradient that is unrealistic.

All predictions in areas with few survey data (Fig. 2B) or sightings should be interpreted with caution, and predictions in these areas that exhibit a vertical banding pattern are likely an artifact of the bug. The bug has been corrected for the second phase of the project.

3. Results

3.1 Model selection and performance

3.1.1 Example species-season combinations

Detailed model selection and performance results are presented here for four example species-season combinations: Common Tern (summer), Northern Gannet (fall), Razorbill (winter), and White-winged Scoter (winter). We chose these examples to illustrate: 1) offshore distribution of a seasonal breeder (Common Tern); concentrated migratory patterns (Northern Gannet); and highly aggregated wintertime distributions of diving birds with disparate feeding ecologies (Razorbill – pelagic feeder; White-winged Scoter – benthivore).

3.1.1.1 Model selection---The performances of the two models for each species and season (Table 7) in terms of multiple performance metrics (Table 6) were compared, and the 'best' model was selected on the basis of the lowest thresholded continuous rank probability score from cross validation tuning of the number of boosting iterations (CRPS_Zinf_CV).

Table 9 presents these model comparisons for the four example species-season combinations. The value of CRPS_Zinf_CV was very similar between models for a given species and season, but this was not always the case with other performance metrics. The zero-inflated Poisson model was selected for three of the example species-season combinations, while the zero-inflated negative binomial model was selected for White-winged scoter (winter). It is possible that the negative binomial distribution provided a better description of the distribution of counts for the latter, highly aggregated species, although the zero-inflated Poisson model performed better in terms of some performance metrics.

3.1.1.2 Cross validation performance during tuning of the number of boosting iterations---Figs 5.1-5.4 illustrate cross validation performance during the tuning of the number of boosting iterations (mstop) for the final selected models for the four example species-season combinations (Table 9). Six performance metrics (Table 6) were calculated with respect to out-of-bag data for each of 20 cross validation replicates. The negative log-likelihood (risk) was minimized to determine the optimal number of boosting iterations (indicated by the vertical red line in the figures).

The Brier score (CRPS_0), thresholded continuous rank probability score (CRPS_Zinf), and the negative log-likelihood (risk) all decreased with the number of boosting iterations indicating improving performance. Performance in terms of the other metrics as a function of the number of boosting iterations was more variable.

3.1.1.3 Receiver Operating Characteristic (ROC) curves---Receiver operating characteristic (ROC) curves and the area under them (AUC) were calculated to assess the ability of a model to classify transect segments with at least one sighting versus segments with no sightings (i.e., occurrence), and to classify numbers of individuals below versus above the median count on segments with sightings.

For the four example species-season combinations (Figs 7.1-7.4), AUC statistics indicated better classification in terms of occurrence (0.91-0.95) than in terms of the median count (0.62-0.72).

3.1.1.4 Brier scores---Brier scores were calculated for zero and different quantiles of the observed non-zero count distribution for each species-season combination. The Brier score for a given quantile indicates the accuracy of the model when predicting the occurrence of a count above or below that value.

For the four example species-season combinations the Brier score decreased with increasing count values indicating increasing prediction accuracy (Figs 8.1-8.4). For example, the predicted probability of a count greater than a very high value is low, and the frequency of occurrence of a count greater than a very high value is also consistently low, which means accurate prediction in the sense of the Brier score as calculated here. Predictive accuracy would be lower near the mean or median where there is substantial probability of counts above and below those values.

3.1.2 All species

Table 10 presents the best models for all species-combinations. Zero-inflated negative binomial models were selected more frequently as the best model than zero-inflated Poisson models, but there were a substantial number of the latter.

Table 11 and Fig. 6 present the performance of the final selected models across all species and seasons in terms of a range of performance metrics (Table 6). In general, performance was highly variable among species and seasons. About half of the best models did not converge within 8000 boosting iterations (the maximum tried), and a large proportion of the remaining models may not have converged (m values close or equal to 6000 or 7000 possibly indicate lack of convergence) (Fig. 6A). Performance metrics calculated for both final fitted models and during cross-validation tuning of mstop were highly correlated between the two versions ('Fit' and 'CV' columns in Table 11). Also, the Brier score calculated for occupancy (CRPS_0) was highly correlated with the thresholded continuous rank probability score (CRPS_Zinf or 'CRPS').

3.2 Predictor variable relative importance

Our modelling framework was designed to provide the most accurate predictions. It was not designed to determine which environmental predictors were most ecologically relevant in determining the distribution of birds. Ecological inferences from the variable importance results should be cautious. Nevertheless, these results may suggest interesting hypotheses for future research.

3.2.1 Example species-season combinations

For the four example species-season combinations, a large number of predictor variables were ranked as relatively important (Figs 9.1 - 9.4). For three of these combinations the same predictor variable was ranked most important for both the np and mu model components, although which variable that was varied among the combinations. The model for Northern Gannet (fall) had the most skewed distribution of variable importance with day of the year accounting for about 40-60% of the total variable importance for both the np and mu components.

3.2.2 All species and seasons

The most important predictor variables varied across species (Fig. 10). Day of the year was relatively important in the np and mu components of the best models for many species. Mean sea surface temperature appeared as relatively important for some alcid species, particularly in the summer. Turbidity appeared as relatively important for some nearshore species (e.g., ducks, Horned Grebe, Double-crested Cormorant, Brown Pelican), at least during some seasons. Year was relatively important in the models for many species and seasons. The Atlantic Multidecadal Oscillation (AMO) climate index appeared as relatively important in the models for a few species-season combinations.

3.2.3 Seasonal

Averaged across species, day of the year was the most important predictor variable in spring and fall models for both the np and mu model components (Figs 11-13). This result may reflect the movement of migratory species in and out of the study area during the transition between summer and winter. Mean sea surface temperature was the most important variable in summer, while turbidity ranked as first (np component) or second (mu component) most important in winter.

3.3 Predictor variable effects (example species-season combinations)

As with predictor variable importance, our modelling framework was not designed to determine the functional relationships between environmental predictors and the distribution of birds, so ecological inferences from the predictor effect results should be cautious. However, again, these results may suggest interesting hypotheses for future research.

3.3.1 Marginal effects

Estimated marginal univariate effects of predictor variables on the np (zero inflation) and mu (count distribution mean) components of predictions exhibited a wide variety of patterns. Figs 14.1-14.4 illustrate some example effects for the four example species-season combinations. In some cases the effect of a given predictor was consistent between the np and mu components. For example, in the best Common Tern (summer) model the probability of an extra zero (np) decreased and the mean of the count distribution (mu) increased at higher values of the upwelling index, both indicating an increase in the expected number of birds sighted per transect segment. As another example, the probability of an extra zero generally decreased and the mean of the count distribution generally increased throughout the fall in the best Northern Gannet model suggesting an average increase in bird numbers in the study area, which is consistent with birds migrating south from their more northern summer breeding areas.

3.3.2 Bivariate effect interactions

The tree base-learners in the model allowed for interactions among the effects of different spatially explicit predictor variables. As a result, the marginal univariate effect of a given predictor variable was sometimes different depending on the value of other predictor variables. Figs 15.1-15.4 illustrate some example marginal bivariate effects of predictor variables on the np and mu components of predictions for the four example species-season combinations.

3.4 Predicted spatial distributions

3.4.1 Example species-season combinations

In this section we present a very brief review of the ecology and what is known of the distribution of the four example species: Common Tern (*Sterna hirundo*), White-winged Scoter (*Melanitta fusca*), Razorbill

(*Alca torda*), and Northern Gannet (*Morus bassanus*). For each species' example season we then present eight prediction maps organized into two groups: relative occupancy (4 maps; Figs 16.1-16.4 ABCD), and relative abundance (4 maps; Figs 16.1-16.4 EFGH). We also present two annual maps (relative occupancy and abundance) for each of these species (Figs 17.1-17.4 AB), representing the predictions averaged across seasons that were modeled. For species that were modeled in more than one season, these annual maps represent their average spatial distribution during the year or part of the year during which they are present in substantial numbers in the study area. Seasons in which a species was more abundant contributed more to the annual pattern. Finally, we discuss the correspondence between these predicted maps and what is known of the distribution of these species.

3.4.1.1 Common Tern--- Increasing population trend. Common Terns nest on islands, beaches, and saltmarshes on the coast, where it is a common breeder from the Bay of Fundy to northern South Carolina (Nisbet et al. 2013). During spring and fall migration, they generally occur on the entire Atlantic coast and winter mainly in Central and South America. Small numbers winter on the Gulf Coast from Texas to Florida and fewer to North Carolina; these are likely first winter birds from the Great Lakes (Nisbet 2002; Nisbet et al. 2013).

Common Terns take live prey on the surface and usually forage within 20 km from shore during the breeding season when they consume and provision chicks with small forage fish, of which American sand lance (*Ammodytes americanus)* is a major food item (Nisbet 1983; Veit and Petersen 1993). In Long Island Sound, large foraging groups of Common Terns had greater success than smaller groups when exploiting dense patchy prey (Duffy 1986). Feeding associations may form with sub-surface predatory fish, such as schools of blue fish that drive prey to the surface during feeding frenzies; also over tidal rips (e.g., sand rips of Cape Cod, Nantucket, Tuckernuck, and Muskeget Islands) and shoals, where prey is concentrated and brought to the surface by means of rapid tidal flux and convergent flow (Duffy 1986; Safina et al. 1988; Schneider 1990; Veit and Petersen 1993).

Modeled relative occurrence and abundance of Common Tern in summer reflect this species' breeding distribution, a period when adults are nesting and provisioning chicks (Fig. 16.1). Bootstrapped median occupancy and abundance models reveal similar patterns (Fig. 16.1 C,G). Highest predictions of occupancy are closest to shore near documented nesting sites and local foraging areas; e.g., coastal Maine; Grand Manan Archipelago; Petit Manan; Monomoy National Wildlife Refuge, Cape Cod, Massachusetts; Nantucket Sound, Massachusetts; shoals surrounding Muskeget and Tuckernuck Islands, Massachusetts; and Muskeget Channel, Massachusetts. East of Cape Cod, a local area of predicted high relative occupancy and abundance is predicted in Franklin Basin over Franklin Swell (Fig. 16.1). This shoal is within range of major breeding colonies on Cape Cod and may produce favorable foraging conditions for nesting terns. Other areas of predicted high relative occupancy and abundance include east of Long Island, New York; Sandy Hook, New Jersey; and barrier beaches of New Jersey, Delaware, and Maryland. These coastal zones support local breeding colonies in spring and summer.

The average annual modeled distribution of Common Tern (average of spring, summer, and fall model predictions) indicates high relative occupancy and abundance near the coast reflecting migratory distributions and associations with breeding colonies, e.g. Maine's coastal islands, Cape Cod, Long Island and New Jersey (Fig. 17.1).

It is possible that the number of Common Tern sightings in the South Atlantic Bight (Cape Hatteras to Southern Florida) in the survey dataset was biased low due to the challenges of identifying terns from fixed-winged aircraft. Sightings of terns from aerial and ship surveys in spring, summer, and fall suggest

that observers on ships positively identify Common Terns more often than observers on aerial surveys. A total of 2883 terns were sighted from ship surveys of which 883 (31%) were identified as Common Tern, 765 (27%) were identified as other tern species, and 1235 (43%) were not identified to species. From aerial surveys a total of 2361 terns were sighted of which none were identified as Common Tern, 673 (29%) were identified as other tern species, and 1688 (71%) were not identified to species. Because the ratio of aerial survey effort to ship survey effort was higher in the South Atlantic Bight (Fig. 2A), the information in the survey data about Common Tern in this region was lower, so model predictions for this species in this area should be interpreted cautiously. In particular, predictions of high relative occupancy and abundance offshore in this area are questionable (Fig. 17.1).

3.4.1.2 Northern Gannet--- Increasing population trend. In North America, breeding occurs on colonies in the Gulf of St. Lawrence and off the coast of Newfoundland, Canada. Northern Gannets can form dense feeding aggregations composed of 1000s individuals that frenetically plunge-dive into ephemeral sub-surface schooling fish, such as herring and menhaden. In spring and fall, gannets form large migratory groups that stream by headlands and are easily observed from shore-based vantage points. Standardized counts and radar studies of gannets and other seabirds are organized along the coast; e.g. Avalon Seawatch, where a high count of approximately 20,000 gannets occurred on 12 November 2008 (New Jersey Audubon 2006); however, migratory movements also occur over a broad swath of the continental shelf (Powers 1984; Stenhouse et al. 2015). On Georges Bank, gannets were most abundant during spring and fall (Powers and Brown 1987), with reported high concentrations in New York and New Jersey waters during winter. Stenhouse et al. (2015) used satellite transmitters to track gannets across three winter periods and observed core areas south of Gloucester, Massachusetts, an area known for its commercial fishing fleet; Chesapeake and Delaware Bay; the Outer Banks, North Carolina; and in the vicinity of a Frying Pan Shoals in southern North Carolina. Also in winter, Veit and Petersen (1993) reported high concentrations at the shelf break in association with fishing trawlers. Data from Christmas Bird Counts (CBCs) report 93% of observations between MA-NC (data available from National Audubon Society 2016; Nisbet et al. 2013). Juveniles tend to travel farther south to offshore areas from North Carolina to Florida (Palmer 1976, Nelson 1978; Nisbet et al 2013).

Model predictions of median relative occupancy and abundance generally support what has been reported about the distribution and abundance of Northern Gannets in fall in US waters (Fig. 16.2). Relative occupancy is predicted to be broad across the continental shelf, with highest probabilities in close proximity to the coast, specifically east of New York, New Jersey, Delaware, and Virginia (Fig. 16.2 A-D). Predicted median relative abundance reveals similar patterns close to the coast and offshore; e.g., Georges Bank (Fig. 16.2 E-H). Relative abundance predictions generally agree with reports of low abundance off Cape Hatteras in autumn (Sep – Nov) and off east Florida (Nisbet et al. 2013). Predicted higher relative abundance off southern NJ is generally supported by shore-based estimates during late fall (New Jersey Audubon 2006; Nisbet et al. 2013). Predicted high relative occupancy and abundance east of the shelf break and far offshore in the South Atlantic Bight are questionable (Nisbet et al. 2013).

The average annual modeled distribution of Northern Gannet (average of spring, summer, fall, and winter model predictions) generally reflects patterns of spring and fall migration and the species' winter distribution (Fig. 17.2). Predicted high relative occupancy and abundance offshore of the shelf break and slope likely do not reflect persistent areas of aggregation as they fall outside regions of concentrated survey effort (Fig. 2).

3.4.1.3 Razorbill---Increasing population trend. There are approximately 1000 breeding pairs on islands in the Bay of Fundy and Gulf of Maine. The bulk of the North American breeding distribution is in low-arctic waters of southern Labrador and the lower North Shore of the Gulf of St. Lawrence (Lavers et al. 2009; Nisbet et al. 2013). In winter, 94% of total birds reported on CBC surveys stretch between Nova Scotia and Massachusetts (data available from National Audubon Society 2016; Nisbet et al. 2013). Birds winter mainly in waters south to 40°, and are highly concentrated in the Bay of Fundy and in productive waters of Georges Bank, Nantucket Shoals, Nantucket Sound, and east of Cape Cod (Powers and Brown 1987; Veit and Petersen 1993; Nisbet et al. 2013; White 2011; White et al. 2013); however, numbers have increased off Cape Hatteras in recent years (Veit and Guris 2009). Razorbills often form highly aggregative foraging flocks in association with tidal fronts that manifest in the vicinity of sloped topography on shallow banks and ledges (Durazo et al. 1998; White 2011). Their diet is primarily composed of small forage fish (e.g., sand lance, young herring) and crustaceans (e.g., krill), that also form dense aggregations in association with hydrographic fronts (Huettmann et al. 2005; Gaston and Woo 2008; White 2011). Abundant sand lance populations occur in the Gulf of Maine and southern New England where they burrow in sandy bottom, particularly in the waters of Cape Cod, Nantucket Shoals, and Georges Bank. Strong topographically rectified currents, tidal fronts, and vertical mixing occur within these regions and spatially correspond with high model predictions of Razorbills. In winter 2012-2013, the Atlantic coast witnessed an incursion of Razorbills in unprecedented numbers that spanned from the Gulf of Maine to the Gulf of Mexico. Many emaciated carcasses were found onshore indicating a lack of suitable prey, which was likely due to anomalous warm water conditions in the Atlantic (Brinkley 2013).

Model predictions of median relative occupancy and abundance of Razorbills in winter reveal similar patterns (Fig. 16.3). Patterns of relative occupancy and abundance broadly agree with recent at-sea surveys and published reports, especially in the vicinity Cape Cod (Nantucket Sound, east of outer Cape Cod, Stellwagen Bank), Nantucket Shoals, Georges Bank, and the Bay of Fundy. Modeled median relative occupancy appears to reflect increasing presence of Razorbills in the Mid-Atlantic Bight (Fig. 16.3).

The average annual modeled distribution of Razorbill (average of spring, summer, fall, and winter model predictions) generally reflects the summer distribution associated with breeding islands in the Gulf of Maine (Fig. 17.3). Winter, spring, and fall distributions coalesce around shallow banks and ledges and Georges Bank in the Gulf of Maine; Cape Cod, Nantucket Sound and Nantucket Shoals in southern New England; and to a lesser extent, off eastern Long Island, NY and southern New Jersey (Fig 17.3).

3.4.1.4 White-winged Scoter---Decreasing population trend. This largest scoter species nests in the northwestern interior of North America and winters on both coasts. White-winged Scoters arrive to the US east coast in September, increase in numbers throughout fall and winter, and depart for breeding areas in mid-May. Also known as diving ducks, they prey mainly upon molluscs attached to substrate; e.g. blue mussels, and infaunal clams embedded in the seafloor, and sometimes select soft-bodied crustaceans. White-winged Scoters are generally found in close proximity to the coast between depths of 5 and 40 m. They are highly gregarious and form patchy feeding flocks, which can comprise 1000s of individuals and stretch across miles of ocean; e.g., Nantucket Shoals (White 2013; White et al. 2013). The Nantucket Shoals feeding hotspot is associated with high concentrations of clams and pelagic crustaceans and overlaps with a hotspot of wintering Long-tailed Ducks (White 2013). The majority or 86% of the total number of White-winged Scoters reported on CBCs concentrate between Maine and New York (data available from National Audubon Society 2016; Nisbet et al. 2013).

Model predictions of median relative occupancy and abundance in winter are similar for White-winged Scoters (Fig. 16.4). Both relative occupancy and abundance is predicted to be higher in and around Cape Cod Bay, Nantucket Sound, and Nantucket Shoals and agree with reported areas of high abundance. Reasonably high predicted relative occupancy and abundance also occur east of Long Island, NY and the New Jersey coast. Use of these areas in winter is supported by satellite telemetry (birds fixed with GPS transmitters; Environment Canada 2013), systematic surveys, and local reports (Nisbet et al. 2013). Predictions of high relative occupancy and abundance of this species in offshore waters are questionable. The model predicts White-winged Scoters in deep waters (> 90 m) and approximately 100 nm south of Nova Scotia. These zones appear unlikely to be favored by White-winged Scoters given what is known of their wintering ecology. Predictions of high relative occupancy and abundance south of Nantucket Shoals and offshore of the shelf break are also questionable.

The average annual modeled distribution of White-winged Scoter (average of fall, winter, and spring) reflects core winter foraging areas in the vicinity of Nantucket Island (Nantucket Sound and Nantucket Shoals) and Cape Cod Bay (Fig. 7.4). Lower predicted coastal relative occupancy and abundance extend south into the mid-Atlantic region, and reveal a peak along eastern Long Island, NY and in the vicinity of Montauk Point. Predicted relative occupancy and abundance attenuates south until the barrier islands of New Jersey, and mouths of Delaware and Chesapeake Bay. Higher predicted relative occupancy and abundance greater than 20 nm from the New England coast suggest migratory groups travelling to southern foraging destinations in fall, and should not be interpreted as persistent foraging areas. Predictions of moderate relative occupancy and abundance far offshore from the mid-Atlantic coast are almost certainly spurious (Fig. 17.4).

3.4.2 Species groups

Figs 18-20 show modeled annual distributions of relative occupancy and abundance averaged across species within three species groups: nearshore, pelagic, and gulls and gannets (Table 12). Each species' annual predictions were normalized (divided by their sum) prior to averaging so that each species contributed equally to the multi-species average. Because each species' predictions were divided by their sum, the actual numeric values of these normalized predictions are very small. As with all predictions of occupancy and abundance presented in this report, it is the relative differences in predictions across space that are relevant, not the actual numbers themselves.

Figs 18-20 should be regarded as an exploratory exercise to generate multi-species products. These species groupings were based on loosely similar spatial domains and should not be interpreted as ecological groups. Some member species of the 'pelagic' group are more of a 'nearshore' species during the breeding season (e.g. Atlantic Puffin, Razorbill) as revealed in the modeled distribution for this group which exhibits predictions of high relative occupancy and abundance around breeding colonies in the Gulf of Maine (Fig. 19).

4. Discussion

This report describes the first phase of a project aimed at producing maps of the spatial distributions of marine bird species in U.S. Atlantic Outer Continental Shelf waters (Fig. 1) that can be used to inform marine spatial planning in the region. Maps were developed for 40 species and 118 species-season combinations.

4.1 Interpretation of maps

The maps presented in this report represent spatial predictions of relative occurrence and relative abundance averaged over time. The maps do not provide predictions of the absolute number of individuals of a given species that would be expected in a specific location at a specific time. The maps only provide information about where a given species may be more or less likely to occur and where a species may be more or less abundant.

The maps presented here represent model predictions that ultimately rely on the underlying survey data that the models were fit to. The distribution of survey effort was highly uneven across the study area (Fig. 2), so some areas were much better sampled than others. For example, there were many fewer data from offshore areas than nearshore areas. Model predictions in areas with low survey effort should be interpreted cautiously. The survey effort contours provided can be used to identify such areas. For example, Fig. 21 shows the map of predicted relative abundance for Razorbill in winter with the survey effort contours overlaid. The area of predicted high relative abundance off southern Nova Scotia at the northeast end of the study area is outside of the 95% survey effort contour indicating that these model predictions are based on few, if any local data.

Predictions very close to shore (i.e., within 1-2 km) should be interpreted with caution for several reasons. First, survey effort was limited very close to shore (i.e., within 1-2 km). Second, the boundaries of the square study grid cells did not perfectly align with the shoreline, so there may be gaps between the shoreline and the nearest study grid cell. Third, data for some remotely-sensed predictor variables were less reliable or missing (precluding prediction) very close to shore. As a result, predictions for species that tend to be very close to shore (e.g., Brown Pelican, Laughing Gull, and Least Tern) should be interpreted with caution.

Large variations in model predictions at the 2-km resolution of the prediction grid may not be realistic. For example, the modeled annual average distribution of Common Tern exhibits patchy predictions in offshore areas of the South Atlantic Bight and Gulf of Maine (Fig. 17.1). Such large variation in average long-term relative occurrence and abundance at such fine spatial scales is likely unrealistic in many cases. Management applications should not assume that fine-scale variation in model predictions from one grid cell to the next is realistic. Interpretation of the maps presented here to inform spatial planning is probably more reliable at the regional scale (i.e., 10-100 km).

Some model predictions of high relative occurrence and abundance may partially reflect large temporal and spatial aggregations of birds coinciding with survey effort rather than average long-term spatial patterns per se. For example, pockets of very high predicted relative occurrence and abundance in offshore areas often reflect high counts on a limited number of survey transects (e.g., Audubon Shearwater fall model). In many cases, it is unlikely that these are persistent areas of much higher relative occurrence and abundance than adjacent areas that had no survey effort. While our spatial predictive modeling framework theoretically accounts for effort and attempts to account for the aggregated nature of animal distributions and sightings, limited sample size combined with extreme aggregations can unduly influence model predictions.

The maps of predicted relative occurrence and abundance presented here are accompanied by corresponding maps of the estimated uncertainty in those predictions including bootstrapped quantiles, confidence intervals, and coefficients of variation. It is important that the uncertainty products are considered alongside the prediction maps. In many cases the confidence intervals and coefficients of

variation are very large indicating substantial statistical uncertainty and variability associated with the corresponding predictions, and those predictions should be interpreted cautiously.

4.2 Model performance

The performance of the models varied among species and seasons (Table 11). We provide two assessments of the quality of each model.

First, a suite of performance metrics were calculated to determine the statistical fit of each model to the data. Four of these metrics were combined to provide an overall model performance class, and a badge indicating this performance is included on the map products. It is important to recognize that the model performance metrics and badge reflect only the statistical fit of the model to the data that were analyzed, and they do not reflect the quality of model predictions away from the data. For example, the accuracy of predictions in areas with little survey effort is not necessarily reflected by the model performance metrics. Nevertheless, the performance metrics and overall performance class give a relative indication of how accurately a model was able to predict the observed data, and better performance provides a measure of confidence in the model predictions, especially within the temporal and spatial coverage of the observed survey data. On the other hand, when metrics indicate poor performance (e.g., zero percent deviance explained, negative Gaussian rank correlation coefficient, or extremely high median absolute error) those models should be interpreted cautiously.

Second, we provide a judgement about the quality of each model based on an expert review of the maps by one of the authors of this report (TPW). This assessment is more subjective than the performance assessment, and it is the opinion of one expert, but it provides a broader evaluation of how the modeled distributions of relative occurrence and abundance match what is known about the distributions of these marine bird species in the study area.

4.3 Species identification

The survey data analyzed in this project were from a large number of surveys representing numerous survey platforms and protocols. A fundamental assumption of the analysis presented here is that all species, when present, were recorded. This assumption might have been violated on one or more surveys if observers were focused on particular groups of species and failed to record occurrences of other species. A related issue is the identification of observed birds to the species level. From some survey platforms, or again if observers were more focused on some species than others, some birds might have been less likely to be identified to species. For example, it can be difficult to identify the species of some small birds from typical aerial surveys. Birds that were not identified to species were not included in the analysis here. The result of failure to record some species or failure to identify the species of some types of birds is the same: the expected count of those species will vary among survey datasets, independent of other factors.

Our statistical modeling framework allowed for differences in the expected count of a given species among survey platforms and transects, so theoretically the models could account for differences arising from failure to record or identify species. However, if a geographic area is covered by a limited number of surveys or platforms, then it would be difficult or impossible for the model to determine whether differences in counts in that area were because of fewer birds in that area or because of differences in species recording and identification in that area. Model predictions in such instances should be interpreted

cautiously. For example, model predictions for species that are difficult to identify from aircraft should be interpreted cautiously in areas where most of the survey effort was aerial.

4.4 Project Phase II

A second phase of this project is currently underway that will expand, refine, and improve the modeling and results presented in this report. The results presented here should be considered preliminary. In particular, an error in the computer code used for Phase I of the analysis resulted in spurious spatial patterns in some of the predictions (Section 2.6). The error has been corrected for the second phase of the project.

5. Literature Cited

Bodenhofer, U., Krone, M., and Klawonn, F. 2013. Testing noisy numerical data for monotonic association. Information Sciences 245:21-37.

Boudt, K., Cornelissen, J., and Croux, C. 2012. The Gaussian rank correlation estimator: robustness properties. Statistics and Computing 22:471-483.

Brinkley, E.S. 2013. The Changing Seasons: Strangers in a strange land. In North American Birds. Vol 67(2): 216-228.

Bühlmann, P. and Hothorn, T. 2007. Boosting algorithms: Regularization, prediction and model fitting. Statistical Science 22(4):477-505.

Duffy, D. C. 1986. Foraging at patches: interactions between Common and Roseate Terns. Ornis Scandinavica 17:47-52.

Durazo, R., Harrison, N.M., and Hill, A.E. 1998. Seabird observations at a tidal mixing front in the Irish Sea. Estuarine, Coastal and Shelf Science 47(2):153-164.

Environment Canada. 2013. URL: http://www.seaturtle.org/tracking/index.shtml?tag_id=39274. Accessed 2016-04-14.

Friedman, J. H. 2002. Stochastic gradient boosting. Computational Statistics & Data Analysis 38:367-378.

Gaston, A.J. and Woo, K. 2008. Razorbills (*Alca torda*) follow subarctic prey into the Canadian Arctic: colonization results from climate change? The Auk 125(4):939-942.

Hahsler, M. and Hornik, K. 2015. TSP: Traveling Salesperson Problem (TSP). R package version 1.1-1. https://CRAN.R-project.org/package=TSP.

Hofner, B., Mayr, A., Robinzonov, N., and Schmid, M. 2012. Model-based boosting in R: A hands-on tutorial using the R package mboost. Technical Report 120, Department of Statistics, University of Munich, Germany.

Hothorn, T., Buehlmann, P., Kneib, T., Schmid, M., and Hofner, B. 2014. mboost: Model-Based Boosting, R package version 2.4-0. URL: http://CRAN.R-project.org/package=mboost. Accessed 2016-04-14.

Huettmann F.A., Diamond A.W., Dalzell B.R., and Macintosh, K. 2005. Winter distribution, ecology and movements of Razorbills *Alca torda* and other auks in the outer Bay of Fundy, Atlantic Canada. Marine Ornithology 33:161-171.

Lavers, J., Hipfner, M., Chapdelaine, G., and Hipfner, J. M. 2009. Razorbill (*Alca torda*). No. 635 in The Birds of North America (Poole, A., ed.). Cornell Lab of Ornithology, Ithaca, NY.

Mayr, A., Fenske, N., Hofner, B., Kneib, T., and Schmid, M. 2012. Generalized additive models for location, scale and shape for high dimensional data---a flexible approach based on boosting. Applied Statistics 61(3):403-427.

National Audubon Society. 2016. URL: http://www.audubon.org. Accessed 2016-04-14.

New Jersey Audubon. 2006. URL: http://www.njaudubon.org. Accessed 2016-04-14.

Nelson, J. B. 1978. The Gannet. Buteo Books, Vermillion, SD.

Nisbet, I. C. 1983. Territorial feeding by Common Terns. Colonial Waterbirds 6:64-70.

Nisbet, I. C. 2002. Common Tern (*Sterna hirundo*). No. 618 in The Birds of North America (Poole, A., ed.). Cornell Lab of Ornithology, Ithaca, NY.

Nisbet, I. C., Veit, R. R., Auer, S. A., and White, T. P. 2013. Marine birds of the eastern United States and the Bay of Fundy: Distribution, numbers, trends, threats, and management. Nuttall Ornithological Club, Cambridge, MA.

NROC (Northeast Regional Ocean Council). 2016. URL: http://neoceanplanning.org/projects/marine-life/. 'Work Groups' section. Accessed 2016-04-14.

O'Connell, A., Gardner, B., Gilbert, A., and Laurent, K. 2009. Compendium of Avian Occurrence Information for the Continental Shelf Waters along the Atlantic Coast of the United States. Final report to the U.S. Fish and Wildlife Service under USGS Quick Response and Science Support Partnership Funding and Minerals Management Service under reimbursable agreement M08PG20033.

Palmer, R. S. 1976. Handbook of North American birds, Vol. 2: Waterfowl. Part 1. Yale University Press, New Haven, CT.

Powers, K. D. 1984. Pelagic distributions of marine birds off the northeastern United States. US Department of Commerce, National Oceanic and Atmospheric Administration, National Marine Fisheries Service, Northeast Fisheries Center.

Powers, K. D. and Brown, R. G. B. 1987. Seabirds. Pages 372–384 in Georges Bank (Backus, R. H. and Bourne, D. W., eds.). MIT Press, Cambridge, MA.

R Core Team. 2014. R: A language and environment for statistical computing. R Foundation for Statistical Computing, Vienna, Austria. URL: http://www.R-project.org/. Accessed 2016-04-14.

Robinson Willmott, J. C., G. Forcey, and A. Kent. 2013. The relative vulnerability of migratory bird species to offshore wind energy projects on the Atlantic Outer Continental Shelf: An assessment method and database. Final Report to the U.S. Department of the Interior, Bureau of Ocean Energy Management, Office of Renewable Energy Programs. OCS Study BOEM 2013-207. 275 pp.

Safina, C., Burger, J., Gochfeld, M., and Wagner, R. H. 1988. Evidence for prey limitation of Common and Roseate Tern reproduction. Condor 90:832-839.

Schmid, M., Potapov, S., Pfahlberg, A., and Hothorn, T. 2008. Estimation and regularization techniques for regression models with multidimensional prediction functions. Technical Report 42, Department of Statistics, University of Munich, Germany.

Schneider, D. C. 1990. Seabirds and fronts: a brief overview. Polar Research 8:17-21.

Stenhouse, I. J., Gray, C. E., Gilbert, A. T., Montevecchi, W. A. 2015. Wintering movements and habitat use of Northern Gannets (*Morus bassanus*) in the mid-Atlantic U.S. In: Wildlife Densities and Habitat Use Across Temporal and Spatial Scales on the Mid-Atlantic Outer Continental Shelf: Final Report to the Department of Energy EERE Wind & Water Power Technologies Office. Williams, K. A., Connelly, E. E., Johnson, S. M., and Stenhouse, I. J. (eds.) Award Number: DE-EE0005362. Report BRI 2015-11, Biodiversity Research Institute, Portland, ME. 23 pp.

Veit, R. and Petersen, W. 1993. Birds of Massachusetts. Massachusetts Audubon Society, Lincoln, MA.

Veit, R. R. and Guris, P. A. 2009. Recent increases in alcid abundance in the New York Bight and New England waters. New Jersey Birds 34: 83–87.

White, T. P. 2011. Associations of diving birds and prey at hydrographic fronts during winter. Paper presented at the AMBCC meeting (February), Portland, ME.

White, T. P. 2013. Spatial ecology of Long-tailed Ducks and White-Winged Scoters on Nantucket Shoals, Massachusetts. PhD thesis. City University of New York, NY.

White, T. P., Veit, R. R., Perkins, S. A. 2013. Aerial surveys of pelagic birds south of Nantucket Massachusetts. Report to The Massachusetts Clean Energy Center.

Table 1. Datasets analyzed. Data from these surveys were extracted from the USGS Avian Compendium Database (O'Connell et al. 2009) and standardized to 15-minute ship survey equivalent transect segments as described in the text. Transect counts reflect all transect segments within the study area, including some records that were later excluded from analysis due to incomplete records (missing predictor data).

			Year		Number of transect segments surveyed[c] (15-minute-ship-survey-equivalents[d])				
Source Dataset ID[a]	Platform	Method[b]	Start	End	Total	Spring	Summer	Fall	Winter
AMAPPS_FWS_Aerial_Fall2012	Aerial	cts	2012	2012	5157	0	0	5157	0
AMAPPS_FWS_Aerial_Preliminary_Summer2010	Aerial	cts	2010	2010	1863	0	1863	0	0
AMAPPS_FWS_Aerial_Spring2012	Aerial	cts	2012	2012	5270	5270	0	0	0
AMAPPS_FWS_Aerial_Summer2011	Aerial	cts	2011	2011	5177	0	5177	0	0
AMAPPS_FWS_Aerial_Winter2010-2011	Aerial	cts	2010	2011	914	0	0	0	914
AMAPPS_NOAA/NMFS_NEFSCBoat2011	Boat	cts	2011	2011	1274	0	1274	0	0
AMAPPS_NOAA/NMFS_NEFSCBoat2013	Boat	cts	2013	2013	1318	0	1318	0	0
AMAPPS_NOAA/NMFS_NEFSCBoat2014	Boat	cts	2014	2014	859	859	0	0	0
AMAPPS_NOAA/NMFS_SEFSCBoat2011	Boat	cts	2011	2011	822	0	822	0	0
AMAPPS_NOAA/NMFS_SEFSCBoat2013	Boat	cts	2013	2013	813	0	582	231	0
BarHarborWW05	Boat	cts	2005	2005	911	0	755	156	0
BarHarborWW06	Boat	cts	2006	2006	1022	0	730	292	0
CapeHatteras0405	Boat	cts	2004	2005	276	0	154	0	122
CapeWindAerial	Aerial	cts	2002	2004	4035	963	959	1014	1099
CapeWindBoat	Boat	cts	2002	2003	252	100	123	29	0
CDASMidAtlantic	Aerial	cts	2001	2003	1402	201	0	0	1201
CSAP	Boat	dts	1980	1988	26271	7640	7028	7368	4235
DOEBRIBoatApr2014	Boat	cts	2014	2014	140	140	0	0	0
DOEBRIBoatApril2012	Boat	cts	2012	2012	142	142	0	0	0
DOEBRIBoatAug2012	Boat	cts	2012	2012	142	0	142	0	0
DOEBRIBoatAug2013	Boat	cts	2013	2013	145	0	145	0	0
DOEBRIBoatDec2012	Boat	cts	2012	2013	139	0	0	0	139
DOEBRIBoatDec2013	Boat	cts	2013	2013	147	0	0	0	147
DOEBRIBoatJan2013	Boat	cts	2013	2013	143	0	0	0	143
DOEBRIBoatJan2014	Boat	cts	2014	2014	143	0	0	0	143
DOEBRIBoatJune2012	Boat	cts	2012	2012	143	0	143	0	0
DOEBRIBoatJune2013	Boat	cts	2013	2013	146	0	146	0	0
DOEBRIBoatMar2013	Boat	cts	2013	2013	145	145	0	0	0
DOEBRIBoatMay2013	Boat	cts	2013	2013	147	147	0	0	0
DOEBRIBoatNov2012	Boat	cts	2012	2012	142	0	0	142	0
DOEBRIBoatOct2013	Boat	cts	2013	2013	147	0	0	147	0
DOEBRIBoatSep2012	Boat	cts	2012	2012	144	0	0	144	0
DOEBRIBoatSep2013	Boat	cts	2013	2013	148	0	0	148	0
EcoMonAug08	Boat	cts	2008	2008	411	0	411	0	0
EcoMonAug09	Boat	cts	2009	2009	395	0	395	0	0
EcoMonAug10	Boat	cts	2010	2010	427	0	415	12	0
EcoMonAug2012	Boat	cts	2012	2012	560	0	560	0	0
EcoMonFeb10	Boat	cts	2010	2010	292	0	0	0	292
EcoMonFeb2012	Boat	cts	2012	2012	472	0	0	0	472
EcoMonJan09	Boat	cts	2009	2009	341	0	0	0	341
EcoMonJun2012	Boat	cts	2012	2012	389	27	362	0	0
EcoMonMay07	Boat	cts	2007	2007	435	374	61	0	0
EcoMonMay09	Boat	cts	2009	2009	543	173	370	0	0
EcoMonMay10	Boat	cts	2010	2010	550	235	315	0	0
EcoMonNov09	Boat	cts	2009	2009	379	0	0	379	0
EcoMonNov10	Boat	cts	2010	2010	356	0	0	356	0
EcoMonNov2011	Boat	cts	2011	2011	391	0	0	391	0
EcoMonOct2012	Boat	cts	2012	2012	428	0	0	428	0
FWS_MidAtlanticDetection	Aerial	cts	2012	2012	456	456	0	0	0

_Spring2012									
FWS_SouthernBLSC_Winter2012	Aerial	cts	2012	2012	1582	0	0	0	1582
FWSAtlanticWinterSeaduck2008	Aerial	cts	2008	2011	14377	128	0	0	14249
GeorgiaPelagic	Boat	dts	1982	1985	2187	681	699	576	231
HatterasEddyCruise2004	Boat	cts	2004	2004	93	0	93	0	0
HerringAcoustic06	Boat	cts	2006	2006	243	0	0	243	0
HerringAcoustic07	Boat	cts	2007	2007	283	0	0	283	0
HerringAcoustic08	Boat	cts	2008	2008	710	0	0	710	0
HerringAcoustic09Leg1	Boat	cts	2009	2009	109	0	0	109	0
HerringAcoustic09Leg2	Boat	cts	2009	2009	245	0	0	245	0
HerringAcoustic09Leg3	Boat	cts	2009	2009	227	0	0	227	0
HerringAcoustic2010	Boat	cts	2010	2010	482	0	0	482	0
HerringAcoustic2011	Boat	cts	2011	2011	690	0	0	690	0
MassAudNanAerial	Aerial	cts	2002	2006	4131	753	604	1034	1740
NewEnglandSeamount06	Boat	dts	2006	2007	66	61	4	1	0
NJDEP2009	Boat	cts	2008	2009	4446	1094	1191	1272	889
NOAA/NMFS_NEFSCBoat2004	Boat	cts	2004	2004	1017	0	1017	0	0
NOAA/NMFS_NEFSCBoat2007	Boat	cts	2007	2007	516	0	516	0	0
NOAAMBO7880	Boat	dts	1978	1979	6979	1682	2462	2044	791
PlattsBankAerial	Aerial	cts	2005	2005	732	0	732	0	0
RISAMPAerial	Aerial	cts	2009	2010	2158	849	663	0	646
RISAMPBoat	Boat	cts	2009	2010	716	185	239	142	150
SEFSC1992	Boat	cts	1992	1992	674	0	0	0	674
SEFSC1998	Boat	cts	1998	1998	1146	0	1146	0	0
SEFSC1999	Boat	cts	1999	1999	1058	0	611	447	0
WHOIJuly2010	Boat	cts	2010	2010	71	0	71	0	0
WHOISept2010	Boat	cts	2010	2010	74	0	0	74	0
TOTALS	ALL	ALL	1978	2014	111776	22305	34298	24973	30200

[a]The Source Dataset ID can be used to look up datasets in Appendix A, Table A1, which gives detailed additional background information about each survey. Table A1 lists several additional datasets; these additional datasets are available but did not contain any segments that fell within the study area.

[b]Survey method: cts, continuous-time strip transects; dts, discrete-time strip transects

[c]Counts exclude segments whose midpoint falls outside the study area (as shown in Figure 1), and any partial segments that were less than 60% of standard transect segment length (i.e., only segments >2.778km in length were included).

[d]A15-minute-ship-survey-equivalent is defined as the distance a ship would travel in 15 minutes at 10 knots.

Table 2. List of species analyzed. Four-letter species codes in the first column are generally used in place of the full common or scientific name throughout this report. For each season, only species with >=50 sightings were modeled. Number of sightings includes some records that were later excluded from analysis due to incomplete records (missing predictor data). Shaded cells indicate model runs that were successfully completed.

Species code	Common name	Scientific name	Family	Number of sightings				
				Total	Spring	Summer	Fall	Winter
arte	Arctic Tern	*Sterna paradisaea*	Sternidae	242	44	154	44	0
atpu	Atlantic Puffin	*Fratercula arctica*	Alcidae	795	209	246	91	249
aush	Audubon's Shearwater	*Puffinus lherminieri*	Procellariidae	1460	129	876	286	169
bcpe	Black-capped Petrel	*Pterodroma hasitata*	Procellariidae	689	158	356	92	83
blgu	Black Guillemot	*Cepphus grylle*	Alcidae	141	7	93	7	34
blki	Black-legged Kittiwake	*Rissa tridactyla*	Laridae	6434	621	24	2083	3706
blsc	Black Scoter	*Melanitta americana*	Anatidae	1958	423	16	356	1163
bogu	Bonaparte's Gull	*Chroicocephalus philadelphia*	Laridae	1678	397	20	280	981
brpe	Brown Pelican	*Pelecanus occidentalis*	Pelecanidae	356	66	127	87	76
brsp	Band-rumped Storm-Petrel	*Oceanodroma castro*	Hydrobatidae	290	14	266	10	0
coei	Common Eider	*Somateria mollissima*	Anatidae	3800	893	159	537	2211
colo	Common Loon	*Gavia immer*	Gaviidae	6949	2367	182	1185	3215
comu	Common Murre	*Uria aalge*	Alcidae	277	90	22	5	160
cosh	Cory's Shearwater	*Calonectris diomedea*	Procellariidae	4579	106	2925	1547	1
cote	Common Tern	*Sterna hirundo*	Sternidae	2713	488	1538	683	4
dcco	Double-crested Cormorant	*Phalacrocorax auritus*	Phalacrocoracidae	700	145	187	206	162
dove	Dovekie	*Alle alle*	Alcidae	1675	260	49	404	962
gbbg	Great Black-backed Gull	*Larus marinus*	Laridae	15654	3423	3186	5390	3655
grsh	Great Shearwater	*Puffinus gravis*	Procellariidae	12907	586	6011	6176	134
herg	Herring Gull	*Larus argentatus*	Laridae	21087	5721	2941	7439	4986
hogr	Horned Grebe	*Podiceps auritus*	Podicipedidae	128	21	0	13	94
lagu	Laughing Gull	*Leucophaeus atricilla*	Laridae	3987	711	1602	1560	114
lesp	Leach's Storm-Petrel	*Oceanodroma leucorhoa*	Hydrobatidae	2816	223	2140	452	1
lete	Least Tern	*Sterna antillarum*	Sternidae	185	27	121	37	0

ltdu	Long-tailed Duck	*Clangula hyemalis*	Anatidae	4852	1152	1	485	3214
mash	Manx Shearwater	*Puffinus puffinus*	Procellariidae	689	100	309	264	16
nofu	Northern Fulmar	*Fulmarus glacialis*	Procellariidae	6613	2244	737	1823	1809
noga	Northern Gannet	*Morus bassanus*	Sulidae	17270	5667	1187	4002	6414
poja	Pomarine Jaeger	*Stercorarius pomarinus*	Stercorariidae	984	110	144	709	21
razo	Razorbill	*Alca torda*	Alcidae	2527	720	78	170	1559
rbgu	Ring-billed Gull	*Larus delawarensis*	Laridae	1243	181	46	312	704
reph	Red Phalarope	*Phalaropus fulicarius*	Scolopacidae	1005	461	214	286	44
rnph	Red-necked Phalarope	*Phalaropus lobatus*	Scolopacidae	469	132	167	156	14
rost	Roseate Tern	*Sterna dougallii*	Sternidae	328	56	195	74	3
royt	Royal Tern	*Sterna maxima*	Sternidae	842	269	283	279	11
rtlo	Red-throated Loon	*Gavia stellata*	Gaviidae	3999	1699	11	387	1902
sosh	Sooty Shearwater	*Puffinus griseus*	Procellariidae	2439	790	1542	104	3
susc	Surf Scoter	*Melanitta perspicillata*	Anatidae	3260	745	8	761	1746
wisp	Wilson's Storm-Petrel	*Oceanites oceanicus*	Hydrobatidae	11400	1650	8392	1348	10
wwsc	White-winged Scoter	*Melanitta fusca*	Anatidae	2302	415	5	550	1332

Table 3. Predictor variables used in model with codenames, resolutions, and sources.

Predictor variable	Codename	Native resolution	Source
Survey variables			
Survey platform	boatplane	Categorical variable	USGS/USFWS Compendium of Avian Information Database
Survey ID	sid	Categorical variable	USGS/USFWS Compendium of Avian Information Database
Transect ID	tid	Categorical variable	USGS/USFWS Compendium of Avian Information Database
Temporal variables			
Year	yearscaled	1 year	n/a
Day of year	jday	1 day	n/a
Atlantic Multidecadal Oscillation (AMO) index (current and 1 year lag)	index_amo, index_amo_lag1	Monthly	NOAA ESRL http://www.esrl.noaa.gov/psd/data/correlation/amon.us.data
Multivariate El Niño-Southern Oscillation Index (MEI) (current and 1 year lag)	index_mei, index_mei_lag1	Monthly	NOAA ESRL http://www.esrl.noaa.gov/psd/data/correlation/mei.data
North Atlantic Oscillation (NAO) index (current and 1 year lag)	index_nao, index_nao_lag1	Monthly	NOAA ESRL http://www.esrl.noaa.gov/psd/data/correlation/nao.data
Trans-Niño Index (TNI) (current and 1 year lag)	index_tni, index_tni_lag1	Monthly	NOAA ESRL http://www.esrl.noaa.gov/psd/data/correlation/tni.data
Geographic variables			
Longitude projected (oblique Mercator)	prlon	n/a	n/a
Latitude projected (oblique Mercator)	prlat	n/a	n/a
Distance to land[1]	dland	50 m	Derived from Prototype Global Shoreline Data (http://msi.nga.mil/NGAPortal/DNC.portal?_nfpb=true&_pageLabel=dnc_portal_page_72)
Distance to shelf break[1]	dshelf	Same as depth (approx. 25 m to 927 m)	Derived from depth (200-m isobath)
Terrain variables			
Depth[2]	depth	CRM: 3 arc-seconds (approx. 92 m); ACUMEN: approx. 25 m; CCOM: approx. 111 m; GEBCO: 30 arc-seconds (approx. 927 m)	NOAA National Geophysical Data Center Coastal Relief Model (CRM) (http://www.ngdc.noaa.gov/mgg/coastal/crm.html); NOAA Atlantic Canyons Undersea Mapping Expeditions (ACUMEN) (http://oceanexplorer.noaa.gov/okeanos/explorations/acumen12/summary/welcome.html); University of New Hampshire Center for Coastal and Ocean Mapping (CCOM) / Joint Hydrographic Center (http://ccom.unh.edu/about-ccomjhc); General Bathymetric Chart of the Oceans (GEBCO) GEBCO_08 grid (http://www.gebco.net/data_and_products/gridded_bathymetry_data/)

Slope (derived at 1500 m scale)[1,4]	slp1500m	approx. 1500 m	Derived from depth
Slope (derived at 10 km scale)[1,4]	slp10km	approx. 10 km	Derived from depth
Slope of slope (derived at 10 km scale)[1,4]	slpslp10km	approx. 10 km	Derived from depth
Planform curvature (derived at 10 km scale)[1,3,4]	plcurv10km	approx. 10 km	Derived from depth
Profile curvature (derived at 10 km scale)[1,3,4]	prcurv10km	approx. 10 km	Derived from depth
Physical variables (seasonal climatologies)			
Sea surface height	sshmean	1/3 degree (approx. 37km)	AVISO Global DT-Upd Merged MADT weekly sea surface altimetry product (1992-2013) (http://www.aviso.altimetry.fr/en/data/products/sea-surface-height-products/global/madt.html; note that 'Upd' is now referred to as 'all sat merged')
Sea surface height standard deviation	sshsd	1/3 degree (approx. 37km)	Derived from sea surface height
Probability of anticyclonic eddy ring[5]	peddacyc	1/3 degree (approx. 37km)	Derived from sea surface height
Probability of cyclonic eddy ring[5]	peddcyc	1/3 degree (approx. 37km)	Derived from sea surface height
Sea surface temperature	sstmean	approx. 1 km	AVHRR Pathfinder daily or sub-daily SST (1985-2010) from Peter Cornillon (University of Rhode Island) served at http://www.sstfronts.org/opendap/
Sea surface temperature standard deviation	sstsd	approx. 1 km	Derived from sea surface temperature
Probability of sea surface temperature front[6]	sstfront	0.011 degree (approx. 1.2 km)	Monthly 'climatologies' from Peter Miller (Plymouth Marine Laboratory) derived from monthly front presence/absence in turn derived from daily NASA MUR 1-km SST data (2002-2013)
Current velocity (u direction)	wateru	1/6 degree (approx. 19 km)	Hybrid vertical coordinate system ocean model (HYCOM) reanalysis (GLBu0.16 grid, experiments 19.0 and 19.1) 3-hourly data (1992-2005) (http://hycom.org/dataserver)
Current velocity (v direction)	waterv	1/6 degree (approx. 19 km)	Hybrid vertical coordinate system ocean model (HYCOM) reanalysis (GLBu0.16 grid, experiments 19.0 and 19.1) 3-hourly data (1992-2005) (http://hycom.org/dataserver)
Current divergence	diverg	1/6 degree (approx. 19 km)	Derived from current velocity
Current vorticity	vort	1/6 degree (approx. 19 km)	Derived from current velocity
Wind stress (x direction)	windstrx	0.25 degrees (approx. 28 km)	NOAA CoastWatch monthly grids (1999-2009) derived from NASA Quick Scatterometer (QuikSCAT) data (http://coastwatch.pfeg.noaa.gov/erddap/griddap/erdQSstressmday.html)
Wind stress (y direction)	windstry	0.25 degrees (approx. 28 km)	NOAA CoastWatch monthly grids (1999-2009) derived from NASA Quick Scatterometer (QuikSCAT) data (http://coastwatch.pfeg.noaa.gov/erddap/griddap/erdQSstressmday.html)

Wind divergence	divw	0.25 degrees (approx. 28 km)	NOAA CoastWatch monthly grids (1999-2009) derived from NASA Quick Scatterometer (QuikSCAT) data (http://coastwatch.pfeg.noaa.gov/erddap/griddap/erdQSdivmodmday.html)
Upwelling index	upwelling	0.25 degrees (approx. 28 km)	NOAA CoastWatch monthly grids (1999-2009) derived from NASA Quick Scatterometer (QuikSCAT) data (http://coastwatch.pfeg.noaa.gov/erddap/griddap/erdQSstressmday.html)
Turbidity (reflectance at 670 nm)	turb	approx. 1 km	Monthly products (1997-2010) from Tim Wynne (NOAA NCCOS) derived from daily Sea-Viewing Wide Field of-View Sensor (SeaWiFS) data processed using the Naval Research Laboratories' Automated Processing System software
Biological variables (seasonal climatologies)			
Surface chlorophyll-a	chla	approx. 1 km	Monthly products (1997-2010) from Tim Wynne (NOAA NCCOS) derived from daily Sea-Viewing Wide Field of-View Sensor (SeaWiFS) data processed using the Naval Research Laboratories' Automated Processing System software

[1] Derived using ArcGIS 10.2 Spatial Analyst Tools.

[2] Datasets were converted to a common 100-m grid then mosaicked in order of decreasing priority: CRM, ACUMEN, CCOM, and GEBCO.

[3] Derived using the ArcGIS 10.2 extension DEM Surface Tools (Jenness 2012).

[4] Calculated from depth grids that were smoothed using a Gaussian low-pass filter for each spatial scale.

[5] Derived using Duke University's Marine Geospatial Ecology Lab's Marine Geospatial Ecology Tools (MGET) for ArcGIS 10.2 (Okubo-Weiss algorithm).

[6] A low-pass filter was applied to the climatologies to remove banding artifacts.

Table 4a. Predictor correlation table (spring). Pairwise Spearman rank correlation coefficients for spatial predictor variables. High correlations are highlighted (|tau|>0.7 in yellow, |tau|>0.8 in orange, |tau|>0.9 in red).

	chla	diverg	divw	peddacyc	peddcyc	sshmean	sshsd	sstfront	sstmean	sstsd	turb	upwelling	vort	wateru	waterv	windstrx	windstry	depth	dland	dshelf	plcurv10km	prcurv10km	prlat	prlon	slp10km	slp1500m	slpslp10km
chla		0.2	0.28	-0.47	-0.59	-0.7	-0.48	0.06	-0.87	0.77	0.89	0.27	0.14	-0.22	-0.33	-0.04	-0.62	0.59	-0.53	-0.47	0.04	-0.08	0.8	0.47	-0.24	-0.22	-0.18
diverg			0.02	0	-0.11	-0.22	-0.04	0	-0.14	0.17	0.19	0.28	0.09	0.01	0.08	-0.04	-0.25	0.12	-0.12	-0.12	0.02	0.05	0.16	0.12	0	-0.01	0.04
divw				-0.16	-0.17	-0.44	-0.37	0.16	-0.29	0.34	0.26	0.05	0.21	-0.23	-0.25	-0.23	-0.29	0.26	-0.19	-0.33	0.01	-0.06	0.12	0	-0.01	-0.06	0.05
peddacyc					0.24	0.21	0.53	0.09	0.29	-0.09	-0.38	0.03	-0.13	0.25	0.17	0.28	0.06	-0.61	0.55	0.45	-0.05	0.24	-0.21	0.1	0.27	0.27	0.11
peddcyc						0.59	0.61	-0.04	0.5	-0.39	-0.5	-0.36	0.14	0.12	0.04	0.2	0.46	-0.55	0.54	0.6	-0.01	0.02	-0.54	-0.26	0.07	0.08	0.02
sshmean							0.52	-0.29	0.66	-0.72	-0.64	-0.34	-0.32	0.18	0.22	0.23	0.77	-0.52	0.46	0.61	-0.03	0.02	-0.63	-0.35	-0.06	-0.04	-0.11
sshsd								0.15	0.43	-0.11	-0.35	-0.04	0.02	0.47	0.26	0.63	0.13	-0.72	0.69	0.68	-0.01	0.16	-0.27	0.07	0.2	0.24	0.01
sstfront									0.07	0.47	0.12	0.13	0.35	0.29	0.23	0.29	-0.47	0	0.01	-0.33	0.01	-0.01	0.1	0.03	0.53	0.44	0.35
sstmean										-0.66	-0.76	-0.23	-0.07	0.38	0.54	-0.07	0.55	-0.29	0.24	0.22	-0.02	0.01	-0.9	-0.73	0.21	0.16	0.14
sstsd											0.74	0.32	0.27	0.02	-0.19	0.18	-0.78	0.29	-0.24	-0.33	0.01	0.05	0.66	0.44	0.08	0.07	-0.02
turb												0.26	0.12	-0.14	-0.28	-0.01	-0.61	0.49	-0.42	-0.36	0.05	-0.06	0.7	0.43	-0.18	-0.16	-0.14
upwelling													-0.07	0.18	0.14	0.13	-0.43	0.17	-0.14	-0.24	0.05	0.06	0.35	0.26	-0.01	0	0
vort														0.04	0.05	-0.08	-0.35	0.06	-0.09	-0.23	0.01	-0.09	0.01	-0.02	0.2	0.18	0.21
wateru															0.58	0.37	-0.12	-0.22	0.16	0.09	0.01	0.12	-0.15	-0.09	0.19	0.19	0.02
waterv																0.06	0.01	0.01	-0.05	-0.1	0	0.04	-0.36	-0.36	0.16	0.15	0.07
windstrx																	-0.2	-0.63	0.61	0.39	0.02	0.15	0.3	0.53	0.22	0.26	0.01
windstry																		-0.21	0.2	0.45	-0.06	-0.06	-0.65	-0.5	-0.19	-0.17	-0.12
depth																			-0.9	-0.76	0.07	-0.29	0.21	-0.26	-0.24	-0.29	-0.08
dland																				0.76	-0.02	0.15	-0.18	0.3	0.16	0.2	0.07
dshelf																					-0.06	0.16	-0.25	0.14	-0.14	-0.05	-0.21
plcurv10km																						-0.21	0.03	0.03	0.02	0.01	0
prcurv10km																							0.05	0.12	0.16	0.18	0.09
prlat																								0.84	-0.03	0.03	-0.04
prlon																									0.03	0.11	-0.01
slp10km																										0.88	0.74
slp1500m																											0.63
slpslp10km																											

Table 4b. Predictor correlation table (summer). Pairwise Spearman rank correlation coefficients for spatial predictor variables. High correlations are highlighted (|tau|>0.7 in yellow, |tau|>0.8 in orange, |tau|>0.9 in red).

	chla	diverg	divw	peddacyc	peddcyc	sshmean	sshsd	sstfront	sstmean	sstsd	turb	upwelling	vort	wateru	waterv	windstrx	windstry	depth	dland	dshelf	plcurv10km	prcurv10km	prlat	prlon	slp10km	slp1500m	slpslp10km
chla		0.24	0.2	-0.52	-0.7	-0.78	-0.6	0.67	-0.66	0.63	0.48	0.39	0.14	-0.03	-0.14	-0.15	-0.72	0.76	-0.71	-0.66	0.05	-0.11	0.72	0.31	-0.2	-0.19	-0.13
diverg			0.07	-0.07	-0.14	-0.2	-0.07	0.1	-0.1	0.11	0.06	0.19	0.08	0.01	0.12	-0.02	-0.2	0.16	-0.18	-0.09	0	0.04	0.12	0.05	-0.1	-0.08	-0.06
divw				-0.24	-0.11	-0.24	-0.3	-0.06	-0.07	0.11	0.04	-0.09	0.17	-0.23	-0.15	-0.25	-0.27	0.28	-0.23	-0.26	0.02	-0.14	-0.03	-0.13	-0.09	-0.15	0
peddacyc					0.37	0.29	0.6	-0.17	0.13	-0.11	-0.52	-0.04	-0.12	0.09	0.03	0.4	0.33	-0.65	0.59	0.48	-0.04	0.23	-0.14	0.16	0.39	0.4	0.2
peddcyc						0.57	0.65	-0.46	0.39	-0.39	-0.27	-0.37	0.14	-0.06	-0.05	0.22	0.6	-0.61	0.61	0.65	-0.01	0.06	-0.48	-0.18	0.1	0.11	0.05
sshmean							0.6	-0.6	0.63	-0.67	-0.13	-0.42	-0.25	0.09	0.22	0.25	0.87	-0.61	0.55	0.64	-0.03	0.05	-0.64	-0.32	0	0.02	-0.1
sshsd								-0.16	0.32	-0.3	-0.42	-0.13	0.07	0.31	0.19	0.62	0.59	-0.77	0.76	0.68	-0.01	0.17	-0.27	0.1	0.25	0.28	0.05
sstfront									-0.55	0.6	0.11	0.45	0.2	0.22	0.01	0.24	-0.58	0.32	-0.28	-0.48	0.03	-0.02	0.7	0.5	0.2	0.18	0.14
sstmean										-0.96	-0.09	-0.39	0.02	0.23	0.52	-0.23	0.49	-0.16	0.11	0.15	-0.03	-0.03	-0.94	-0.84	0.11	0.05	0.08
sstsd											0.01	0.41	0.03	-0.21	-0.5	0.24	-0.54	0.13	-0.07	-0.19	0.02	0.03	0.9	0.81	-0.05	-0.02	-0.04
turb												0.03	-0.04	-0.03	-0.03	-0.32	-0.12	0.56	-0.52	-0.31	0.04	-0.2	0.13	-0.21	-0.35	-0.35	-0.25
upwelling													-0.13	0.21	0.09	0.16	-0.37	0.18	-0.16	-0.26	-0.01	0.11	0.51	0.38	0.07	0.09	0.05
vort														0.05	0.08	-0.09	-0.31	0.07	-0.09	-0.19	0.04	-0.1	-0.03	-0.04	0.19	0.15	0.19
wateru															0.59	0.3	0.03	-0.1	0.07	-0.02	0.02	0.13	-0.01	-0.01	0.2	0.2	0.02
waterv																0	0.06	0	-0.07	-0.1	-0.01	0.09	-0.35	-0.36	0.17	0.15	0.06
windstrx																	0.39	-0.58	0.56	0.37	0	0.16	0.33	0.55	0.21	0.24	0
windstry																		-0.6	0.58	0.7	-0.06	0.06	-0.51	-0.22	-0.08	-0.04	-0.14
depth																			-0.9	-0.76	0.07	-0.29	0.21	-0.26	-0.24	-0.29	-0.08
dland																				0.76	-0.02	0.15	-0.18	0.3	0.16	0.2	0.07
dshelf																					-0.06	0.16	-0.25	0.14	-0.14	-0.05	-0.21
plcurv10km																						-0.21	0.03	0.03	0.02	0.01	0
prcurv10km																							0.05	0.12	0.16	0.18	0.09
prlat																								0.84	-0.03	0.03	-0.04
prlon																									0.03	0.11	-0.01
slp10km																										0.88	0.74
slp1500m																											0.63
slpslp10km																											

Table 4c. Predictor correlation table (fall). Pairwise Spearman rank correlation coefficients for spatial predictor variables. High correlations are highlighted (|tau|>0.7 in yellow, |tau|>0.8 in orange, |tau|>0.9 in red).

	chla	diverg	divw	peddacyc	peddcyc	sshmean	sshsd	sstfront	sstmean	sstsd	turb	upwelling	vort	wateru	waterv	windstrx	windstry	depth	dland	dshelf	plcurv10km	prcurv10km	prlat	prlon	slp10km	slp1500m	slpslp10km
chla		0.11	0.24	-0.57	-0.68	-0.77	-0.57	0.62	-0.74	0.68	0.49	0.16	0.14	0.09	-0.29	0.53	-0.43	0.77	-0.72	-0.66	0.04	-0.1	0.71	0.3	-0.21	-0.21	-0.13
diverg			0.05	-0.06	-0.06	-0.13	-0.04	0.07	-0.09	0.09	0.07	0.06	0.05	0.03	0.06	0.07	-0.08	0.06	-0.06	-0.04	0.01	0.06	0.13	0.11	-0.04	-0.03	0.02
divw				-0.11	-0.24	-0.29	-0.3	0.05	-0.37	0.39	0.14	0.04	-0.03	-0.21	-0.34	0.21	-0.04	0.18	-0.15	-0.14	0.01	-0.03	0.26	0.16	-0.07	-0.08	0
peddacyc					0.37	0.28	0.54	-0.2	0.32	-0.21	-0.49	0.02	-0.04	0.06	0.21	-0.09	0.19	-0.61	0.54	0.45	-0.03	0.24	-0.24	0.05	0.36	0.35	0.2
peddcyc						0.54	0.68	-0.4	0.5	-0.44	-0.31	-0.32	0.17	-0.07	0.09	-0.36	0.27	-0.58	0.6	0.59	0	0.01	-0.5	-0.18	0.1	0.11	0.05
sshmean							0.56	-0.64	0.66	-0.71	-0.13	-0.13	-0.34	-0.01	0.29	-0.51	0.47	-0.58	0.53	0.64	-0.03	0.04	-0.63	-0.32	-0.03	-0.02	-0.12
sshsd								-0.2	0.38	-0.32	-0.41	-0.14	0.06	0.3	0.32	-0.07	0.17	-0.73	0.72	0.68	-0.01	0.16	-0.26	0.08	0.21	0.24	0.01
sstfront									-0.4	0.48	-0.01	0.14	0.33	0.34	0.04	0.45	-0.59	0.4	-0.35	-0.61	0.04	-0.07	0.52	0.29	0.25	0.19	0.2
sstmean										-0.81	-0.4	-0.18	-0.03	0.1	0.52	-0.85	0.01	-0.29	0.24	0.22	-0.02	-0.01	-0.93	-0.75	0.19	0.13	0.14
sstsd											0.3	0.06	0.2	-0.1	-0.51	0.6	-0.26	0.31	-0.25	-0.26	-0.01	0.01	0.67	0.47	-0.12	-0.12	-0.1
turb												0.03	-0.09	-0.21	-0.35	0.1	0.13	0.46	-0.41	-0.13	0.03	-0.18	0.24	0.07	-0.51	-0.48	-0.34
upwelling													-0.33	0.15	0.07	0.28	-0.04	0.05	-0.04	-0.1	0.01	0.09	0.29	0.25	0.03	0.05	0
vort														0.04	0.03	-0.03	-0.34	0.08	-0.09	-0.25	0.01	-0.09	0	-0.02	0.22	0.19	0.24
wateru															0.57	0.14	-0.33	-0.09	0.03	-0.07	0.04	0.12	0.14	0.11	0.22	0.23	0.05
waterv																-0.28	-0.22	-0.2	0.11	0.03	0	0.11	-0.31	-0.23	0.24	0.23	0.11
windstrx																	0.01	-0.01	0.05	-0.1	0.02	0.09	0.94	0.91	0.04	0.09	-0.01
windstry																		-0.45	0.42	0.67	-0.05	0.04	-0.07	0.23	-0.2	-0.11	-0.13
depth																			-0.9	-0.76	0.07	-0.29	0.21	-0.26	-0.24	-0.29	-0.08
dland																				0.76	-0.02	0.15	-0.18	0.3	0.16	0.2	0.07
dshelf																					-0.06	0.16	-0.25	0.14	-0.14	-0.05	-0.21
plcurv10km																						-0.21	0.03	0.03	0.02	0.01	0
prcurv10km																							0.05	0.12	0.16	0.18	0.09
prlat																								0.84	-0.03	0.03	-0.04
prlon																									0.03	0.11	-0.01
slp10km																										0.88	0.74
slp1500m																											0.63
slpslp10km																											

Table 4d. Predictor correlation table (winter). Predictor correlation table (fall). Pairwise Spearman rank correlation coefficients for spatial predictor variables. High correlations are highlighted (|tau|>0.7 in yellow, |tau|>0.8 in orange, |tau|>0.9 in red).

	chla	diverg	divw	peddacyc	peddcyc	sshmean	sshsd	sstfront	sstmean	sstsd	turb	upwelling	vort	wateru	waterv	windstrx	windstry	depth	dland	dshelf	plcurv10km	prcurv10km	prlat	prlon	slp10km	slp1500m	slpslp10km
chla		0.22	0.36	-0.5	-0.63	-0.74	-0.43	0.4	-0.79	0.74	0.71	0.38	0.09	-0.16	-0.35	0.22	-0.69	0.75	-0.68	-0.62	0.04	-0.12	0.7	0.3	-0.23	-0.24	-0.16
diverg			0.1	-0.02	-0.07	-0.21	0	0.07	-0.15	0.22	0.18	0.22	0.05	0.07	0.11	0.06	-0.19	0.14	-0.13	-0.11	0.02	0.03	0.17	0.12	-0.04	-0.06	0
divw				-0.09	-0.13	-0.43	-0.19	0.33	-0.31	0.39	0.19	0.05	0.22	-0.16	-0.24	-0.06	-0.2	0.29	-0.22	-0.22	0	-0.05	0.12	-0.03	-0.06	-0.11	-0.04
peddacyc					0.29	0.2	0.5	-0.14	0.28	-0.07	-0.27	-0.05	-0.06	0.24	0.26	0.19	0.12	-0.62	0.58	0.48	-0.05	0.24	-0.18	0.13	0.24	0.25	0.08
peddcyc						0.59	0.64	-0.26	0.5	-0.39	-0.36	-0.41	0.16	0.11	0.19	-0.1	0.52	-0.57	0.55	0.59	0	0.04	-0.51	-0.21	0.07	0.09	0.01
sshmean							0.47	-0.51	0.66	-0.71	-0.39	-0.37	-0.32	0.19	0.31	-0.2	0.77	-0.57	0.5	0.64	-0.03	0.03	-0.61	-0.3	-0.06	-0.04	-0.12
sshsd								-0.15	0.34	-0.04	-0.09	-0.17	0.05	0.46	0.3	0.37	0.15	-0.68	0.66	0.65	0	0.14	-0.18	0.11	0.16	0.2	-0.04
sstfront									-0.04	0.48	0.07	0.21	0.35	0.14	0.15	-0.05	-0.44	0.43	-0.43	-0.58	0.02	-0.1	0.07	-0.2	0.32	0.21	0.22
sstmean										-0.71	-0.7	-0.28	-0.03	0.34	0.63	-0.48	0.64	-0.35	0.3	0.25	-0.02	0.01	-0.89	-0.69	0.23	0.18	0.17
sstsd											0.58	0.4	0.22	0.02	-0.25	0.54	-0.77	0.29	-0.23	-0.37	0.03	0.05	0.73	0.53	0.09	0.08	0
turb												0.22	-0.06	-0.09	-0.38	0.45	-0.47	0.32	-0.21	-0.13	0.06	-0.08	0.64	0.5	-0.28	-0.25	-0.24
upwelling													-0.11	0.1	0.07	0.27	-0.45	0.26	-0.22	-0.35	0.02	0.07	0.41	0.27	0.07	0.06	0.06
vort														0.02	0.05	-0.03	-0.25	0.06	-0.08	-0.25	0.01	-0.06	-0.02	-0.04	0.26	0.24	0.26
wateru															0.66	0.17	-0.08	-0.24	0.18	0.14	0.01	0.12	-0.1	-0.04	0.18	0.19	0.01
waterv																-0.2	0.16	-0.14	0.06	0.04	-0.01	0.09	-0.44	-0.37	0.18	0.16	0.05
windstrx																	-0.58	-0.37	0.42	0.15	0.04	0.14	0.71	0.84	0.19	0.24	0.05
windstry																		-0.32	0.32	0.51	-0.05	-0.04	-0.76	-0.53	-0.17	-0.18	-0.12
depth																			-0.9	-0.76	0.07	-0.29	0.21	-0.26	-0.24	-0.29	-0.08
dland																				0.76	-0.02	0.15	-0.18	0.3	0.16	0.2	0.07
dshelf																					-0.06	0.16	-0.25	0.14	-0.14	-0.05	-0.21
plcurv10km																						-0.21	0.03	0.03	0.02	0.01	0
prcurv10km																							0.05	0.12	0.16	0.18	0.09
prlat																								0.84	-0.03	0.03	-0.04
prlon																									0.03	0.11	-0.01
slp10km																										0.88	0.74
slp1500m																											0.63
slpslp10km																											

Table 5. Base-learners employed in the boosted generalized additive modelling framework. Base-learner names are from the 'mboost' package for R (Hothorn et al. 2014; R Core Team. 2014), and predictor variable names are defined in Table 3.

Name	Description	Predictor variables	Model component
bols	linear	intercept	np, mu, th
bols	linear	boatplane	np, mu, th
brandom	random effect	sid	th
brandom	random effect	tid	np, mu
bbs	penalized regression spline[1]	yearscaled	np, mu
bbs	penalized regression spline[1]	jday	np, mu
btree	tree[2]	all climate indexes (current and lagged)	np, mu
bspatial	penalized tensor product[1]	prlon prlat	np, mu
brad	penalized radial basis[3]	prlon prlat	np, mu
btree	tree[4]	dland dshelf all terrain, physical oceanographic and atmospheric, and biological variables	np, mu

[1] P-spline basis

[2] Maximum depth = 1

[3] Matern correlation function

[4] Maximum depth = 5

Table 6. Model performance metrics. In this report performance metrics are presented for cross-validation tuning of the number of boosting iterations and for the final fitted models. The former set of performance metrics are indicated with the suffix '_CV' elsewhere in the report. Sometimes the suffix '_rel' is used to indicate that the performance metric is expressed relative to the mean of the data.

Name	Description
loglikelihood	log-likelihood
risk	negative log-likelihood
RMSE	root mean square error of residual errors
rankR_nz	Spearman's rank correlation coefficient[1]
rankRG_nz	Gaussian rank correlation coefficient[1,2]
MeanAE_nz	mean absolute residual error[1]
MedianAE_nz	median absolute residual error[1]
MeanBias_nz	mean residual error[1]
MedianBias_nz	median residual error[1]
AUC	area under the receiver operating characteristic (ROC) curve[3]
AUC_nz	area under the receiver operating characteristic (ROC) curve[1,4]
Brier[5]	multinomial Brier score
CRPS_Zinf[6]	thresholded continuous rank probability score[7]
CRPS_0	Brier score[8]
CRPS_nz_Q05	Brier score[1,8]
CRPS_ nz_Q25	Brier score[1,8]
CRPS_ nz_Q50	Brier score[1,8]
CRPS_ nz_Q75	Brier score[1,8]
CRPS_ nz_Q95	Brier score[1,8]
PDE[9]	percent deviance explained

[1] Non-zero observed values and corresponding fitted values

[2] Boudt et al. (2012) and Bodenhofer et al. (2013)

[3] Classification as 0/>0

[4] Classification above/below median non-zero observed value

[5] This performance metric should be interpreted with caution because the categories are ordinal, so the standard Brier score is not appropriate

[6] Also simply referred to as 'CRPS'

[7] Classification thresholds at 150 equally spaced quantiles of the observed values

[8] Classification as 0/>0 or indicated quantile of non-zero data (e.g., Q05 classified above/below 5th quantile of non-zero observed values)

[9] To calculate percent deviance explained, the saturated likelihood was assumed to be the maximum possible likelihood value, and the null likelihood was calculated from an intercepts-only zero-inflated model fit to the data (unpublished)

Table 7. Models evaluated for each species/season.

Model Number	Family	Maximum Tree Depth	Start Values
7	ZIP	5	glm
8	ZINB	5	glm

Table 8. Performance metric thresholds used to define model performance categories. Performance metrics are defined in Table 6.

Performance metric	Performance category				
	1	**2**	**3**	**4**	**5**
AUC	x < 0.6	0.6 ≤ x < 0.7	0.7 ≤ x < 0.8	0.8 ≤ x < 0.9	x ≥ 0.9
RankRG_nz	x < 0.1	0.1 ≤ x < 0.2	0.2 ≤ x < 0.4	0.4 ≤ x < 0.6	x ≥ 0.6
MedianAE_nz_CV_rel	x >= 2.0	2.0 > x ≥ 1.0	1.0 > x ≥ 0.5	0.5 > x ≥ 0.25	x < 0.25
PDE	x < 0.1	0.1 ≤ x < 0.2	0.2 ≤ x < 0.4	0.4 ≤ x < 0.6	x ≥ 0.6

Table 9. Model selection table. The model selection process is illustrated for 4 example species/season combinations. Two models were evaluated for each species/season combination (Table 7). Models are sorted in descending order of performance in terms of the thresholded continuous rank probability score (CRPS) from cross-validation tuning of mstop (column marked with an * below). The selected model is in bold font, and all subsequent analyses in this report use this selected model. Other model performance metrics are also provided (see Table 6 for definitions). Note that risk is not directly comparable across model families (ZIP vs. ZINB). For similar model selection information for all species/season combinations evaluated, please see the Digital Data Package (contents listed in Appendix N).

Species code	Season	Mod #[a]	Model Family	Max. depth	Start values	m (iterations)	PDE	AUC (occupancy)	AUC (nz)	Rank R (nz)	Rank RG (nz)	Median AE (nz)		Median bias (nz)		Brier (occup.)		CRPS		Log-likelihood	Risk (CV)
												Fit	CV	Fit	CV	Fit	CV	Fit	CV*		
cote	summer	**7**	**ZIP**	**5**	**glm**	**6996**	**0.44**	**0.93**	**0.62**	**0.26**	**0.3**	**0.27**	**0.29**	**-0.2**	**-0.21**	**0.031**	**0.034**	**0.03**	**0.033**	**-9439**	**2757**
		8	ZINB	5	glm	6999	0.43	0.93	0.63	0.28	0.32	0.27	0.3	-0.2	-0.21	0.031	0.034	0.03	0.033	-6799	-973
noga	fall	**7**	**ZIP**	**5**	**glm**	**7901**	**0.52**	**0.91**	**0.72**	**0.48**	**0.52**	**0.21**	**0.22**	**-0.14**	**-0.14**	**0.082**	**0.088**	**0.075**	**0.08**	**-20417**	**5380**
		8	ZINB	5	glm	7999	0.53	0.91	0.74	0.53	0.55	0.2	0.23	-0.15	-0.16	0.084	0.089	0.076	0.081	-14239	-5690
razo	winter	**7**	**ZIP**	**5**	**glm**	**8000**	**0.44**	**0.93**	**0.72**	**0.45**	**0.47**	**0.29**	**0.31**	**-0.24**	**-0.24**	**0.038**	**0.038**	**0.037**	**0.037**	**-11365**	**3049**
		8	ZINB	5	glm	8000	0.38	0.93	0.71	0.44	0.46	0.26	0.25	-0.22	-0.23	0.038	0.039	0.037	0.038	-7816	-3389
wwsc	winter	**8**	**ZINB**	**5**	**glm**	**8000**	**0.5**	**0.95**	**0.63**	**0.29**	**0.29**	**0.2**	**0.18**	**-0.01**	**-0.03**	**0.027**	**0.028**	**0.027**	**0.028**	**-6766**	**-22354**
		7	ZIP	5	glm	5933	0.59	0.95	0.68	0.39	0.40	0.15	0.14	-0.06	-0.08	0.028	0.03	0.027	0.029	-17676	4957

[a] Model number as in Table 7.

Table 10. Final selected models for all species/season combination evaluated, with number of transect segments with sightings, number of individuals sighted, proportion of transect segments with sightings (prevalence), and mean number of individuals per transect segment with sightings. Numbers of sightings and individuals exclude incomplete records (missing predictor data) that were excluded from the analysis, and therefore may differ from Tables 1 and 2.

Species	Season	No. sightings	No. individuals	Prevalence	Mean non-zero count	Model Family	Max. depth	Start values	m (boosting iterations)
arte	summer	154	507	0.005	3.3	ZIP	5	glm	5623
atpu	spring	209	472	0.009	2.3	ZIP	5	glm	8000
atpu	summer	245	528	0.007	2.2	ZINB	5	glm	8000
atpu	fall	91	129	0.004	1.4	ZIP	5	glm	8000
atpu	winter	248	444	0.008	1.8	ZINB	5	glm	6999
aush	spring	129	443	0.006	3.4	ZINB	5	glm	6994
aush	summer	876	2664	0.026	3	ZINB	5	glm	6999
aush	fall	286	965	0.012	3.4	ZINB	5	glm	5765
aush	winter	163	330	0.006	2	ZINB	5	glm	5548
bcpe	spring	158	314	0.007	2	ZINB	5	glm	5999
bcpe	summer	356	987	0.01	2.8	ZINB	5	glm	5397
bcpe	fall	92	243	0.004	2.6	ZINB	5	glm	5967
bcpe	winter	83	212	0.003	2.6	ZINB	5	glm	5999
blgu	summer	87	159	0.003	1.8	ZINB	5	glm	8000
blki	spring	621	3149	0.028	5.1	ZIP	5	glm	5677
blki	fall	2080	14453	0.084	6.9	ZIP	5	glm	4184
blki	winter	3684	32431	0.126	8.8	ZINB	5	glm	6999
blsc	spring	406	9549	0.018	23.5	ZINB	5	glm	8000
blsc	fall	346	8605	0.014	24.9	ZINB	5	glm	8000
blsc	winter	1091	55798	0.037	51.1	ZINB	5	glm	8000
bogu	spring	394	5425	0.018	13.8	ZINB	5	glm	8000
bogu	fall	269	1963	0.011	7.3	ZINB	5	glm	6998
bogu	winter	959	9163	0.033	9.6	ZIP	5	glm	5998
brpe	spring	62	290	0.003	4.7	ZINB	5	glm	7999
brpe	summer	114	413	0.003	3.6	ZIP	5	glm	5959
brpe	fall	80	268	0.003	3.4	ZIP	5	glm	5287
brpe	winter	65	291	0.002	4.5	ZINB	5	glm	8000
brsp	summer	266	552	0.008	2.1	ZINB	5	glm	7999
coei	winter	2031	553969	0.069	272.8	ZINB	5	glm	8000
colo	spring	2306	5943	0.105	2.6	ZINB	5	glm	8000
colo	summer	178	239	0.005	1.3	ZINB	5	glm	6851
colo	fall	1158	2715	0.047	2.3	ZIP	5	glm	8000
colo	winter	3044	8213	0.104	2.7	ZINB	5	glm	7999
comu	spring	90	252	0.004	2.8	ZIP	5	glm	6902
comu	winter	158	499	0.005	3.2	ZIP	5	glm	8000

cosh	spring	106	235	0.005	2.2	ZINB	5	glm	6999
cosh	summer	2924	13128	0.086	4.5	ZINB	5	glm	8000
cosh	fall	1546	7574	0.063	4.9	ZINB	5	glm	8000
cote	spring	467	2182	0.021	4.7	ZINB	5	glm	8000
cote	summer	1470	6958	0.043	4.7	ZIP	5	glm	6996
cote	fall	663	6509	0.027	9.8	ZINB	5	glm	8000
dcco	spring	114	1232	0.005	10.8	ZIP	5	glm	5896
dcco	summer	168	848	0.005	5	ZIP	5	glm	6999
dcco	fall	196	4600	0.008	23.5	ZIP	5	glm	4735
dcco	winter	138	1933	0.005	14	ZINB	5	glm	8000
dove	spring	259	1919	0.012	7.4	ZINB	5	glm	5902
dove	fall	404	3927	0.016	9.7	ZINB	5	glm	6999
dove	winter	959	7630	0.033	8	ZINB	5	glm	6999
gbbg	spring	3375	26602	0.153	7.9	ZIP	5	glm	5893
gbbg	summer	3138	11222	0.093	3.6	ZINB	5	glm	6998
gbbg	fall	5333	35763	0.216	6.7	ZINB	5	glm	5992
gbbg	winter	3578	31540	0.122	8.8	ZINB	5	glm	6999
grsh	spring	585	5121	0.027	8.8	ZINB	5	glm	7998
grsh	summer	6001	178900	0.177	29.8	ZINB	5	glm	8000
grsh	fall	6175	93255	0.25	15.1	ZINB	5	glm	6998
grsh	winter	133	580	0.005	4.4	ZINB	5	glm	5861
herg	spring	5644	53900	0.256	9.5	ZINB	5	glm	5999
herg	summer	2880	10669	0.085	3.7	ZINB	5	glm	6998
herg	fall	7359	59576	0.298	8.1	ZINB	5	glm	5942
herg	winter	4805	30569	0.164	6.4	ZINB	5	glm	8000
hogr	winter	82	142	0.003	1.7	ZIP	5	glm	8000
lagu	spring	673	1642	0.031	2.4	ZIP	5	glm	8000
lagu	summer	1562	5230	0.046	3.3	ZINB	5	glm	7999
lagu	fall	1512	8343	0.061	5.5	ZINB	5	glm	6978
lagu	winter	110	324	0.004	2.9	ZIP	5	glm	7877
lesp	spring	223	780	0.01	3.5	ZINB	5	glm	8000
lesp	summer	2138	9504	0.063	4.4	ZINB	5	glm	8000
lesp	fall	452	1317	0.018	2.9	ZINB	5	glm	7999
lete	summer	113	414	0.003	3.7	ZIP	5	glm	5890
ltdu	spring	1121	81577	0.051	72.8	ZINB	5	glm	5656
ltdu	fall	473	18625	0.019	39.4	ZINB	5	glm	8000
ltdu	winter	3046	139620	0.104	45.8	ZINB	5	glm	8000
mash	spring	100	152	0.005	1.5	ZIP	5	glm	5987
mash	summer	308	878	0.009	2.9	ZINB	5	glm	8000
mash	fall	264	452	0.011	1.7	ZINB	5	glm	8000
nofu	spring	2244	30593	0.102	13.6	ZINB	5	glm	6964

nofu	summer	737	12835	0.022	17.4	ZINB	5	glm	5999
nofu	fall	1823	10055	0.074	5.5	ZINB	5	glm	5997
nofu	winter	1809	24327	0.062	13.4	ZIP	5	glm	5999
noga	spring	5585	37629	0.253	6.7	ZINB	5	glm	8000
noga	summer	1162	2412	0.034	2.1	ZINB	5	glm	8000
noga	fall	3961	19213	0.16	4.9	ZIP	5	glm	7901
noga	winter	6298	45486	0.215	7.2	ZIP	5	glm	7999
poja	spring	110	142	0.005	1.3	ZIP	5	glm	8000
poja	summer	144	173	0.004	1.2	ZINB	5	glm	8000
poja	fall	709	999	0.029	1.4	ZINB	5	glm	8000
razo	spring	712	4373	0.032	6.1	ZINB	5	glm	8000
razo	summer	78	217	0.002	2.8	ZINB	5	glm	8000
razo	fall	169	1246	0.007	7.4	ZINB	5	glm	6998
razo	winter	1535	11661	0.052	7.6	ZIP	5	glm	8000
rbgu	spring	172	412	0.008	2.4	ZINB	5	glm	8000
rbgu	fall	285	998	0.012	3.5	ZINB	5	glm	8000
rbgu	winter	642	2647	0.022	4.1	ZINB	5	glm	6998
reph	spring	461	85772	0.021	186.1	ZINB	5	glm	8000
reph	summer	214	26267	0.006	122.7	ZINB	5	glm	6999
rnph	summer	167	2272	0.005	13.6	ZINB	5	glm	8000
rnph	fall	156	1105	0.006	7.1	ZIP	5	glm	6999
rost	spring	53	195	0.002	3.7	ZIP	5	glm	8000
rost	summer	176	738	0.005	4.2	ZINB	5	glm	7990
rost	fall	73	467	0.003	6.4	ZINB	5	glm	8000
royt	spring	262	732	0.012	2.8	ZINB	5	glm	5513
royt	summer	272	629	0.008	2.3	ZINB	5	glm	8000
royt	fall	259	624	0.01	2.4	ZINB	5	glm	6993
rtlo	spring	1644	4927	0.075	3	ZINB	5	glm	6992
rtlo	fall	360	1363	0.015	3.8	ZINB	5	glm	8000
rtlo	winter	1802	5583	0.061	3.1	ZINB	5	glm	8000
sosh	spring	788	5925	0.036	7.5	ZIP	5	glm	3901
sosh	summer	1540	35148	0.045	22.8	ZINB	5	glm	5883
sosh	fall	104	284	0.004	2.7	ZINB	5	glm	6632
susc	spring	718	14302	0.033	19.9	ZINB	5	glm	8000
susc	fall	748	28091	0.03	37.6	ZINB	5	glm	5999
susc	winter	1664	48178	0.057	29	ZINB	5	glm	7999
wisp	spring	1650	14890	0.075	9	ZINB	5	glm	7999
wisp	summer	8383	96536	0.247	11.5	ZINB	5	glm	5998
wisp	fall	1348	7214	0.055	5.4	ZINB	5	glm	8000
wwsc	spring	400	4889	0.018	12.2	ZINB	5	glm	8000
wwsc	fall	533	9954	0.022	18.7	ZINB	5	glm	8000

wwsc	winter	1270	20061	0.043	15.8	ZINB	5	glm	8000

Table 11. Best models with model performance metrics. All model performance metrics were calculated on the full dataset, except for columns divided into 'Fit' and 'CV', which denote metrics calculated separately for the full dataset and for out-of-bag data during cross-validation tuning of mstop, respectively. The overall model performance category is the rounded average of performance categories across four performance metrics (PDE, AUC, Rank RG_nz, and MedianAE_nz_CV_rel; see Section 2.4.6). Particularly poor performance in terms of individual performance metrics is indicated in red.

Species code	Season	Model Family	Max. depth	Start values	PDE	AUC	AUC _nz	RankR _nz	RankRG _nz	MedianAE_nz_rel		MedianBias_nz_rel		CRPS_0		CRPS_Zinf			**Overall model performance category**	**Model quality (expert opinion)**
										Fit	CV	Fit	CV	Fit	CV	Fit	CV			
arte	summer	ZIP	5	glm	0.11	0.94	0.74	0.44	0.41	0.36	0.41	-0.32	-0.37	0.000	0.000	0.000	0.000		**4**	**FAIR**
atpu	spring	ZIP	5	glm	0.34	0.93	0.71	0.41	0.4	0.44	0.44	-0.44	-0.44	0.010	0.010	0.010	0.010		**4**	**GOOD**
atpu	summer	ZINB	5	glm	0.53	0.98	0.7	0.41	0.47	0.44	0.46	-0.44	-0.46	0.010	0.010	0.010	0.010		**4**	**GOOD**
atpu	fall	ZIP	5	glm	0.4	0.96	0.7	0.32	0.37	0.69	0.7	-0.69	-0.7	0.000	0.000	0.000	0.000		**4**	**FAIR**
atpu	winter	ZINB	5	glm	0.4	0.95	0.58	0.17	0.22	0.55	0.55	-0.55	-0.55	0.010	0.010	0.010	0.010		**4**	**FAIR**
aush	spring	ZINB	5	glm	0.41	0.99	0.7	0.44	0.49	0.43	0.38	-0.16	-0.26	0.000	0.000	0.000	0.000		**4**	**FAIR**
aush	summer	ZINB	5	glm	0.51	0.95	0.73	0.44	0.46	0.32	0.32	-0.3	-0.31	0.020	0.020	0.020	0.020		**4**	**GOOD**
aush	fall	ZINB	5	glm	0.53	0.95	0.76	0.52	0.54	0.29	0.3	-0.29	-0.29	0.010	0.010	0.010	0.010		**4**	**FAIR**
aush	winter	ZINB	5	glm	0.76	1	0.84	0.61	0.63	0.38	0.48	-0.32	-0.45	0.000	0.000	0.000	0.000		**5**	**FAIR**
bcpe	spring	ZINB	5	glm	0.54	0.99	0.79	0.51	0.49	0.5	0.5	-0.32	-0.48	0.000	0.000	0.000	0.000		**4**	**GOOD**
bcpe	summer	ZINB	5	glm	0.63	0.98	0.78	0.53	0.54	0.34	0.35	-0.32	-0.35	0.010	0.010	0.010	0.010		**5**	**GOOD**
bcpe	fall	ZINB	5	glm	0.33	1	0.82	0.59	0.59	0.36	0.38	-0.17	-0.38	0.000	0.000	0.000	0.000		**4**	**GOOD**
bcpe	winter	ZINB	5	glm	0.28	1	0.95	0.84	0.81	0.39	0.66	-0.28	-0.39	0.000	0.000	0.000	0.000		**4**	**GOOD**
blgu	summer	ZINB	5	glm	0.33	0.99	0.58	-0.17	-0.17	1.7E+9	9.9E+8	1.7E+9	9.9E+8	0.000	0.000	0.000	0.000		**3**	**FAIR**
blki	spring	ZIP	5	glm	0.45	0.93	0.59	0.18	0.22	0.19	0.2	-0.19	-0.19	0.020	0.020	0.020	0.020		**4**	**FAIR**
blki	fall	ZIP	5	glm	0.58	0.94	0.69	0.38	0.4	0.18	0.19	-0.09	-0.1	0.050	0.050	0.040	0.050		**5**	**GOOD**
blki	winter	ZINB	5	glm	0.57	0.95	0.75	0.51	0.53	0.18	0.18	-0.06	-0.07	0.060	0.060	0.050	0.050		**5**	**GOOD**
blsc	spring	ZINB	5	glm	0.43	0.94	0.61	0.3	0.33	0.18	0.17	-0.11	-0.12	0.010	0.020	0.010	0.020		**4**	**FAIR**
blsc	fall	ZINB	5	glm	0.47	0.96	0.55	0.18	0.21	0.23	0.26	-0.09	-0.13	0.010	0.010	0.010	0.010		**4**	**FAIR**
blsc	winter	ZINB	5	glm	0.38	0.91	0.64	0.26	0.28	0.11	0.1	-0.05	-0.06	0.030	0.030	0.030	0.030		**4**	**FAIR**

bogu	spring	ZINB	5	glm	0.27	0.9	0.54	0.08	0.11	0.12	0.13	-0.11	-0.13	0.020	0.020	0.020	0.020		**4**	**POOR**
bogu	fall	ZINB	5	glm	0.4	0.92	0.67	0.34	0.39	0.25	0.26	-0.22	-0.24	0.010	0.010	0.010	0.010		**4**	**POOR**
bogu	winter	ZIP	5	glm	0.44	0.87	0.68	0.39	0.43	0.18	0.18	-0.13	-0.14	0.030	0.030	0.030	0.030		**4**	**FAIR**
brpe	spring	ZINB	5	glm	0	0.98	0.66	0.13	0.15	0.24	0.43	-0.21	-0.37	0.000	0.000	0.000	0.000		**3**	**FAIR**
brpe	summer	ZIP	5	glm	0	0.92	0.58	0.23	0.31	0.28	0.28	-0.28	-0.28	0.000	0.000	0.000	0.000		**3**	**POOR**
brpe	fall	ZIP	5	glm	0.48	0.99	0.65	0.29	0.3	0.3	0.33	-0.29	-0.3	0.000	0.000	0.000	0.000		**4**	**GOOD**
brpe	winter	ZINB	5	glm	0	0.93	0.65	0.35	0.35	0.45	0.34	-0.45	-0.34	0.000	0.000	0.000	0.000		**3**	**POOR**
brsp	summer	ZINB	5	glm	0.52	0.96	0.7	0.39	0.46	0.46	0.47	-0.46	-0.47	0.010	0.010	0.010	0.010		**4**	**GOOD**
coei	winter	ZINB	5	glm	0.55	0.97	0.55	0.1	0.1	0.33	0.35	0.24	0.27	0.030	0.040	0.030	0.030		**4**	**FAIR**
colo	spring	ZINB	5	glm	0.42	0.9	0.7	0.4	0.41	0.35	0.36	-0.32	-0.34	0.060	0.070	0.060	0.070		**4**	**FAIR**
colo	summer	ZINB	5	glm	0.36	0.95	0.63	0.21	0.25	0.73	0.73	-0.73	-0.73	0.000	0.000	0.000	0.000		**4**	**FAIR**
colo	fall	ZIP	5	glm	0.41	0.94	0.68	0.33	0.33	0.4	0.41	-0.37	-0.39	0.030	0.030	0.030	0.030		**4**	**FAIR**
colo	winter	ZINB	5	glm	0.36	0.83	0.65	0.29	0.31	0.32	0.33	-0.32	-0.32	0.080	0.080	0.070	0.070		**4**	**FAIR**
comu	spring	ZIP	5	glm	0.24	0.95	0.69	0.4	0.46	0.48	0.36	-0.48	-0.36	0.000	0.010	0.000	0.010		**4**	**FAIR**
comu	winter	ZIP	5	glm	0.34	0.96	0.74	0.52	0.53	0.5	0.61	-0.45	-0.61	0.000	0.010	0.000	0.010		**4**	**FAIR**
cosh	spring	ZINB	5	glm	0.48	0.98	0.66	0.27	0.27	0.43	0.44	-0.43	-0.44	0.000	0.000	0.000	0.000		**4**	**GOOD**
cosh	summer	ZINB	5	glm	0.33	0.87	0.66	0.33	0.34	0.2	0.21	-0.18	-0.19	0.060	0.070	0.060	0.070		**4**	**GOOD**
cosh	fall	ZINB	5	glm	0.46	0.91	0.72	0.46	0.48	0.22	0.23	-0.19	-0.19	0.040	0.050	0.040	0.040		**5**	**GOOD**
cote	spring	ZINB	5	glm	0.53	0.97	0.6	0.23	0.24	0.34	0.38	-0.29	-0.35	0.010	0.010	0.010	0.010		**4**	**GOOD**
cote	summer	ZIP	5	glm	0.44	0.93	0.62	0.26	0.3	0.27	0.29	-0.2	-0.21	0.030	0.030	0.030	0.030		**4**	**FAIR**
cote	fall	ZINB	5	glm	0.44	0.93	0.66	0.38	0.39	0.24	0.21	-0.15	-0.18	0.020	0.020	0.020	0.020		**4**	**FAIR**
dcco	spring	ZIP	5	glm	0.26	0.93	0.55	0.08	0.11	0.17	0.24	-0.15	-0.22	0.000	0.010	0.000	0.010		**4**	**POOR**
dcco	summer	ZIP	5	glm	0.06	0.92	0.56	0.18	0.24	0.2	0.2	-0.2	-0.2	0.000	0.010	0.000	0.010		**4**	**FAIR**
dcco	fall	ZIP	5	glm	0.42	0.88	0.63	0.27	0.3	0.08	0.08	-0.04	-0.06	0.010	0.010	0.010	0.010		**4**	**POOR**
dcco	winter	ZINB	5	glm	0.34	0.92	0.72	0.47	0.52	0.13	0.09	-0.07	-0.07	0.000	0.000	0.000	0.000		**4**	**FAIR**
dove	spring	ZINB	5	glm	0.41	0.93	0.75	0.56	0.58	0.26	0.27	-0.26	-0.26	0.010	0.010	0.010	0.010		**4**	**GOOD**
dove	fall	ZINB	5	glm	0.62	0.99	0.71	0.46	0.47	0.28	0.28	-0.1	-0.13	0.010	0.010	0.010	0.010		**5**	**GOOD**
dove	winter	ZINB	5	glm	0.49	0.93	0.68	0.45	0.49	0.22	0.23	-0.14	-0.17	0.020	0.020	0.020	0.020		**5**	**GOOD**

gbbg	spring	ZIP	5	glm	0.6	0.87	0.69	0.41	0.44	0.17	0.17	-0.09	-0.09	0.090	0.100	0.090	0.090		**5**	**GOOD**
gbbg	summer	ZINB	5	glm	0.47	0.91	0.67	0.34	0.35	0.26	0.26	-0.21	-0.21	0.060	0.070	0.060	0.060		**4**	**GOOD**
gbbg	fall	ZINB	5	glm	0.37	0.84	0.67	0.36	0.38	0.2	0.2	-0.07	-0.08	0.130	0.130	0.110	0.120		**4**	**GOOD**
gbbg	winter	ZINB	5	glm	0.53	0.9	0.73	0.45	0.48	0.13	0.13	-0.07	-0.07	0.070	0.070	0.070	0.070		**5**	**FAIR**
grsh	spring	ZINB	5	glm	0.72	0.98	0.78	0.59	0.62	0.19	0.21	-0.08	-0.09	0.010	0.010	0.010	0.010		**5**	**FAIR**
grsh	summer	ZINB	5	glm	0.56	0.92	0.72	0.44	0.45	0.1	0.09	0.01	0	0.080	0.090	0.080	0.080		**5**	**GOOD**
grsh	fall	ZINB	5	glm	0.59	0.95	0.72	0.47	0.48	0.26	0.26	0.05	0.04	0.080	0.080	0.080	0.080		**4**	**GOOD**
grsh	winter	ZINB	5	glm	0.71	0.98	0.85	0.65	0.66	0.23	0.23	-0.23	-0.23	0.000	0.000	0.000	0.000		**5**	**FAIR**
herg	spring	ZINB	5	glm	0.41	0.84	0.71	0.47	0.49	0.18	0.18	-0.05	-0.06	0.130	0.140	0.120	0.120		**4**	**FAIR**
herg	summer	ZINB	5	glm	0.48	0.91	0.68	0.37	0.39	0.25	0.25	-0.21	-0.2	0.060	0.060	0.050	0.060		**4**	**FAIR**
herg	fall	ZINB	5	glm	0.38	0.84	0.67	0.39	0.41	0.21	0.21	-0.03	-0.03	0.150	0.150	0.130	0.130		**4**	**GOOD**
herg	winter	ZINB	5	glm	0.43	0.87	0.69	0.41	0.44	0.17	0.16	-0.1	-0.1	0.100	0.100	0.090	0.090		**4**	**FAIR**
hogr	winter	ZIP	5	glm	0.24	0.95	0.71	0.32	0.33	0.57	0.58	-0.57	-0.58	0.000	0.000	0.000	0.000		**4**	**POOR**
lagu	spring	ZIP	5	glm	0.47	0.94	0.67	0.32	0.36	0.38	0.39	-0.38	-0.39	0.020	0.020	0.020	0.020		**4**	**FAIR**
lagu	summer	ZINB	5	glm	0.53	0.95	0.72	0.44	0.47	0.29	0.29	-0.27	-0.28	0.030	0.030	0.030	0.030		**4**	**FAIR**
lagu	fall	ZINB	5	glm	0.52	0.94	0.68	0.42	0.45	0.25	0.27	-0.16	-0.17	0.040	0.040	0.040	0.040		**4**	**GOOD**
lagu	winter	ZIP	5	glm	0.42	0.98	0.74	0.51	0.54	0.34	0.37	-0.34	-0.34	0.000	0.000	0.000	0.000		**4**	**FAIR**
lesp	spring	ZINB	5	glm	0.53	0.97	0.69	0.34	0.37	0.28	0.28	-0.27	-0.28	0.010	0.010	0.010	0.010		**4**	**GOOD**
lesp	summer	ZINB	5	glm	0.54	0.94	0.7	0.43	0.47	0.26	0.28	-0.2	-0.21	0.040	0.040	0.040	0.040		**4**	**GOOD**
lesp	fall	ZINB	5	glm	0.59	0.97	0.72	0.45	0.47	0.33	0.34	-0.31	-0.33	0.010	0.010	0.010	0.010		**4**	**GOOD**
lete	summer	ZIP	5	glm	0.03	0.91	0.62	0.29	0.36	0.27	0.27	-0.27	-0.27	0.000	0.000	0.000	0.000		**3**	**FAIR**
ltdu	spring	ZINB	5	glm	0.64	0.98	0.75	0.55	0.55	0.13	0.14	0.03	0.03	0.020	0.020	0.020	0.020		**5**	**GOOD**
ltdu	fall	ZINB	5	glm	0.72	0.99	0.81	0.62	0.62	0.16	0.15	0.01	0	0.010	0.010	0.010	0.010		**5**	**GOOD**
ltdu	winter	ZINB	5	glm	0.6	0.97	0.73	0.47	0.48	0.23	0.23	0.1	0.08	0.040	0.040	0.040	0.040		**5**	**GOOD**

mash	spring	ZIP	5	glm	0.2	0.89	0.6	0.16	0.25	0.65	0.65	-0.65	-0.65	0.000	0.000	0.000	0.000		**3**	**GOOD**
mash	summer	ZINB	5	glm	0.25	0.83	0.68	0.29	0.33	0.34	0.34	-0.34	-0.34	0.010	0.010	0.010	0.010		**4**	**FAIR**
mash	fall	ZINB	5	glm	0.31	0.9	0.74	0.38	0.41	0.57	0.57	-0.57	-0.57	0.010	0.010	0.010	0.010		**4**	**GOOD**
nofu	spring	ZINB	5	glm	0.62	0.96	0.76	0.57	0.58	0.14	0.14	-0.03	-0.04	0.050	0.050	0.040	0.050		**5**	**GOOD**
nofu	summer	ZINB	5	glm	0.7	0.98	0.72	0.48	0.52	0.07	0.07	-0.04	-0.05	0.010	0.010	0.010	0.010		**5**	**GOOD**
nofu	fall	ZINB	5	glm	0.61	0.95	0.77	0.58	0.59	0.19	0.19	-0.15	-0.15	0.040	0.040	0.040	0.040		**5**	**GOOD**
nofu	winter	ZIP	5	glm	0.62	0.98	0.73	0.49	0.52	0.18	0.17	-0.03	-0.05	0.020	0.020	0.020	0.020		**5**	**GOOD**
noga	spring	ZINB	5	glm	0.39	0.85	0.7	0.44	0.46	0.2	0.19	-0.07	-0.08	0.140	0.150	0.120	0.130		**4**	**GOOD**
noga	summer	ZINB	5	glm	0.47	0.93	0.72	0.41	0.45	0.43	0.45	-0.42	-0.44	0.030	0.030	0.020	0.030		**4**	**POOR**
noga	fall	ZIP	5	glm	0.52	0.91	0.72	0.48	0.52	0.21	0.22	-0.14	-0.14	0.080	0.090	0.070	0.080		**5**	**GOOD**
noga	winter	ZIP	5	glm	0.55	0.85	0.72	0.45	0.48	0.16	0.18	-0.07	-0.07	0.120	0.130	0.110	0.110		**4**	**GOOD**
poja	spring	ZIP	5	glm	0.31	0.93	0.69	0.27	0.31	0.76	0.76	-0.76	-0.76	0.000	0.000	0.000	0.000		**4**	**FAIR**
poja	summer	ZINB	5	glm	0.12	0.83	0.63	0.17	0.2	0.83	0.83	-0.83	-0.83	0.000	0.000	0.000	0.000		**3**	**FAIR**
poja	fall	ZINB	5	glm	0.29	0.89	0.66	0.26	0.28	0.66	0.66	-0.66	-0.66	0.030	0.030	0.020	0.020		**3**	**GOOD**
razo	spring	ZINB	5	glm	0.4	0.94	0.7	0.4	0.44	0.35	0.37	-0.33	-0.32	0.020	0.030	0.020	0.030		**4**	**FAIR**
razo	summer	ZINB	5	glm	0.44	0.98	0.8	0.6	0.63	0.71	0.71	-0.6	-0.6	0.000	0.000	0.000	0.000		**4**	**GOOD**
razo	fall	ZINB	5	glm	0.51	0.97	0.74	0.54	0.57	0.26	0.24	-0.2	-0.15	0.010	0.010	0.010	0.010		**5**	**FAIR**
razo	winter	ZIP	5	glm	0.44	0.93	0.72	0.45	0.47	0.29	0.31	-0.24	-0.24	0.040	0.040	0.040	0.040		**4**	**GOOD**
rbgu	spring	ZINB	5	glm	0.31	0.91	0.67	0.3	0.32	0.41	0.41	-0.41	-0.41	0.010	0.010	0.010	0.010		**4**	**POOR**
rbgu	fall	ZINB	5	glm	0.36	0.9	0.75	0.46	0.5	0.28	0.28	-0.28	-0.28	0.010	0.010	0.010	0.010		**4**	**POOR**
rbgu	winter	ZINB	5	glm	0.28	0.86	0.61	0.2	0.23	0.24	0.24	-0.24	-0.24	0.020	0.020	0.020	0.020		**4**	**FAIR**
reph	spring	ZINB	5	glm	0.48	0.96	0.66	0.35	0.39	0.1	0.09	0	-0.01	0.010	0.020	0.010	0.010		**4**	**GOOD**
reph	summer	ZINB	5	glm	0.51	0.96	0.73	0.45	0.45	0.04	0.05	-0.01	-0.01	0.000	0.000	0.000	0.000		**5**	**GOOD**
rnph	summer	ZINB	5	glm	0.33	0.93	0.65	0.33	0.38	0.31	0.33	-0.26	-0.3	0.000	0.000	0.000	0.000		**4**	**GOOD**

rnph	fall	ZIP	5	glm	0	0.87	0.6	0.2	0.23	0.29	0.31	-0.28	-0.31	0.010	0.010	0.010	0.010		**3**	**FAIR**
rost	spring	ZIP	5	glm	0	0.97	0.56	0.08	0.13	0.31	0.52	-0.31	-0.52	0.000	0.000	0.000	0.000		**3**	**POOR**
rost	summer	ZINB	5	glm	0.45	0.96	0.58	0.25	0.31	0.48	0.48	-0.22	-0.23	0.000	0.010	0.000	0.010		**4**	**FAIR**
rost	fall	ZINB	5	glm	0.54	0.97	0.61	0.27	0.31	0.29	0.29	-0.16	-0.27	0.000	0.000	0.000	0.000		**4**	**FAIR**
royt	spring	ZINB	5	glm	0.49	0.96	0.57	0.15	0.2	0.35	0.36	-0.35	-0.35	0.010	0.010	0.010	0.010		**4**	**FAIR**
royt	summer	ZINB	5	glm	0.52	0.97	0.74	0.47	0.51	0.42	0.43	-0.42	-0.43	0.010	0.010	0.010	0.010		**4**	**GOOD**
royt	fall	ZINB	5	glm	0.44	0.96	0.68	0.39	0.4	0.41	0.41	-0.41	-0.41	0.010	0.010	0.010	0.010		**4**	**GOOD**
rtlo	spring	ZINB	5	glm	0.41	0.9	0.69	0.39	0.42	0.3	0.31	-0.29	-0.3	0.050	0.060	0.050	0.060		**4**	**FAIR**
rtlo	fall	ZINB	5	glm	0.51	0.96	0.72	0.48	0.51	0.26	0.26	-0.25	-0.26	0.010	0.010	0.010	0.010		**4**	**FAIR**
rtlo	winter	ZINB	5	glm	0.34	0.87	0.69	0.39	0.43	0.3	0.31	-0.3	-0.31	0.050	0.050	0.050	0.050		**4**	**FAIR**
sosh	spring	ZIP	5	glm	0.45	0.95	0.67	0.38	0.41	0.17	0.17	-0.11	-0.12	0.020	0.020	0.020	0.020		**5**	**GOOD**
sosh	summer	ZINB	5	glm	0.56	0.93	0.72	0.45	0.48	0.05	0.06	-0.04	-0.04	0.030	0.030	0.030	0.030		**5**	**GOOD**
sosh	fall	ZINB	5	glm	0.22	0.9	0.65	0.29	0.34	0.36	0.36	-0.36	-0.36	0.000	0.000	0.000	0.000		**4**	**GOOD**
susc	spring	ZINB	5	glm	0.54	0.97	0.62	0.24	0.27	0.22	0.23	-0.06	-0.08	0.020	0.020	0.020	0.020		**4**	**FAIR**
susc	fall	ZINB	5	glm	0.62	0.97	0.7	0.42	0.38	0.34	0.32	0.07	0.07	0.010	0.010	0.010	0.010		**4**	**FAIR**
susc	winter	ZINB	5	glm	0.6	0.97	0.73	0.44	0.45	0.28	0.3	0.02	-0.01	0.020	0.030	0.020	0.020		**5**	**FAIR**
wisp	spring	ZINB	5	glm	0.61	0.97	0.69	0.39	0.4	0.21	0.2	-0.01	-0.03	0.040	0.040	0.030	0.040		**5**	**GOOD**
wisp	summer	ZINB	5	glm	0.46	0.86	0.68	0.4	0.42	0.2	0.2	0	-0.01	0.130	0.130	0.110	0.120		**4**	**FAIR**
wisp	fall	ZINB	5	glm	0.5	0.96	0.63	0.3	0.31	0.21	0.21	-0.11	-0.13	0.030	0.040	0.030	0.030		**4**	**GOOD**
wwsc	spring	ZINB	5	glm	0.44	0.95	0.59	0.22	0.24	0.11	0.14	-0.08	-0.12	0.010	0.020	0.010	0.020		**4**	**FAIR**
wwsc	fall	ZINB	5	glm	0.54	0.97	0.74	0.51	0.54	0.21	0.2	-0.07	-0.1	0.010	0.010	0.010	0.010		**5**	**FAIR**
wwsc	winter	ZINB	5	glm	0.5	0.95	0.63	0.29	0.29	0.2	0.18	-0.01	-0.03	0.030	0.030	0.030	0.030		**4**	**FAIR**

Table 12. Groups of species with similar spatial distributions chosen for averaging[a].

Group Number	Family	Number of Species	Species in group	Types of species
1	Nearshore	15	arte, blsc, brpe, coei, colo, cote, dcco, hogr, lete, ltdu, rost, royt, rtlo, susc, wwsc	Seaducks, Loons, Terns,
2	Pelagic	18	atpu, aush, bcpe, blgu, brsp, comu, cosh, dove, grsh, lesp, mash, nofu, poja, razo, reph, rnph, sosh, wisp	Petrels, Shearwaters, Jaegers, Phalaropes, Alcids
3	Gulls and Gannets	7	blki, bogu, gbbg, herg, lagu, noga, rbgu	Small gulls, Large gulls, Gannets

[a] Note that the groups described in this table are not based on similar taxonomy or ecological traits, but rather on broad similarities in patterns of spatial distribution as reflected in species model results.

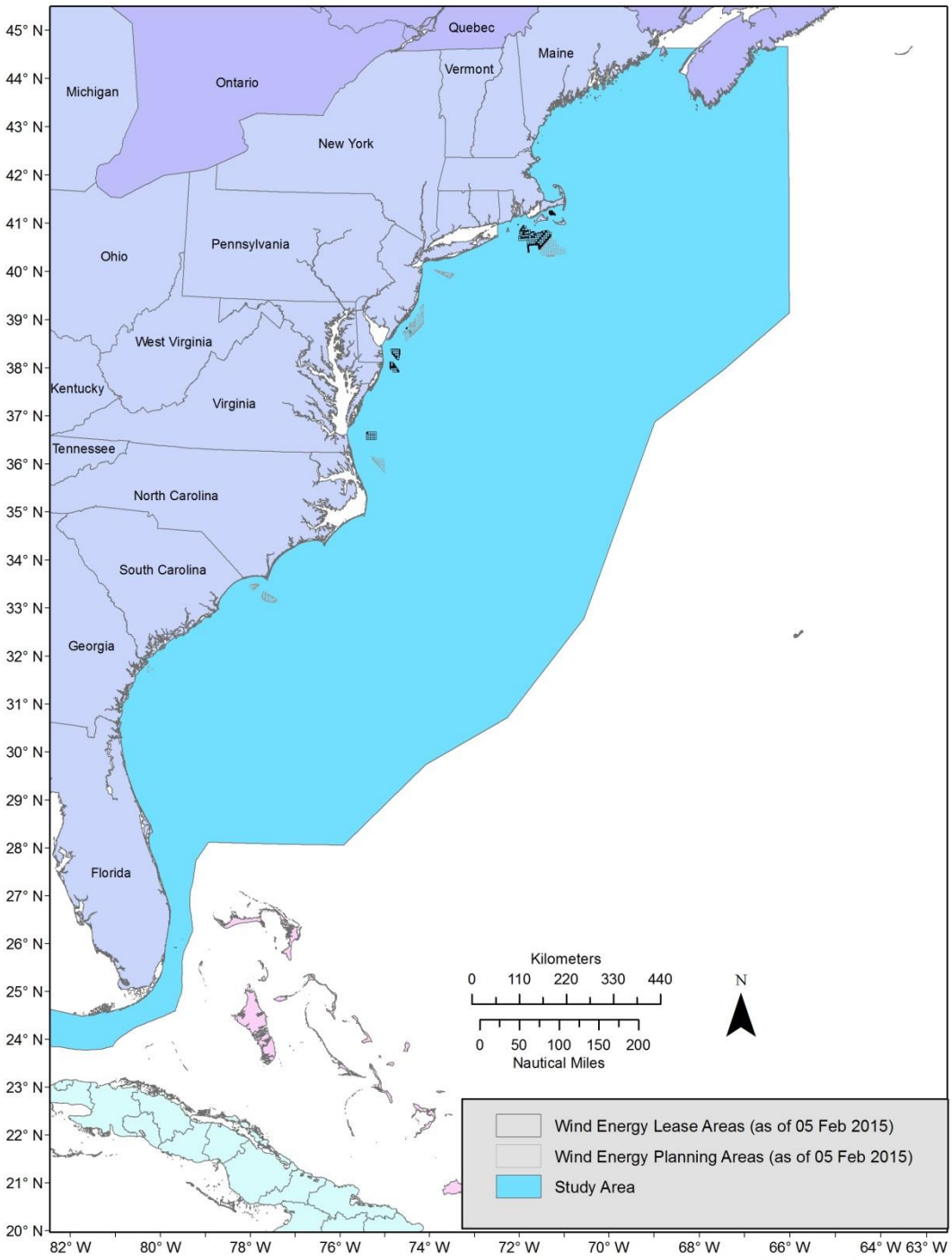

Figure 1. Study area with Wind Energy Planning and Lease Areas overlaid (approximate boundaries current as of 05 Feb 2015).

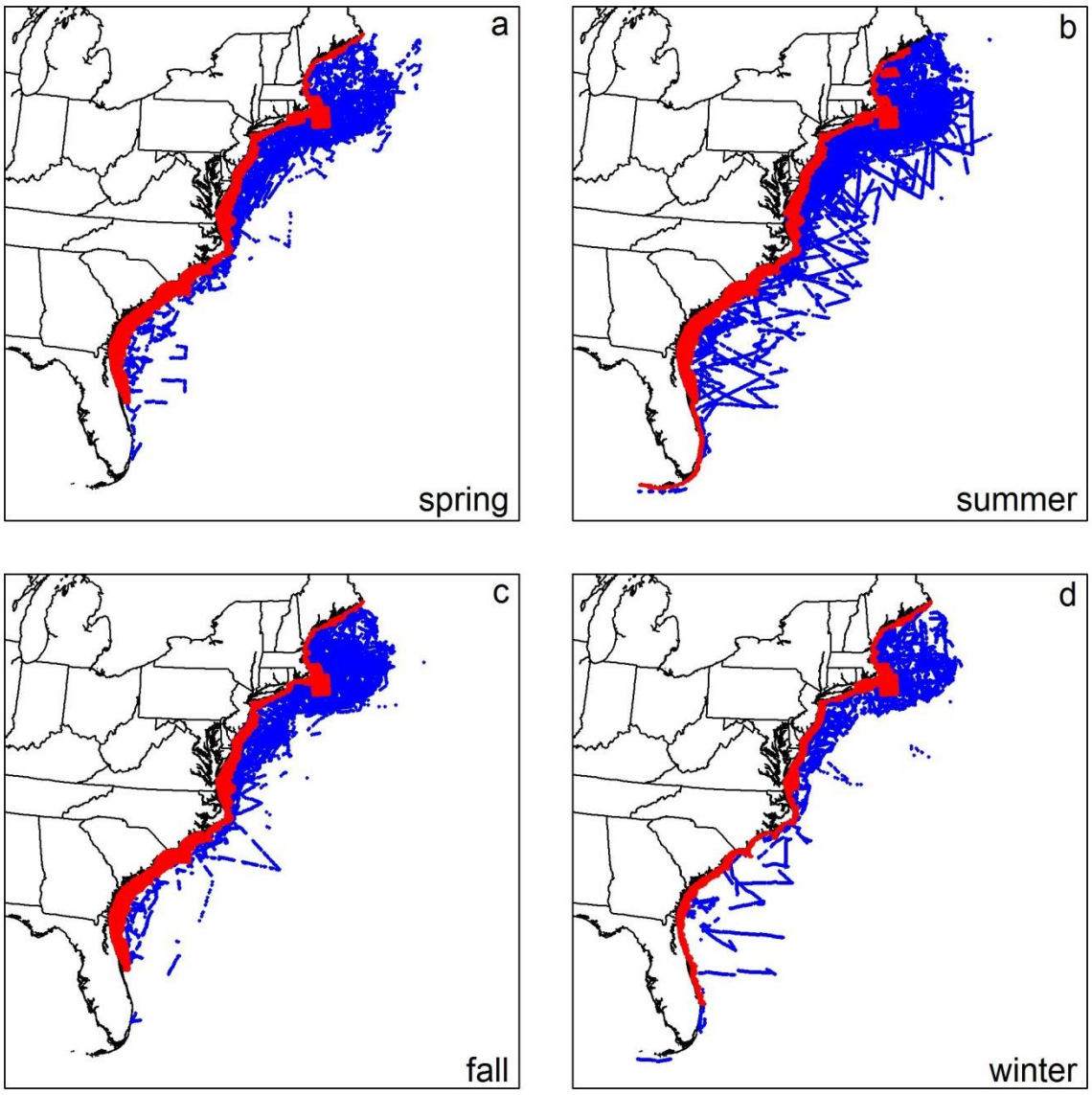

Figure 2A. Map of survey effort. Midpoints of standardized transect segments within the study area are plotted in blue (boat surveys) and red (aerial surveys) for each season analyzed. For complete list of datasets, see Appendix A.

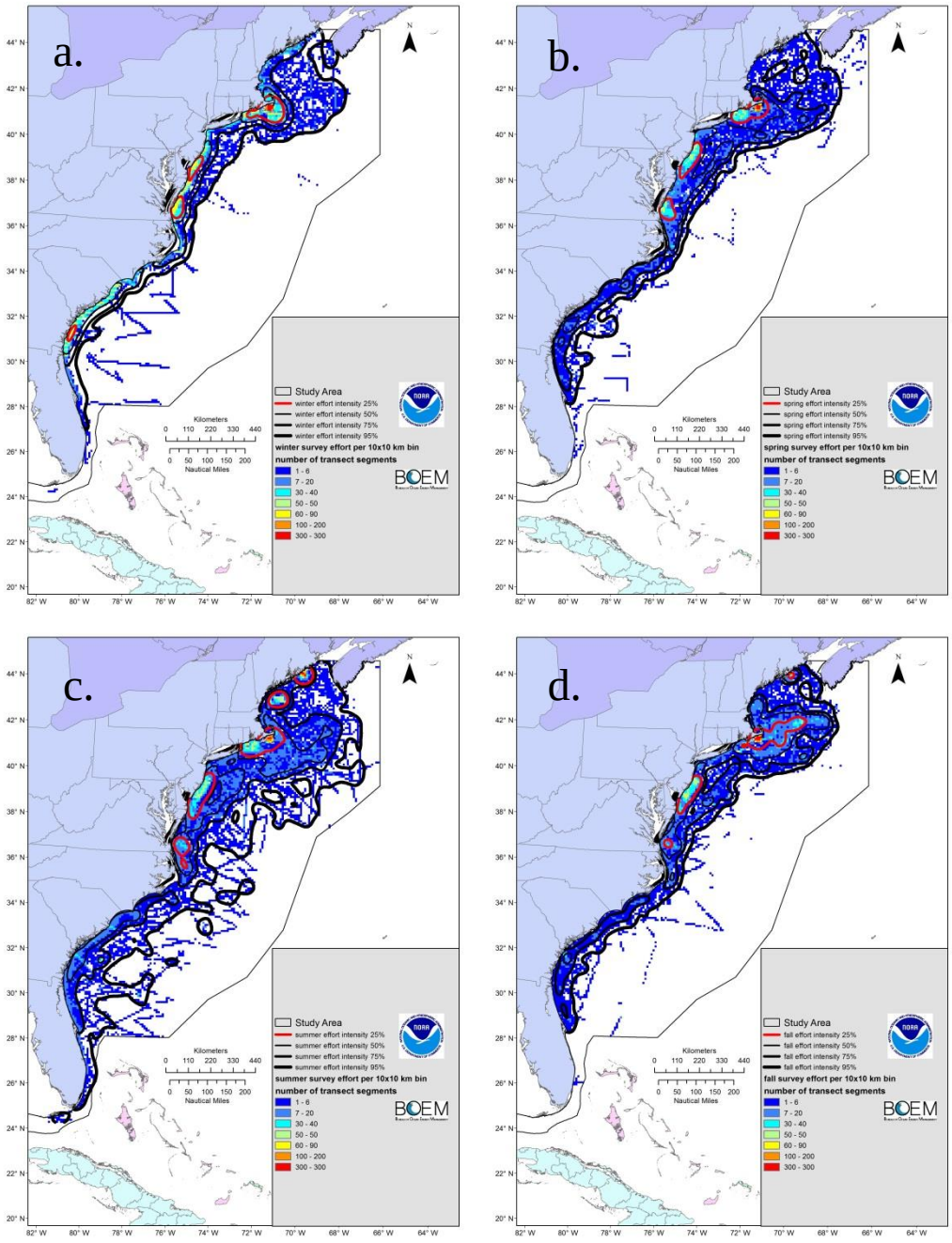

Figure 2B. Map of survey effort. Number of survey midpoints of standardized transect segments summed across 10 x 10 km cells within the study area for each season analyzed: a) winter b) spring c) summer d) fall. Colored contours indicate survey intensity. For complete list of datasets, see Appendix A.

a.

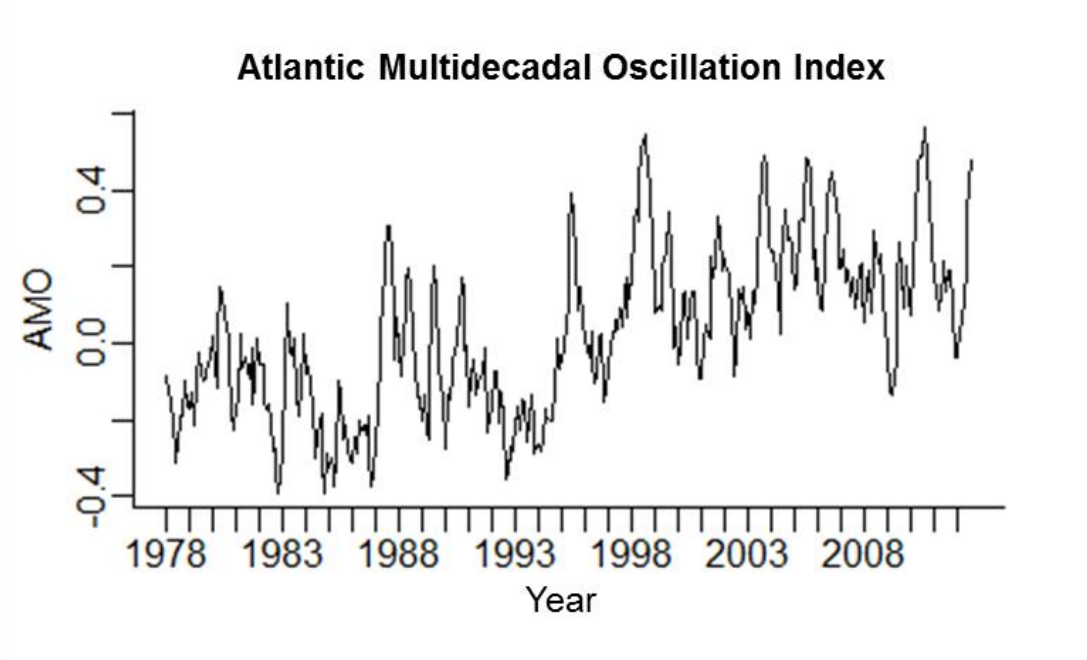

b.

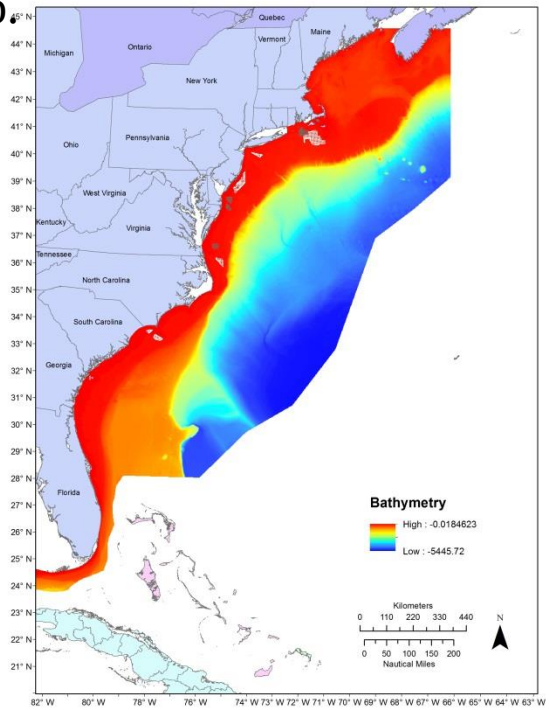

c.

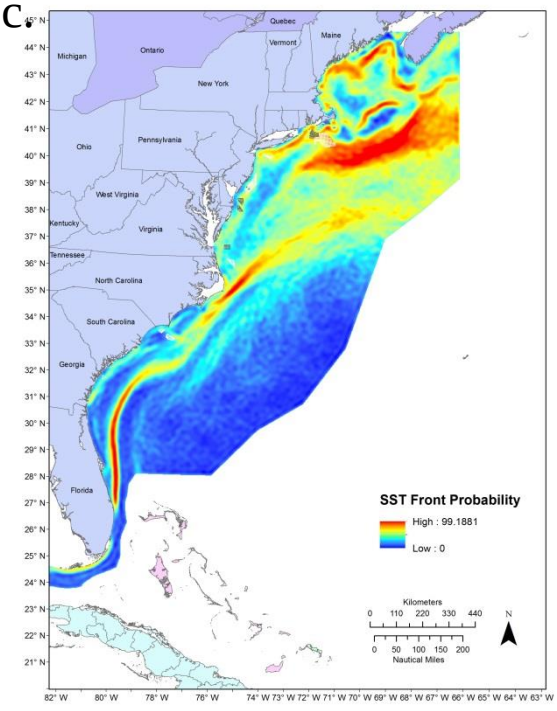

Figure 3. Examples of temporal and spatial predictors used in models; a) Climate index time series (AMO); b) static spatial predictor (depth); c) seasonal spatial predictor (front probability climatology for spring). For complete set of predictor plots, see Appendix B.

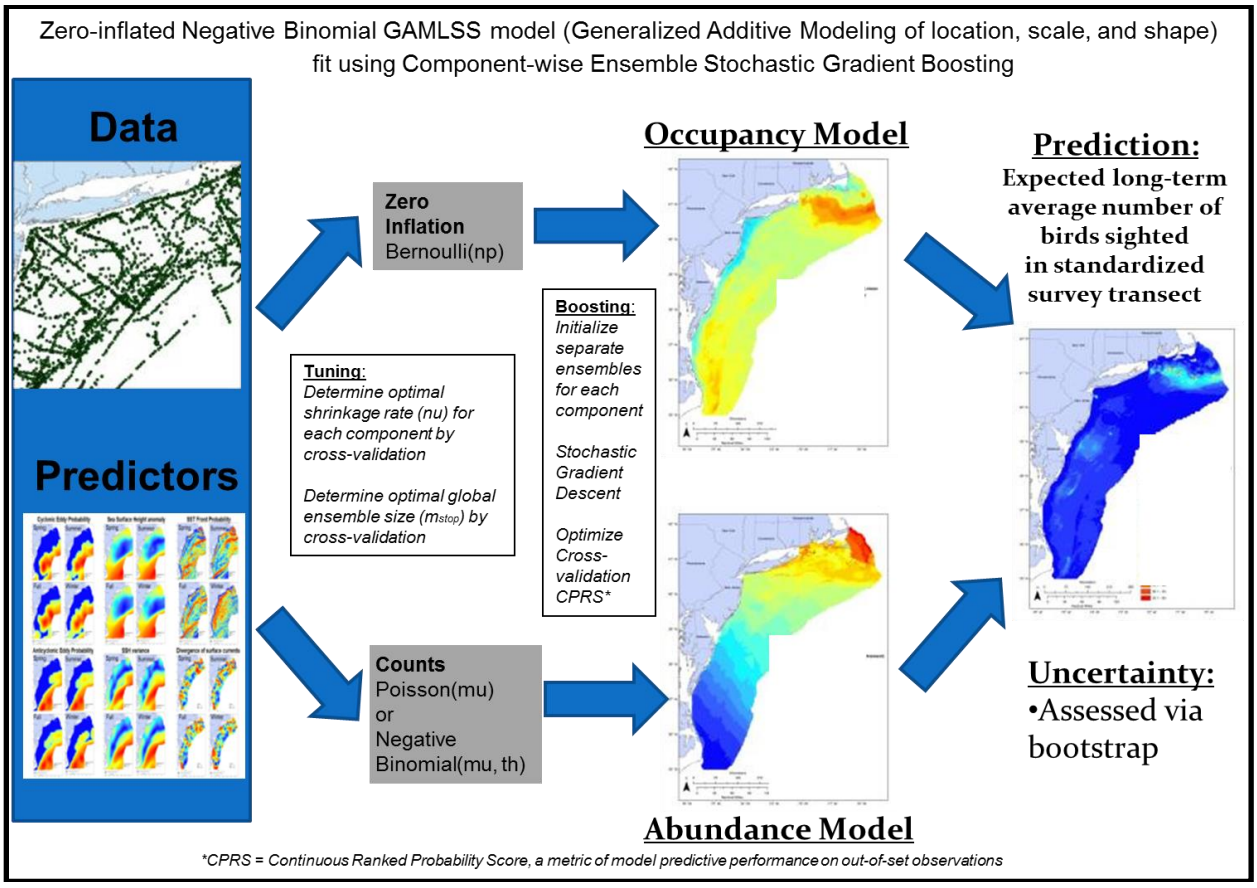

Figure 4. Schematic overview of statistical modeling process. See Section 2 Methods for details.

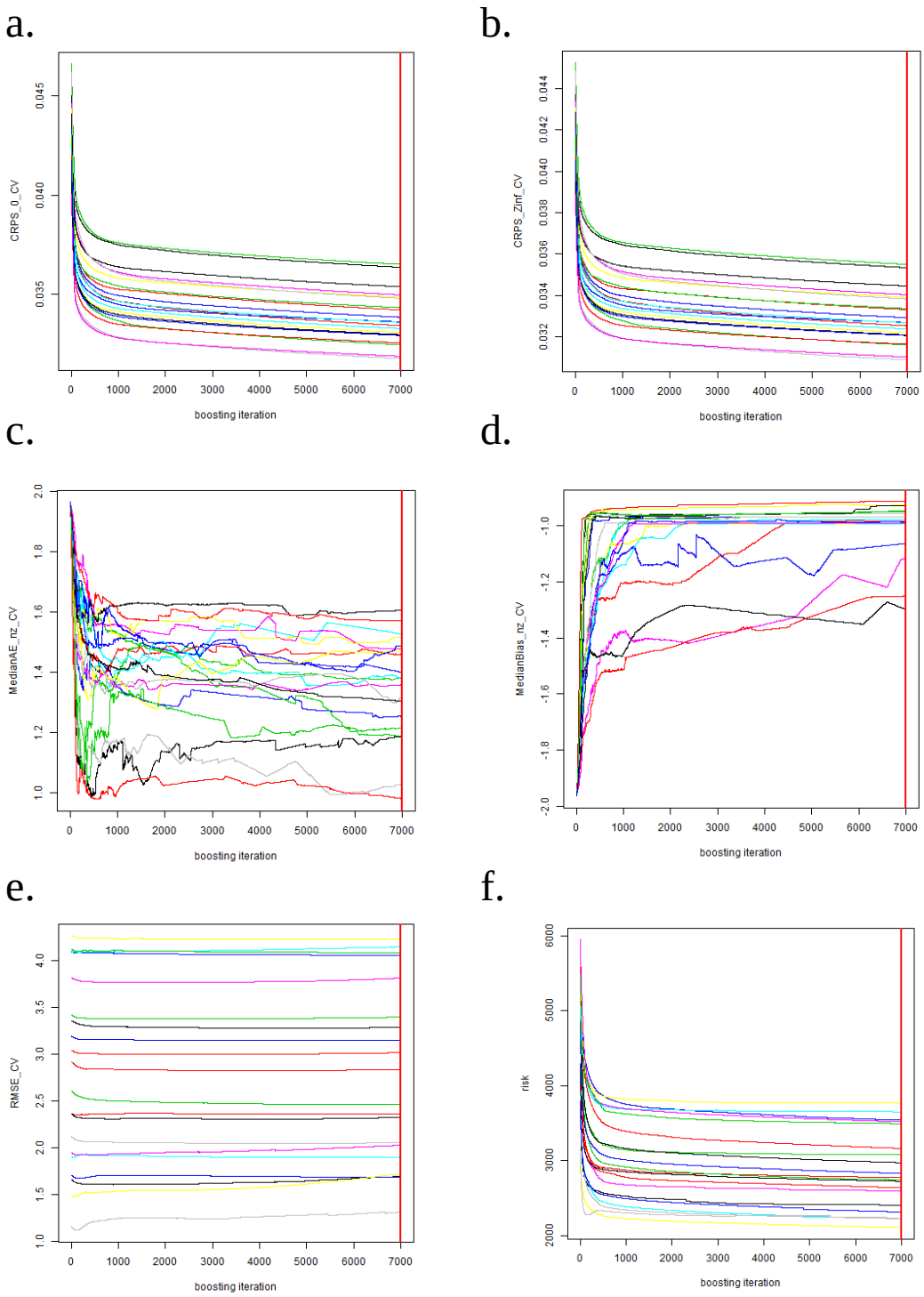

Figure 5.1. Cross-validation model performance metrics during stochastic gradient boosting for example model 7 (COTE/summer). a) Brier score, b) thresholded continuous rank probability score (CRPS), c) Median Absolute Error for non-zero data, d) Median Bias for non-zero data, e) root mean square error (RMSE), f) negative log-likelihood (risk). The optimized metrics were CRPS (panel b) and risk (panel f). For complete set of gradient descent plots, see Appendix C.

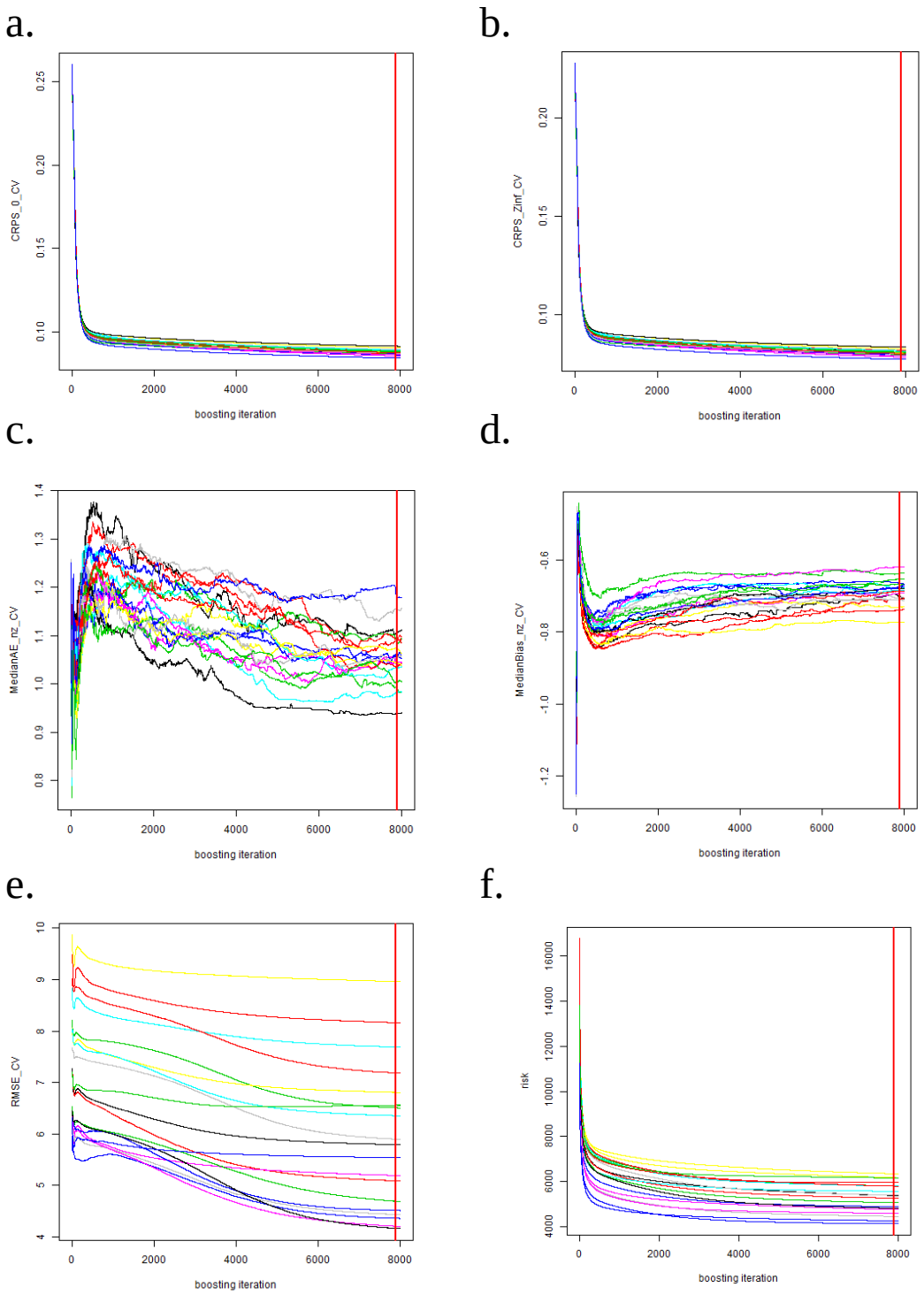

Figure 5.2. Cross-validation model performance metrics during stochastic gradient boosting for example model 7 (NOGA/fall). a) Brier score, b) thresholded continuous rank probability score (CRPS), c) Median Absolute Error for non-zero data, d) Median Bias for non-zero data, e) root mean square error (RMSE), f) negative log-likelihood (risk). The optimized metrics were CRPS (panel b) and risk (panel f). For complete set of gradient descent plots, see Appendix C.

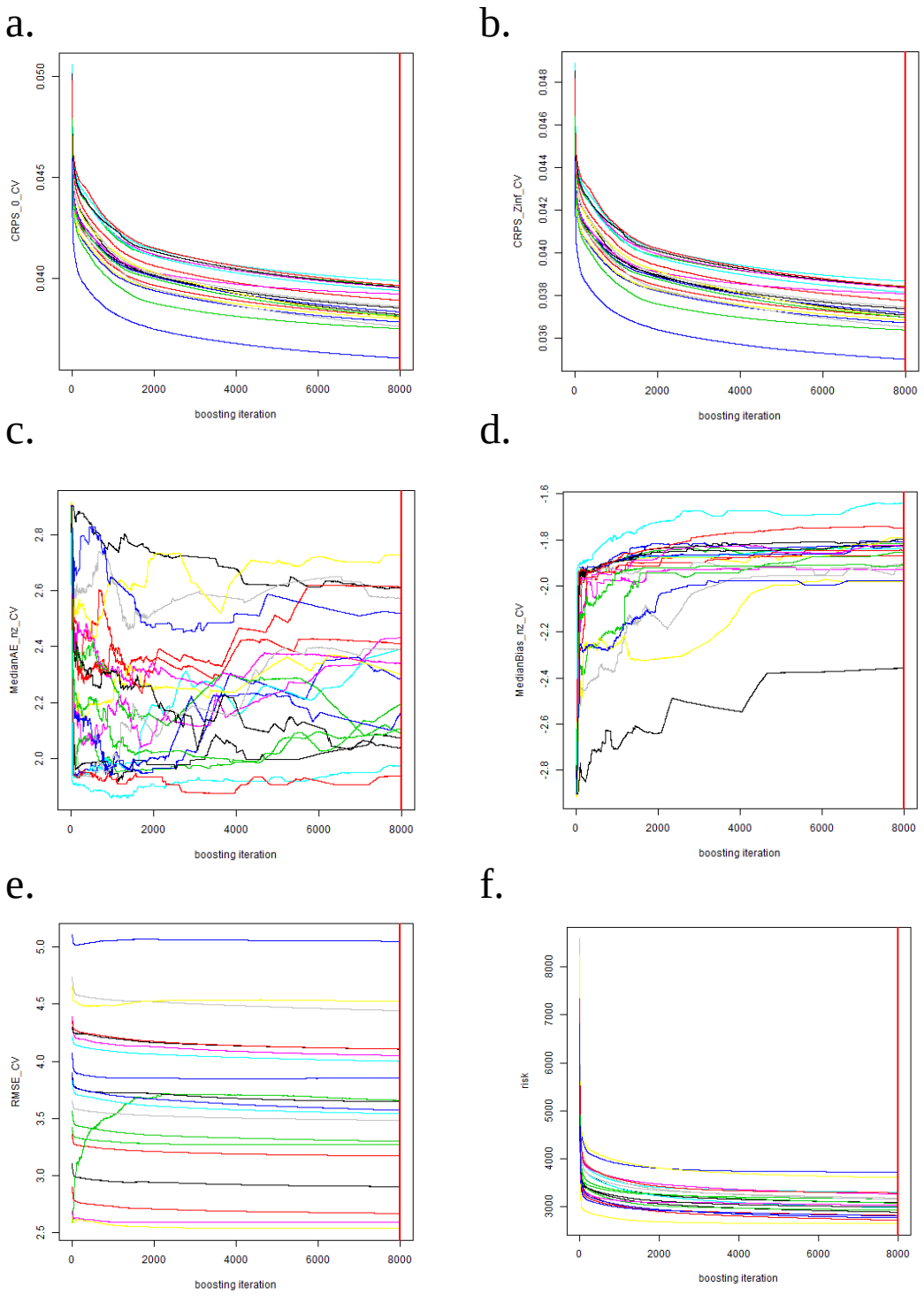

Figure 5.3. Cross-validation model performance metrics during stochastic gradient boosting for example model 7 (RAZO/winter). a) Brier score, b) thresholded continuous rank probability score (CRPS), c) Median Absolute Error for non-zero data, d) Median Bias for non-zero data, e) root mean square error (RMSE), f) negative log-likelihood (risk). The optimized metrics were CRPS (panel b) and risk (panel f). For complete set of gradient descent plots, see Appendix C.

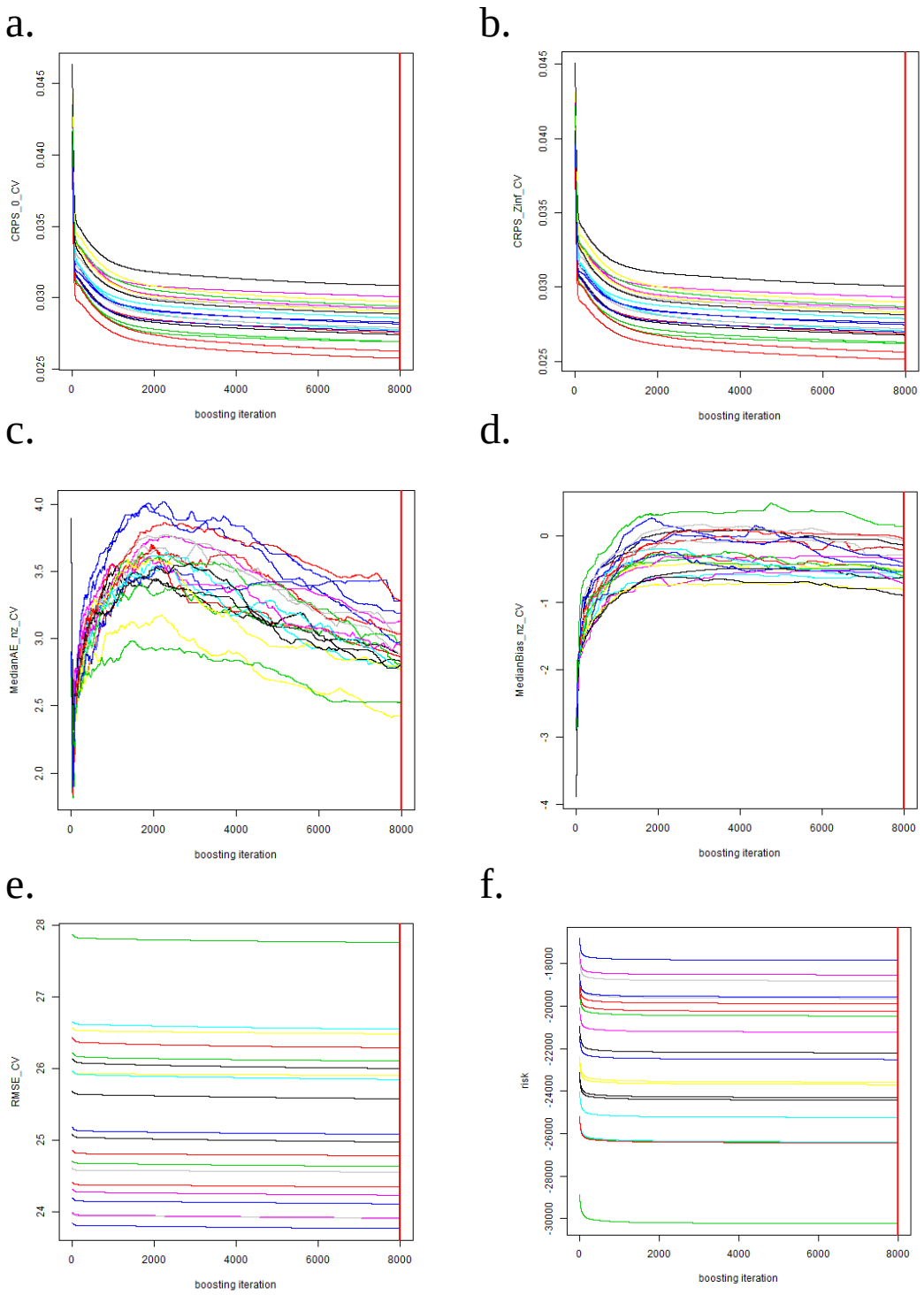

Figure 5.4. Cross-validation model performance metrics during stochastic gradient boosting for example model 8 (WWSC/winter). a) Brier score, b) thresholded continuous rank probability score (CRPS), c) Median Absolute Error for non-zero data, d) Median Bias for non-zero data, e) root mean square error (RMSE), f) negative log-likelihood (risk). The optimized metrics were CRPS (panel b) and risk (panel f). For complete set of gradient descent plots, see Appendix C.

a.

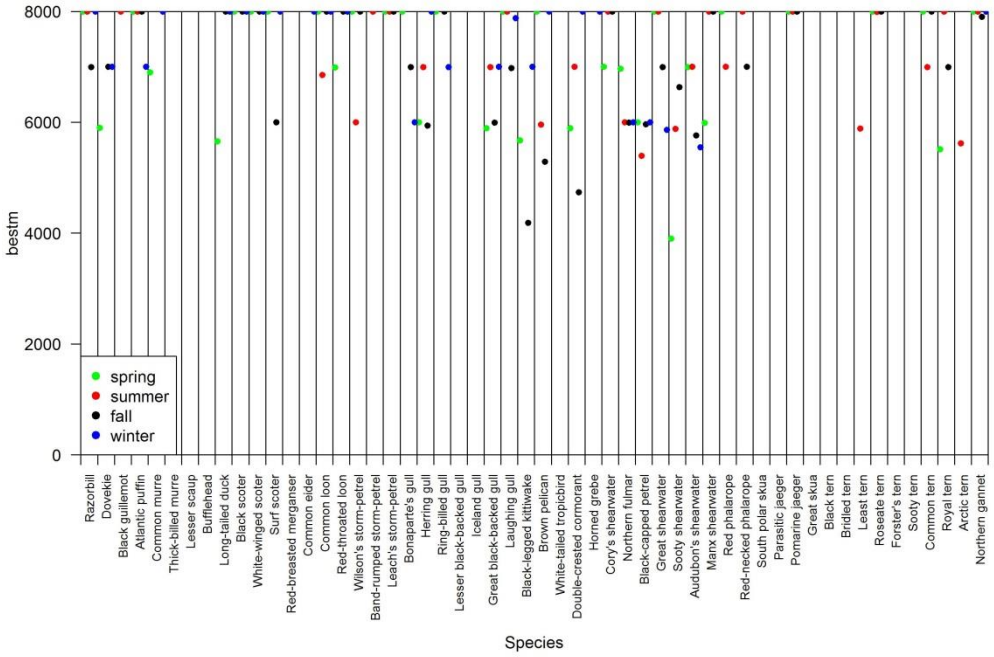

b.

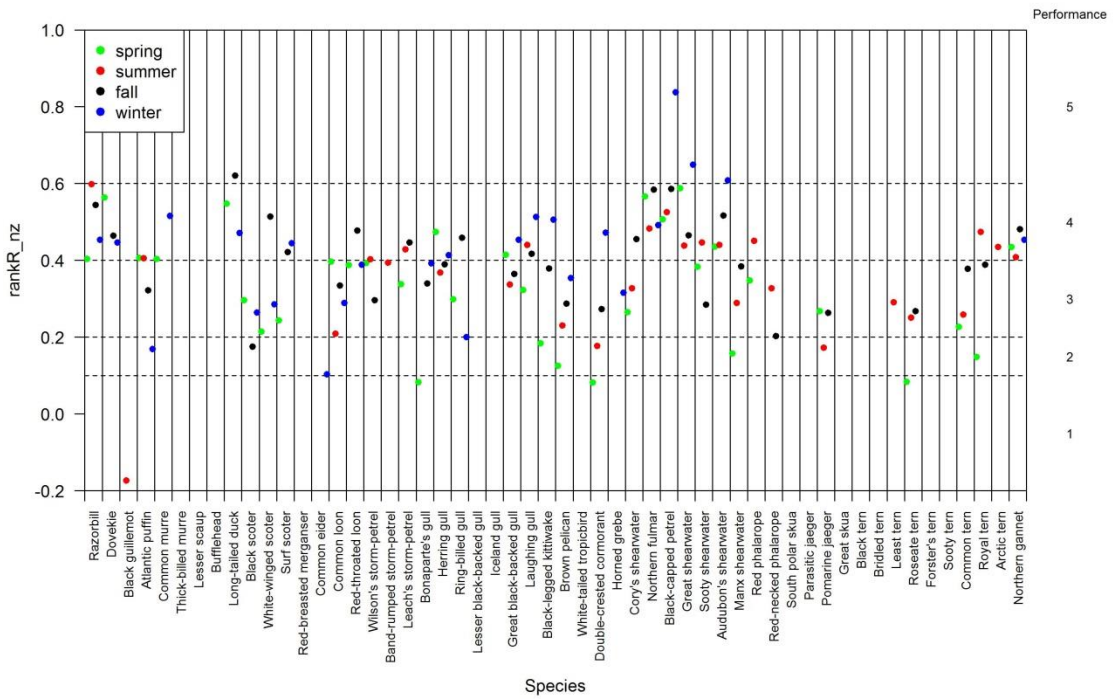

Figure 6AB. Comparison of model performance metrics for the best models (the final selected model out of the two compared) for each species/season combination. a) bestm, number of iterations to model convergence; b) rankR, Spearman rank correlation of observed non-zero data vs. predicted values. See also Tables 10 and 11 and Appendix E.

c.

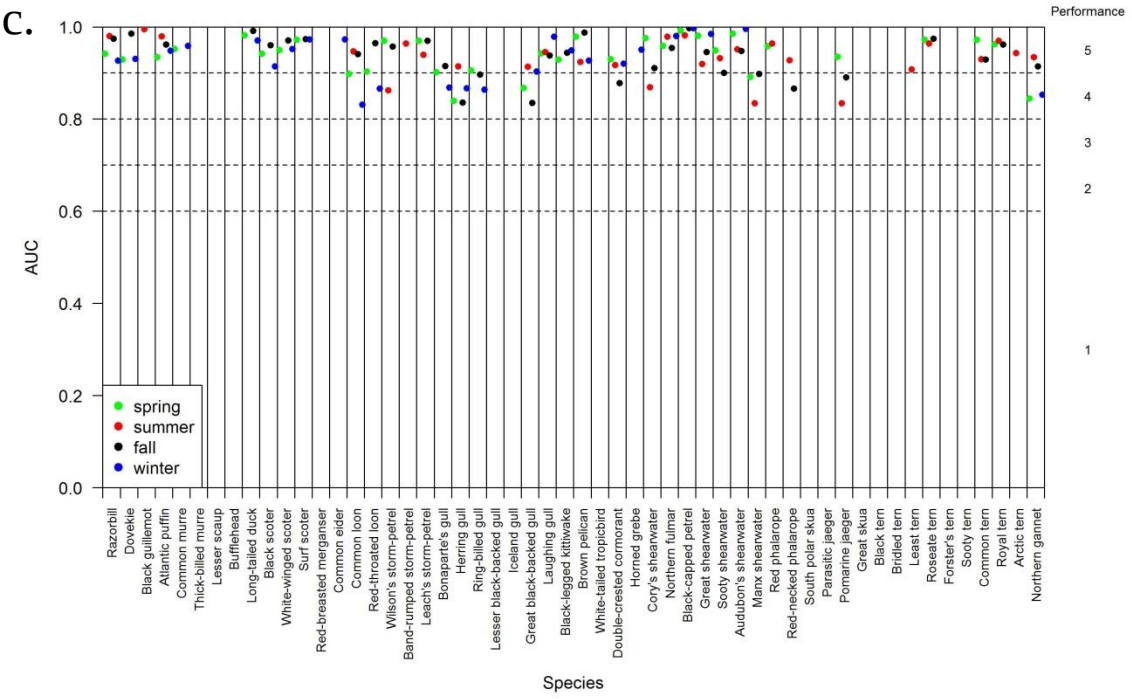

d.

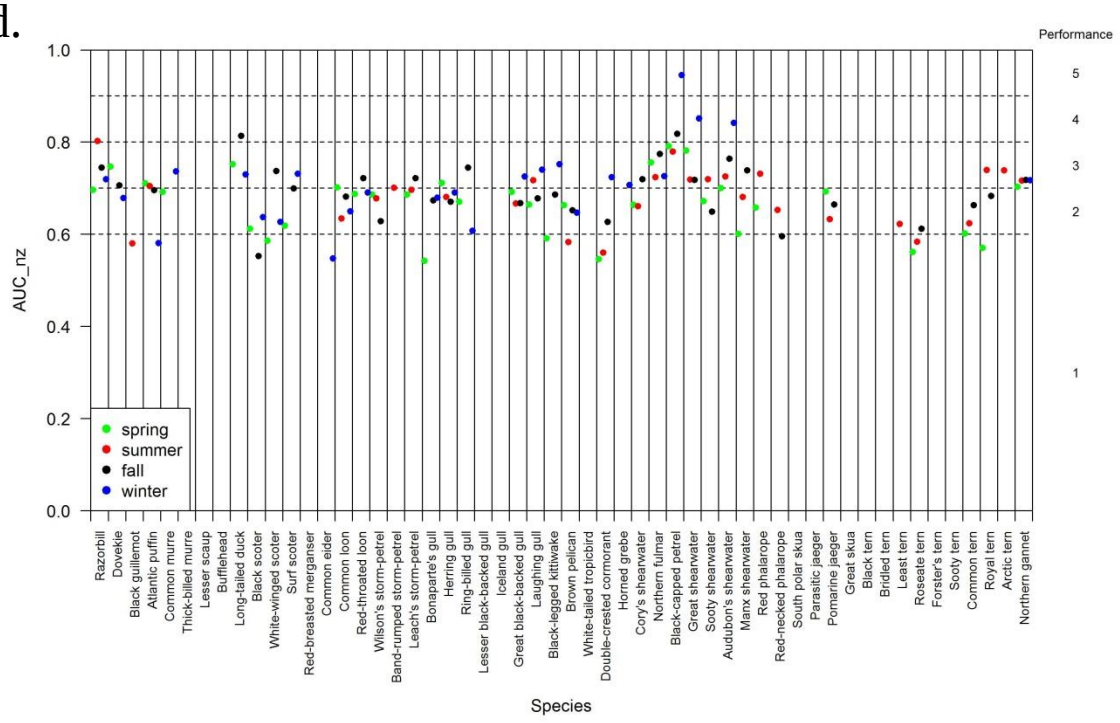

Figure 6CD. Comparison of model performance metrics for the best models (the final selected model out of the two compared) for each species/season combination. c) AUC, area under the receiver operating characteristic curve calculated for all data categorized as 0 or >0; d) AUC_nz, AUC calculated for non-zero data categorized as < the median or > the median. See also Tables 10 and 11 and Appendix E.

e.

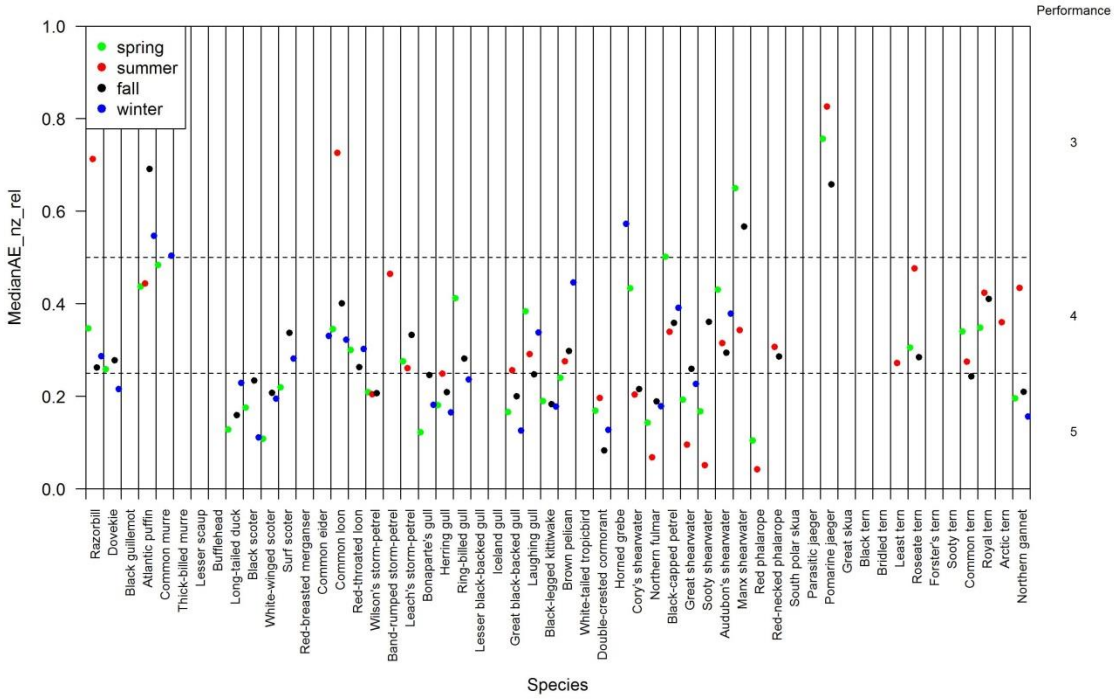

f.

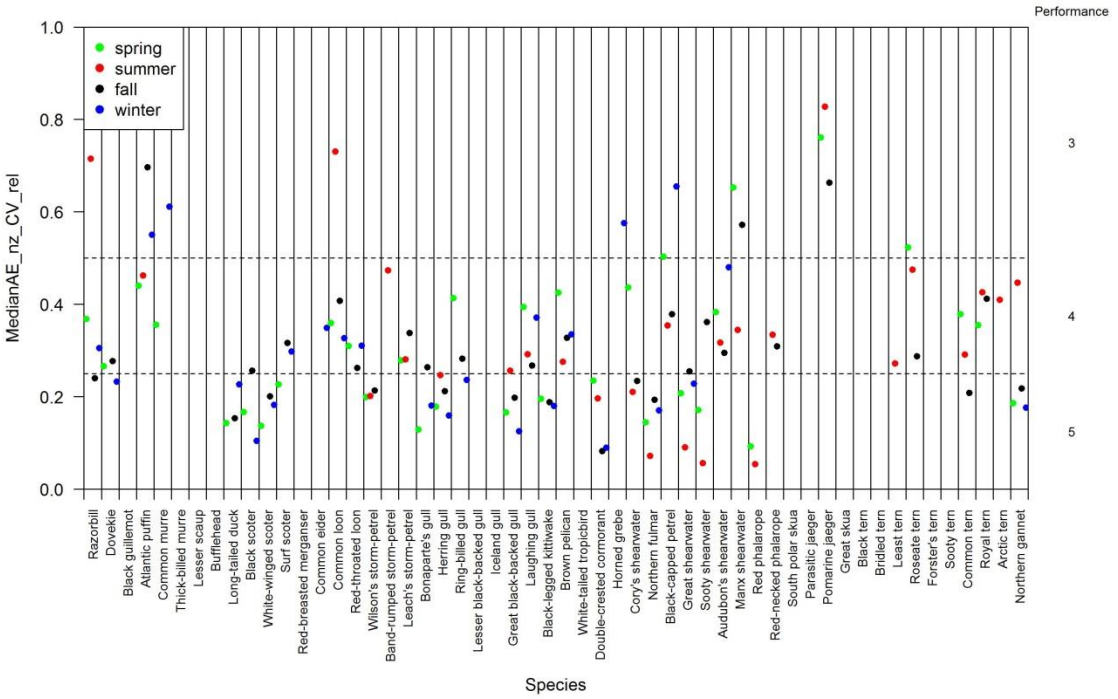

Figure 6EF. Comparison of model performance metrics for the best models (the final selected model out of the two compared) for each species/season combination. e) MedianAE_nz_rel, median absolute error for non-zero data relative to their mean; f) MedianAE_nz_CV_rel, median absolute error for non-zero data relative to their mean during cross-validation tuning. See also Tables 10 and 11 and Appendix E.

g.

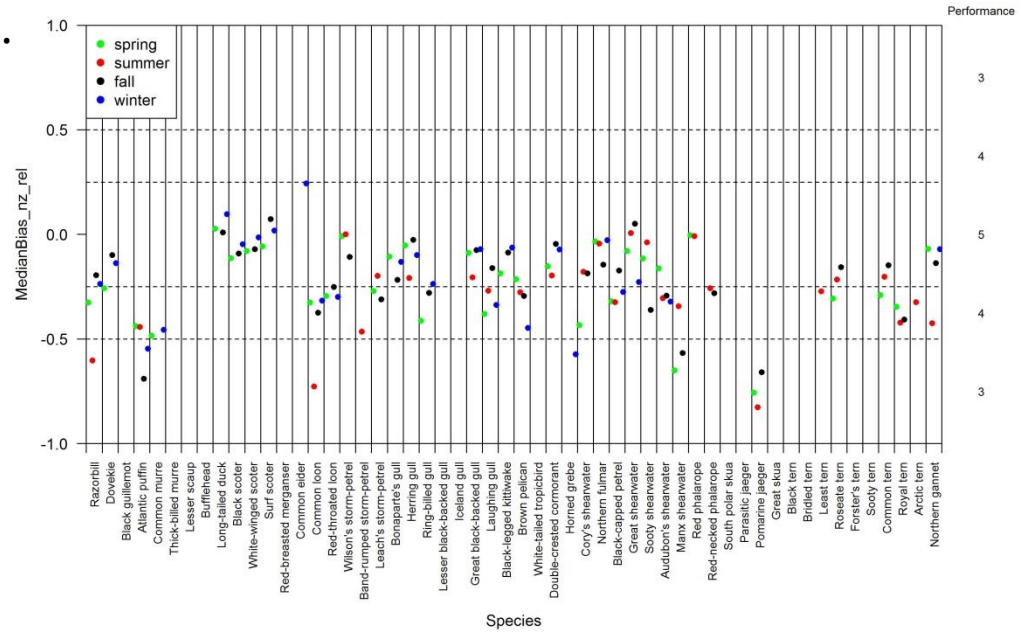

h.

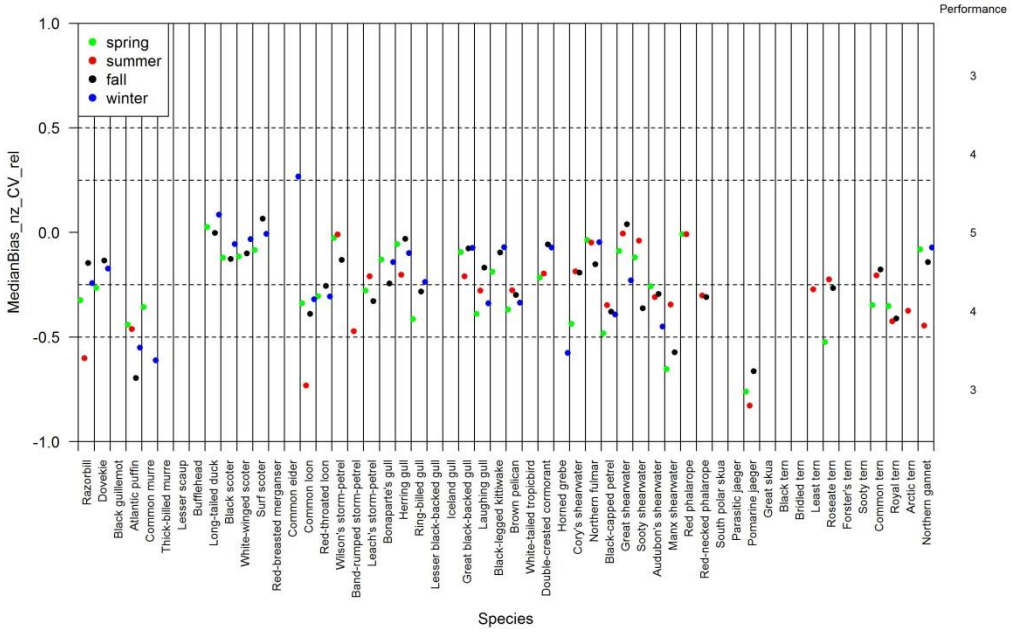

Figure 6GH. Comparison of model performance metrics for the best models (the final selected model out of the two compared) for each species/season combination. g) MedianBias_nz_rel, median error for non-zero data relative to their mean; h) MedianBias_nz_rel, median error for non-zero data relative to their mean during cross-validation tuning. See also Tables 10 and 11 and Appendix E.

i.

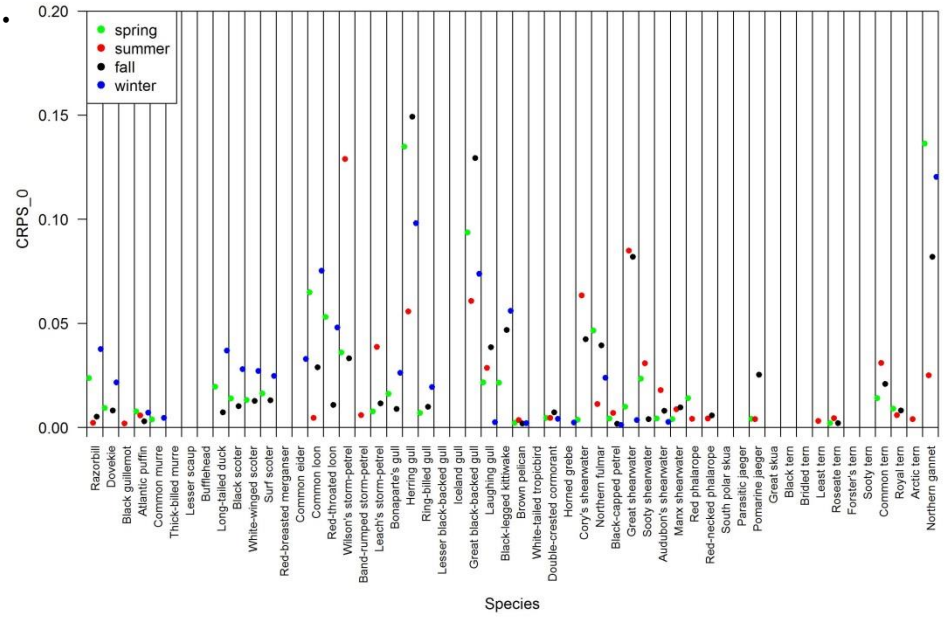

j.

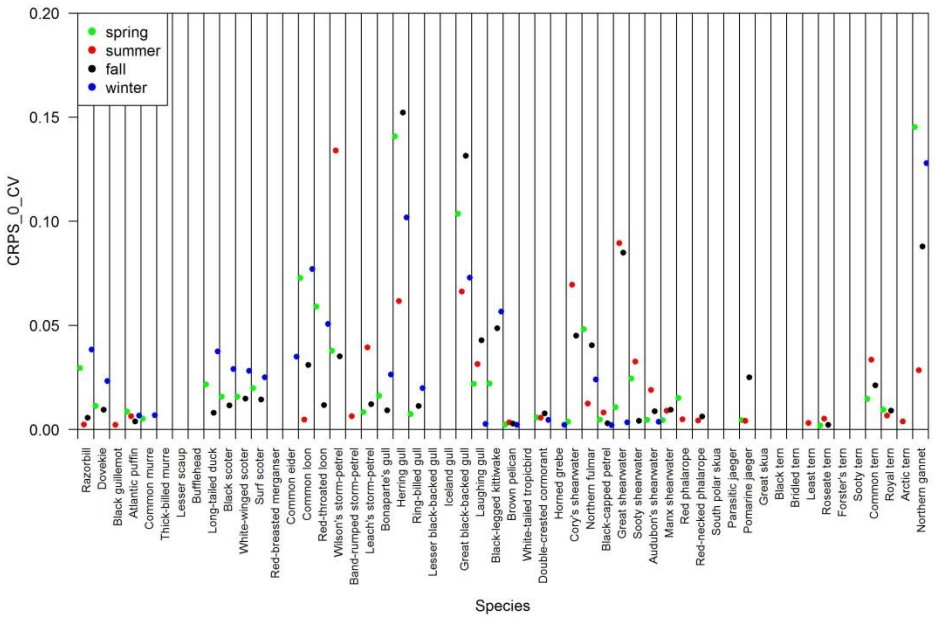

Figure 6IJ. Comparison of model performance metrics for the best models (the final selected model out of the two compared) for each species/season combination. i) CRPS_0, Brier score (occupancy); j) CRPS_0_CV, Brier score during cross-validation tuning. See also Tables 10 and 11 and Appendix E.

k.

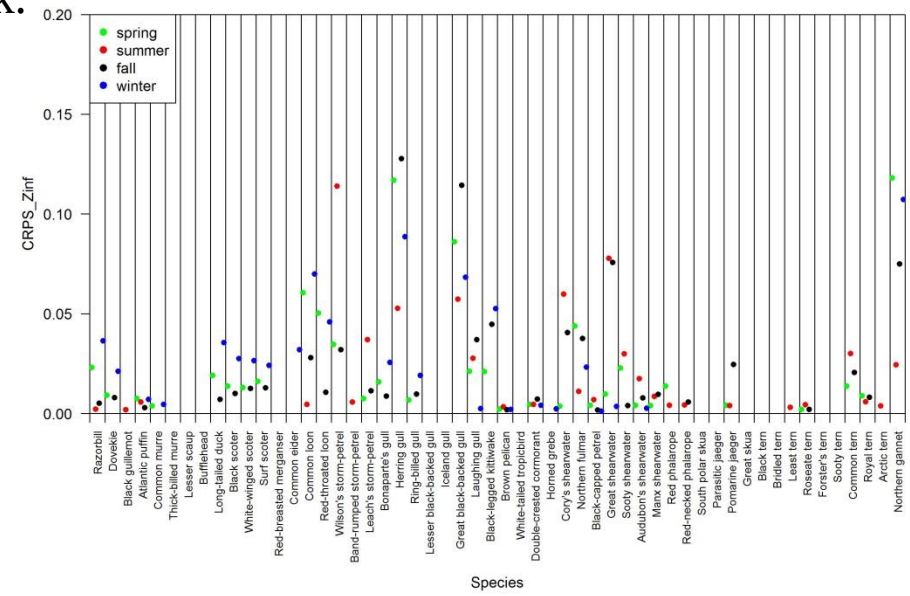

l.

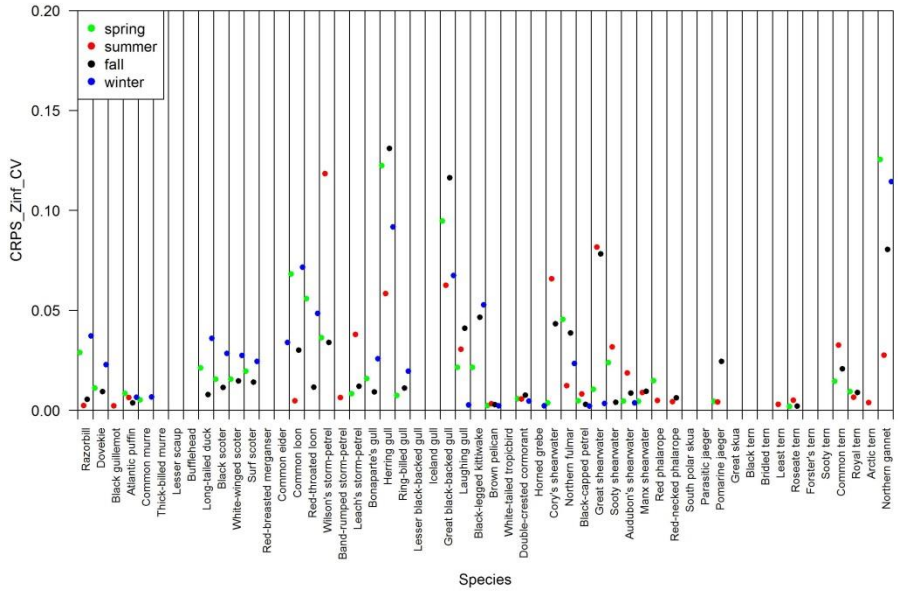

Figure 6KL. Comparison of model performance metrics for the best models (the final selected model out of the two compared) for each species/season combination. k) CRPS_Zinf, thresholded continuous rank probability score (CRPS); l) CRPS_Zinf_CV, CRPS during cross-validation tuning. See also Tables 10 and 11 and Appendix E.

m.

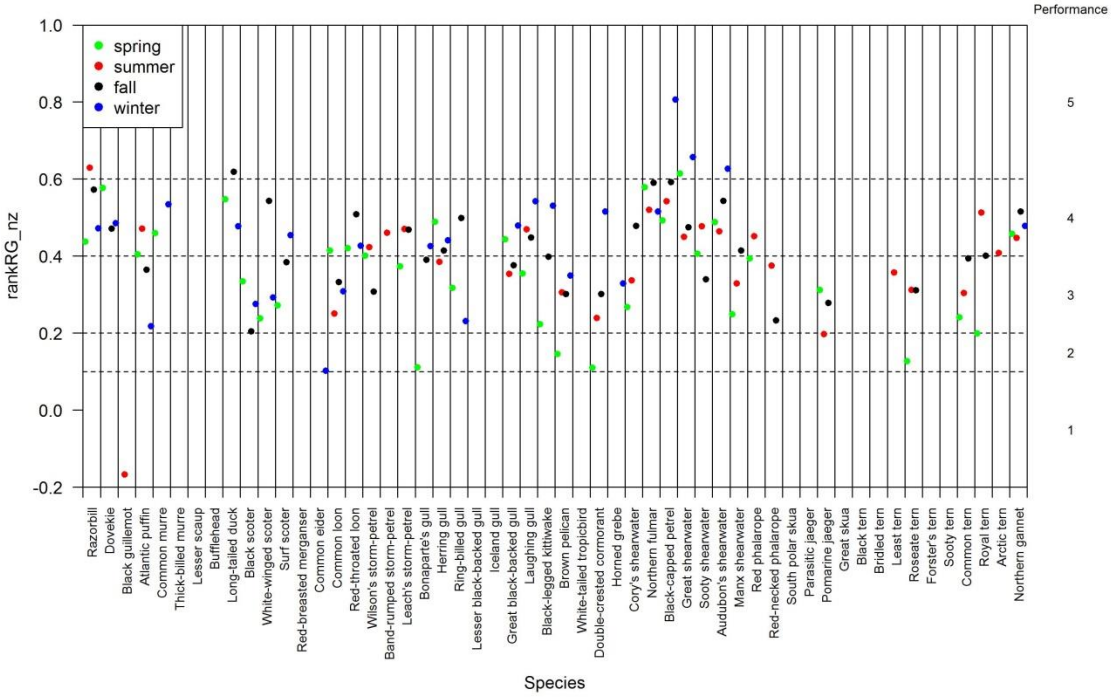

n.

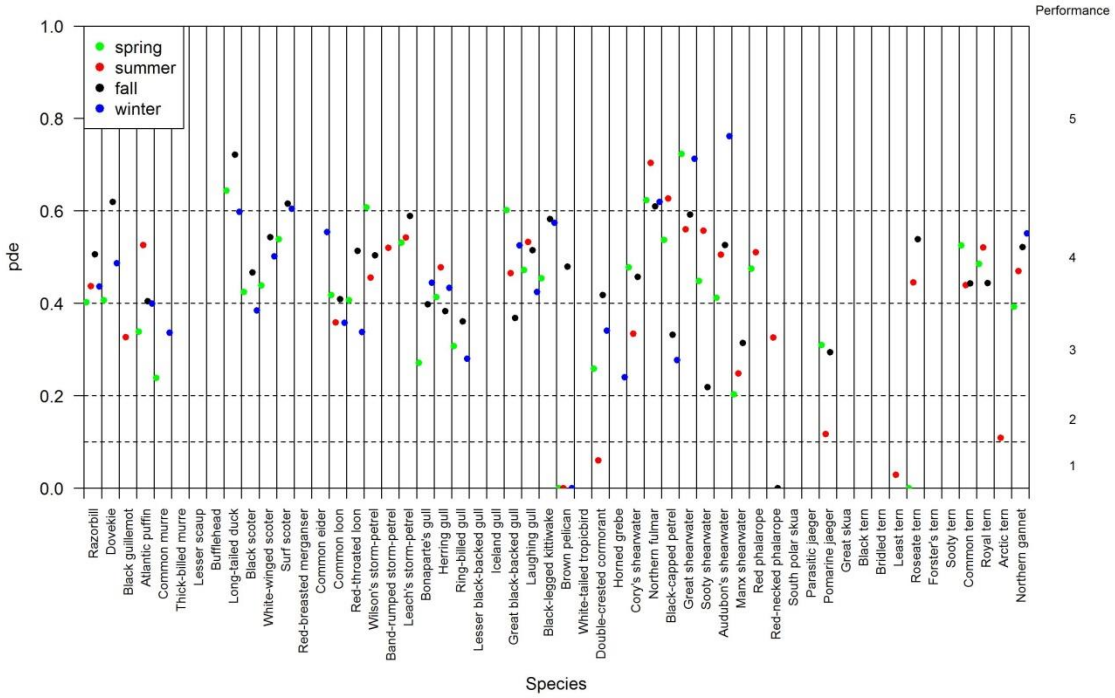

Figure 6MN. Comparison of model performance metrics for the best models (the final selected model out of the two compared) for each species/season combination. m) rankRG_nz, Gaussian rank correlation of observed non-zero data vs. predicted values; n) pde, percent deviance explained. See also Tables 10 and 11 and Appendix E.

a.

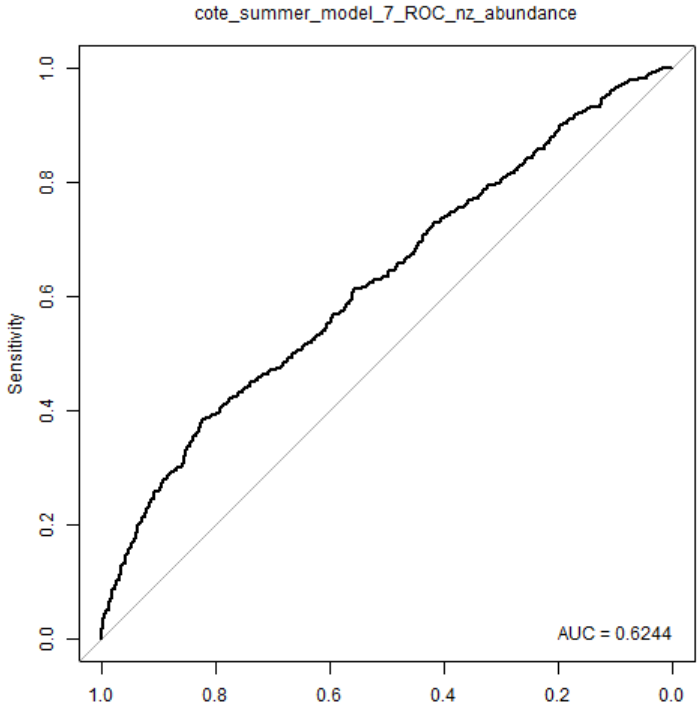

b.

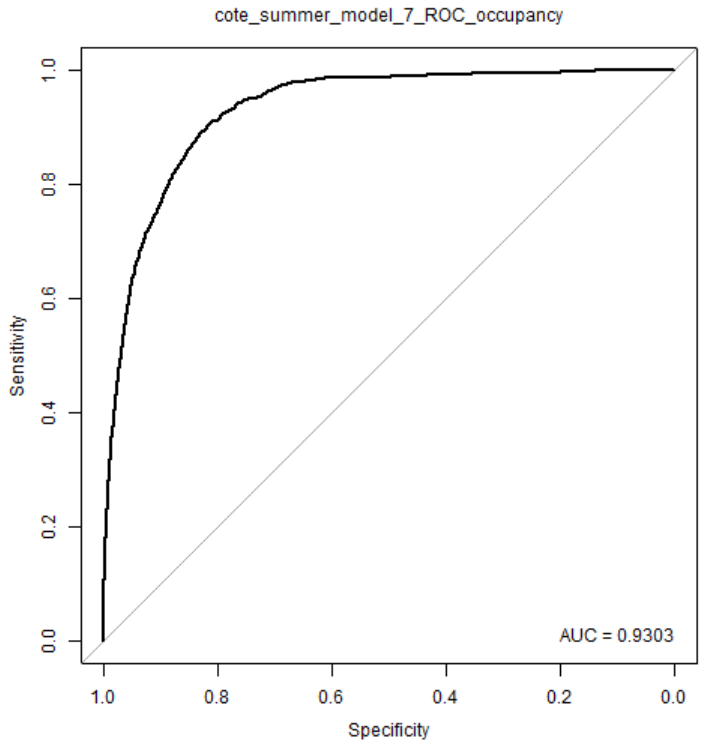

Figure 7.1. Receiver Operating Characteristic (ROC) curves for assessment of predictive accuracy of example model 7 (COTE/summer). a) ROC curve and area under the curve (AUC) statistic for prediction of median-thresholded non-zero data (i.e., non-zero data above/below median observed value), b) ROC curve and AUC statistic for prediction of presence/absence. For complete set of ROC curves for selected models, see Appendix F. For complete set of AUC statistics for selected models, see Table 11.

a.

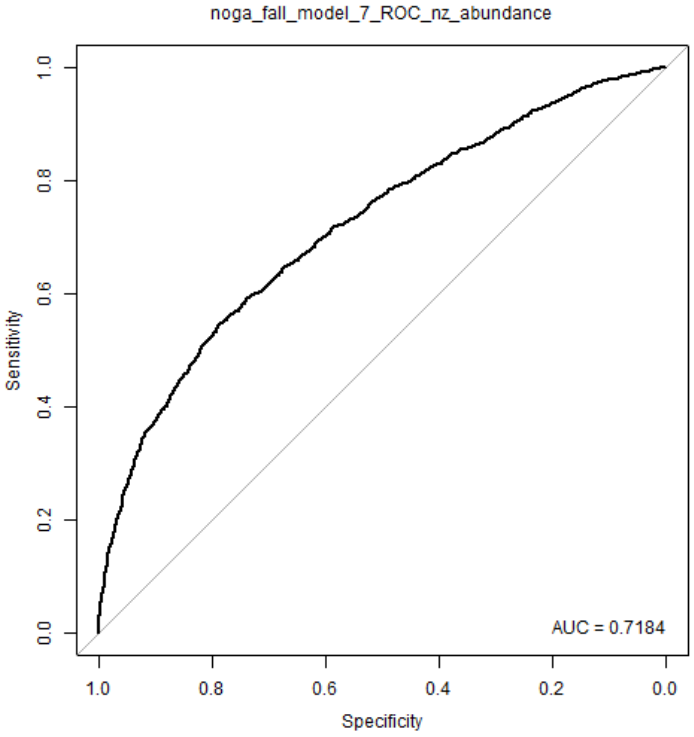

b.

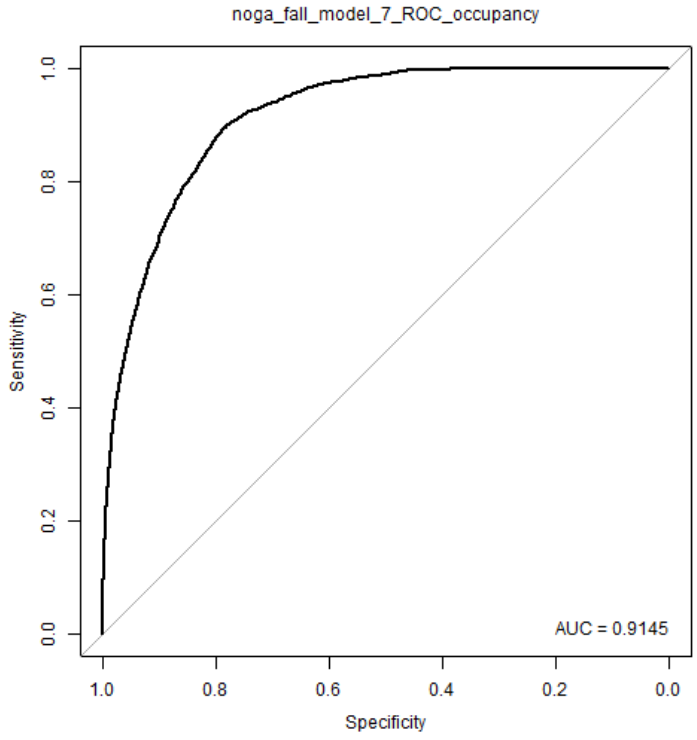

Figure 7.2. Receiver Operating Characteristic (ROC) curves for assessment of predictive accuracy of example model 7 (NOGA/fall). a) ROC curve and area under the curve (AUC) statistic for prediction of median-thresholded non-zero data (i.e., non-zero data above/below median observed value), b) ROC curve and AUC statistic for prediction of presence/absence. For complete set of ROC curves for selected models, see Appendix F. For complete set of AUC statistics for selected models, see Table 11.

a.

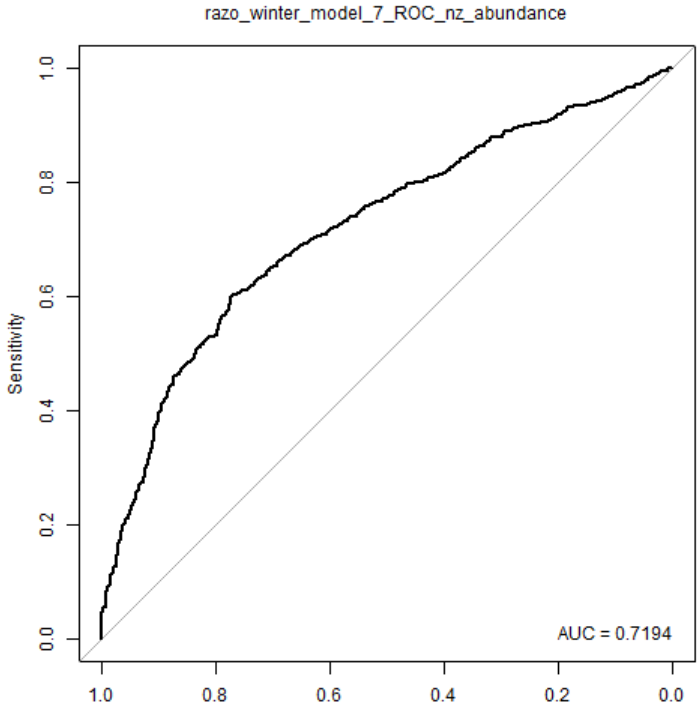

b.

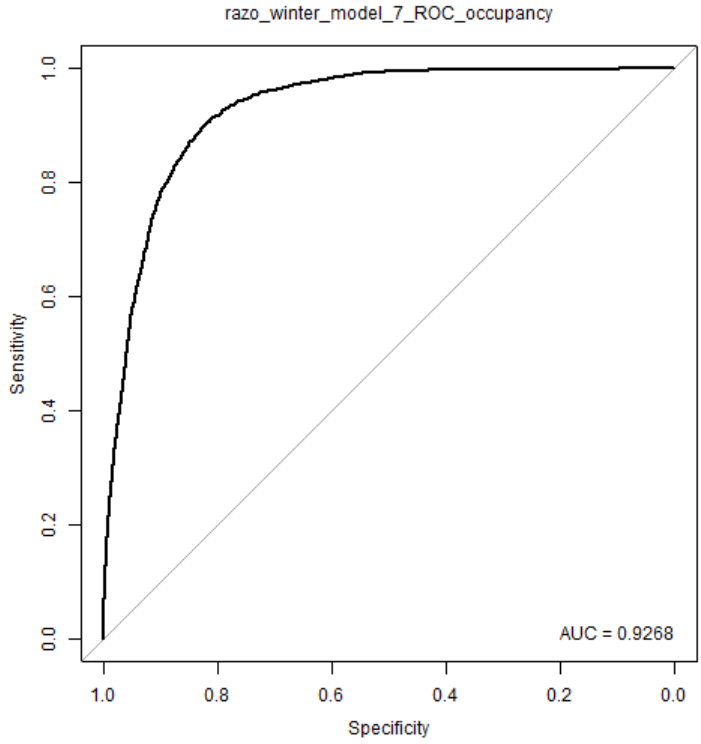

Figure 7.3. Receiver Operating Characteristic (ROC) curves for assessment of predictive accuracy of example model 7 (RAZO/winter). a) ROC curve and area under the curve (AUC) statistic for prediction of median-thresholded non-zero data (i.e., non-zero data above/below median observed value), b) ROC curve and AUC statistic for prediction of presence/absence. For complete set of ROC curves for selected models, see Appendix F. For complete set of AUC statistics for selected models, see Table 11.

a.

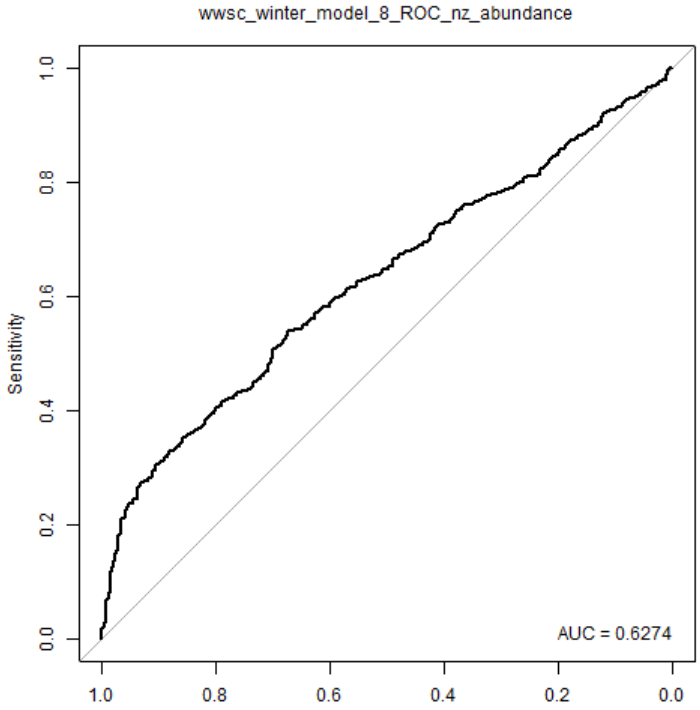

b.

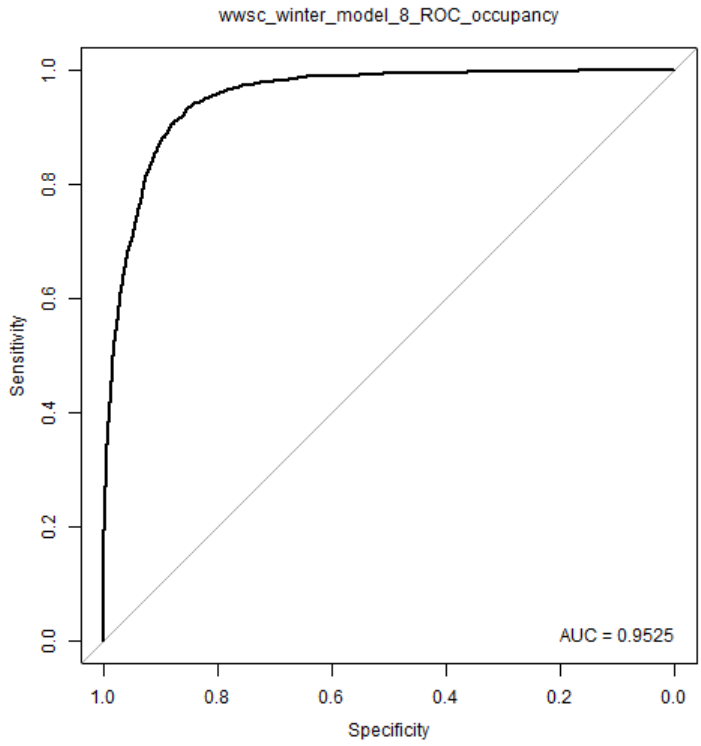

Figure 7.4. Receiver Operating Characteristic (ROC) curves for assessment of predictive accuracy of example model 8 (WWSC/winter). a) ROC curve and area under the curve (AUC) statistic for prediction of median-thresholded non-zero data (i.e., non-zero data above/below median observed value), b) ROC curve and AUC statistic for prediction of presence/absence. For complete set of ROC curves for selected models, see Appendix F. For complete set of AUC statistics for selected models, see Table 11.

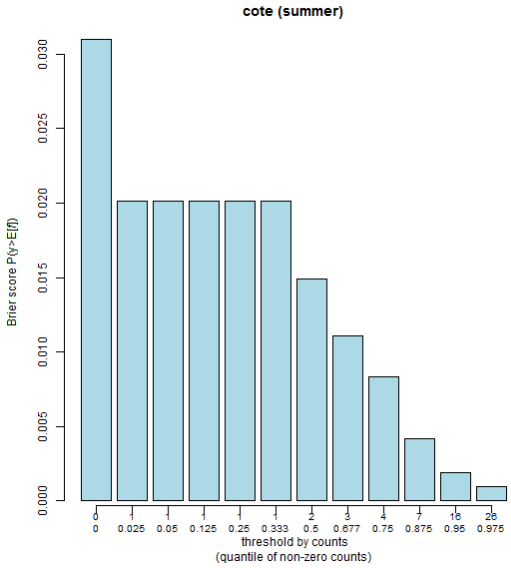

Figure 8.1. Brier score calculated at quantile thresholds of non-zero data for example model 7 (COTE/summer). For complete set of Brier score plots for selected models, see Appendix G. For complete set of Brier score statistics and related thresholded continuous rank probability scores (CPRS) for selected models, see Table 11.

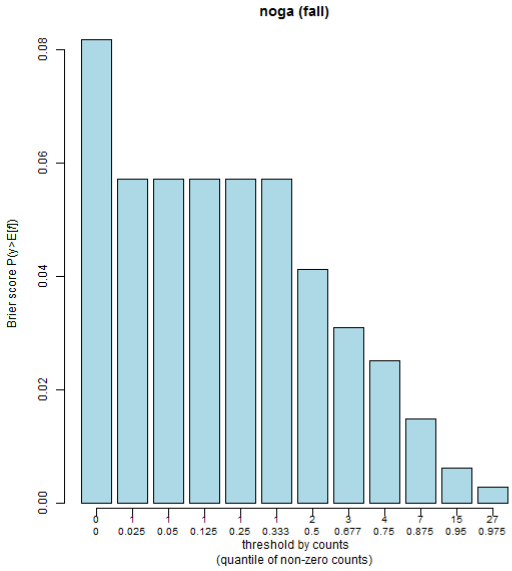

Figure 8.2. Brier score calculated at quantile thresholds of non-zero data for example model 7 (NOGA/fall). For complete set of Brier score plots for selected models, see Appendix G. For complete set of Brier score statistics and related thresholded continuous rank probability scores (CPRS) for selected models, see Table 11.

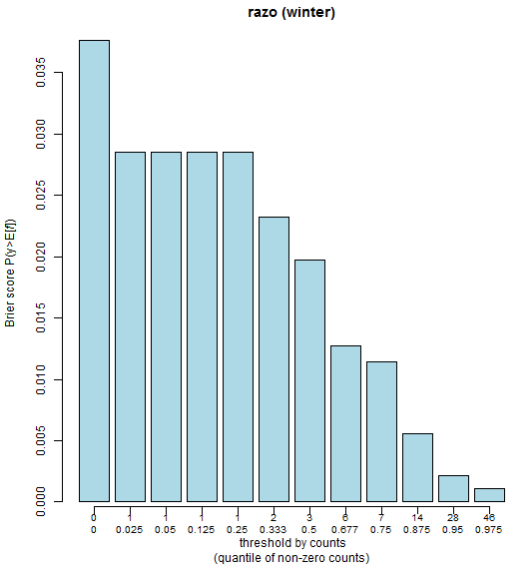

Figure 8.3. Brier score calculated at quantile thresholds of non-zero data for example model 7 (RAZO/winter). For complete set of Brier score plots for selected models, see Appendix G. For complete set of Brier score statistics and related thresholded continuous rank probability scores (CPRS) for selected models, see Table 11.

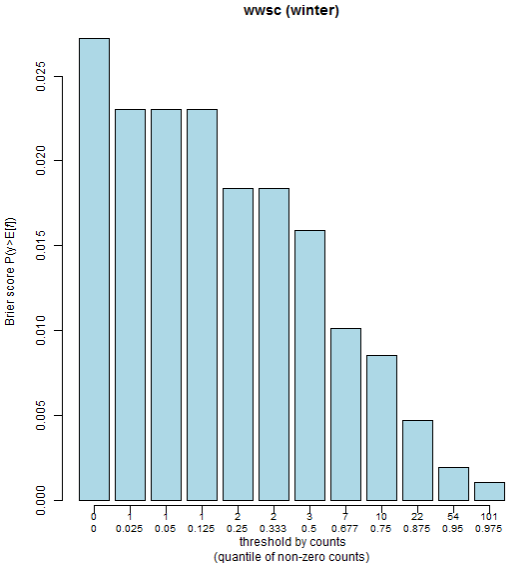

Figure 8.4. Brier score calculated at quantile thresholds of non-zero data for example model 8 (WWSC/winter). For complete set of Brier score plots for selected models, see Appendix G. For complete set of Brier score statistics and related thresholded continuous rank probability scores (CPRS) for selected models, see Table 11.

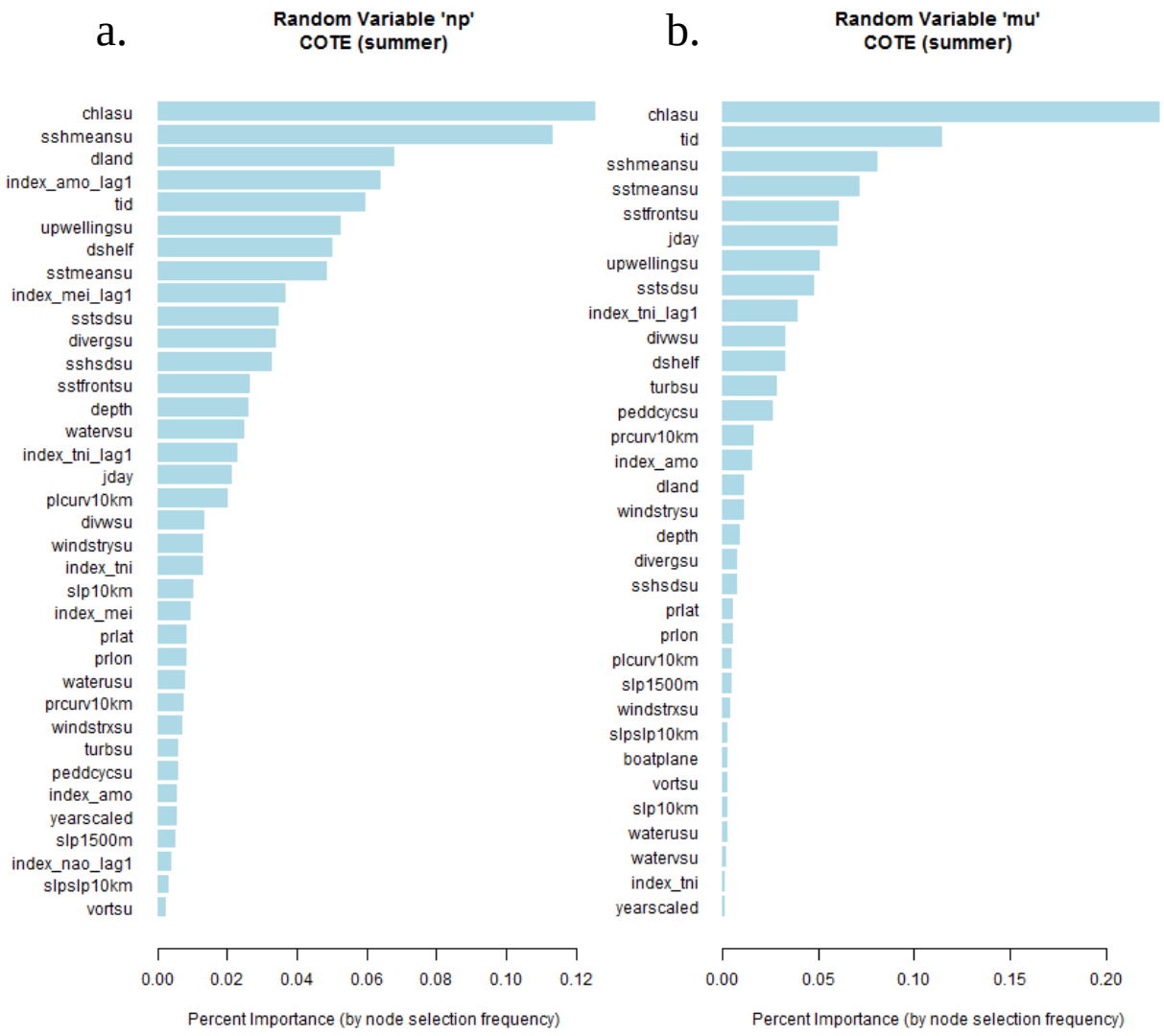

Figure 9.1. Variable importance bar plots for top variables in example model 7 (COTE/summer). a) np component; b) mu component. For complete set of variable importance bar plots, see Appendix H.

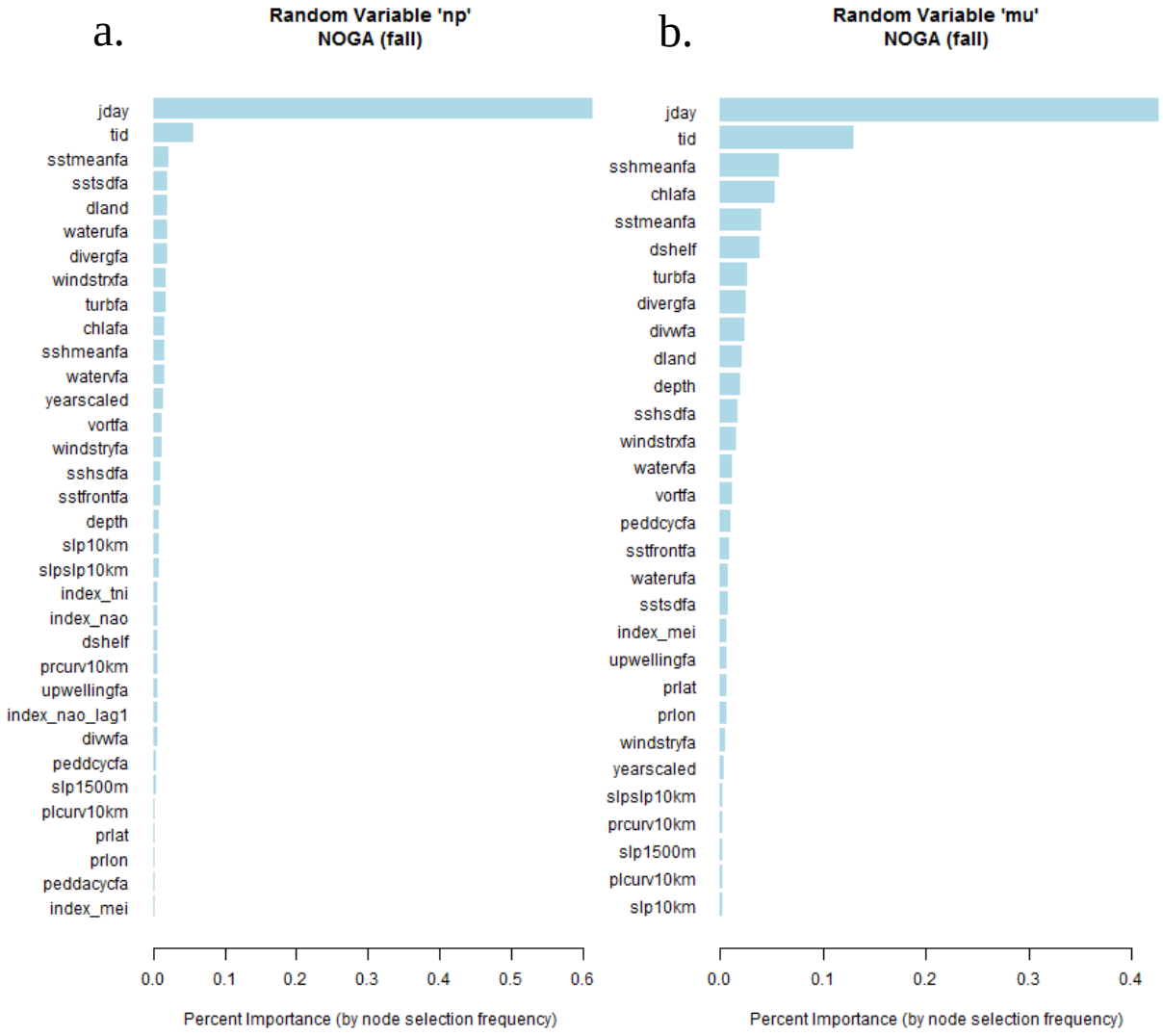

Figure 9.2. Variable importance bar plots for top variables in example model 7 (NOGA/fall). a) np component; b) mu component. For complete set of variable importance bar plots, see Appendix H.

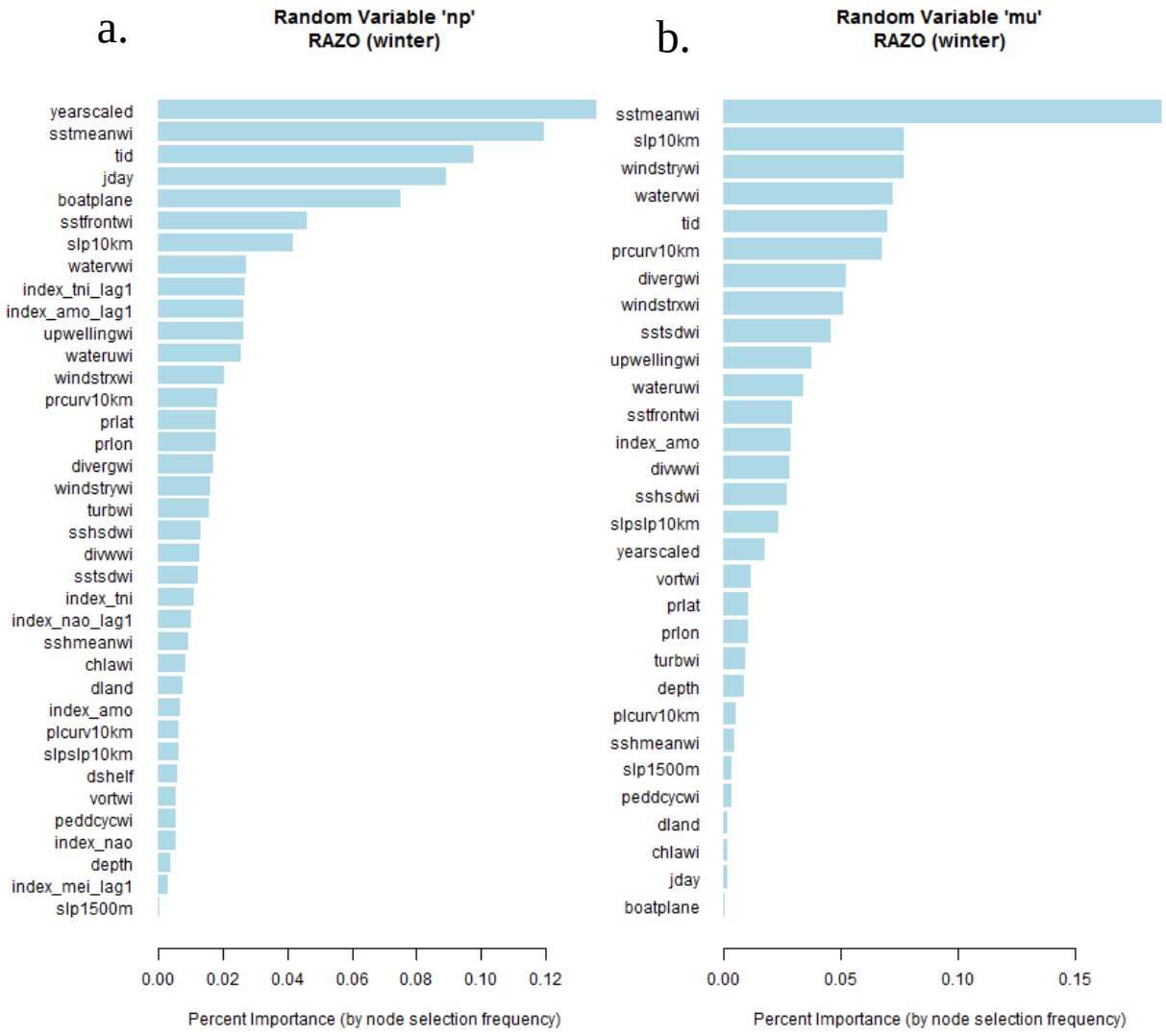

Figure 9.3. Variable importance bar plots for top variables in example model 7 (RAZO/winter). a) np component; b) mu component. For complete set of variable importance bar plots, see Appendix H.

a.

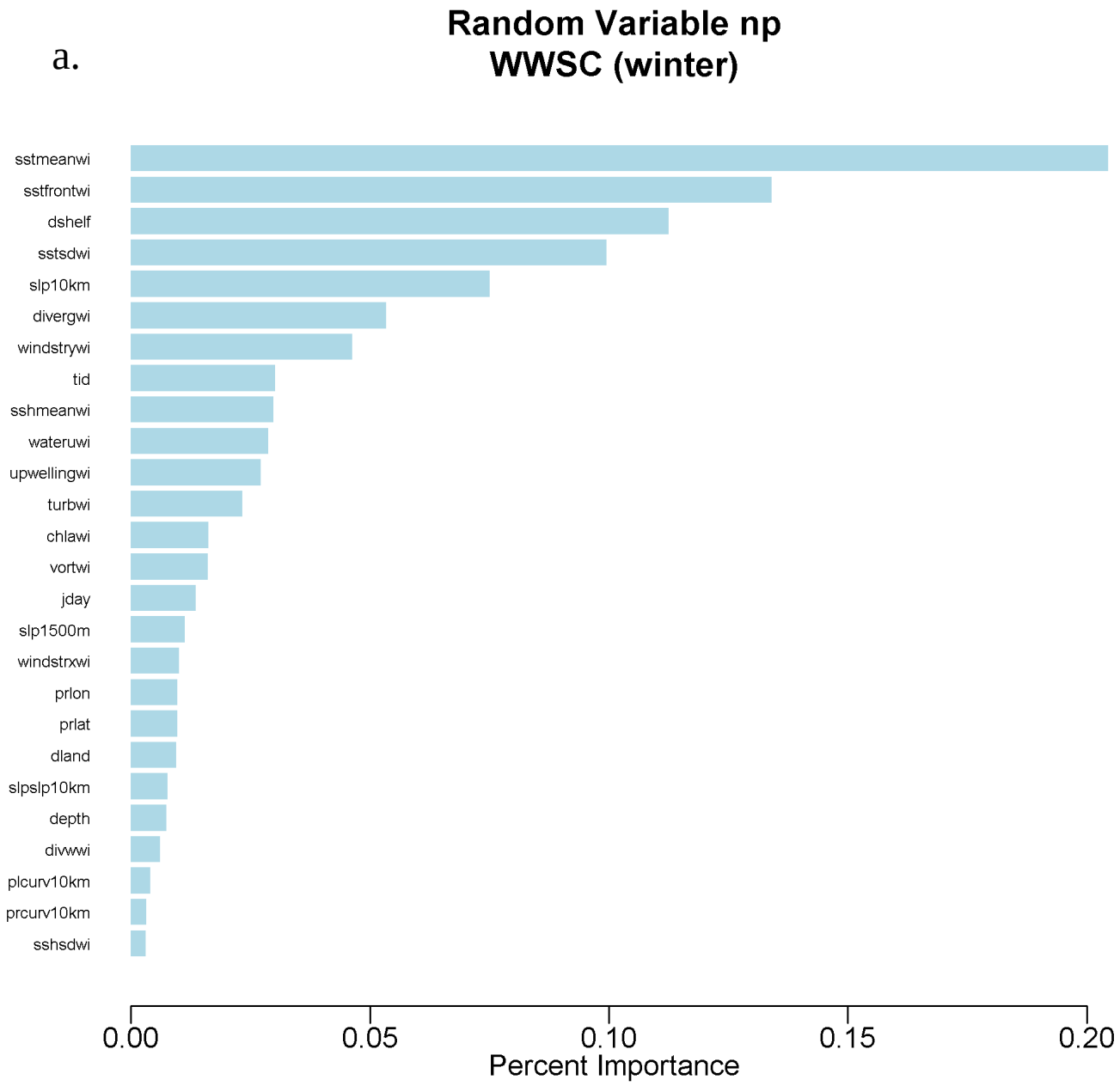

Figure 9.4. Variable importance bar plots for top variables in example model 8 (WWSC/winter). a) np component; b) mu component; c) theta component. For complete set of variable importance bar plots, see Appendix H.

b.

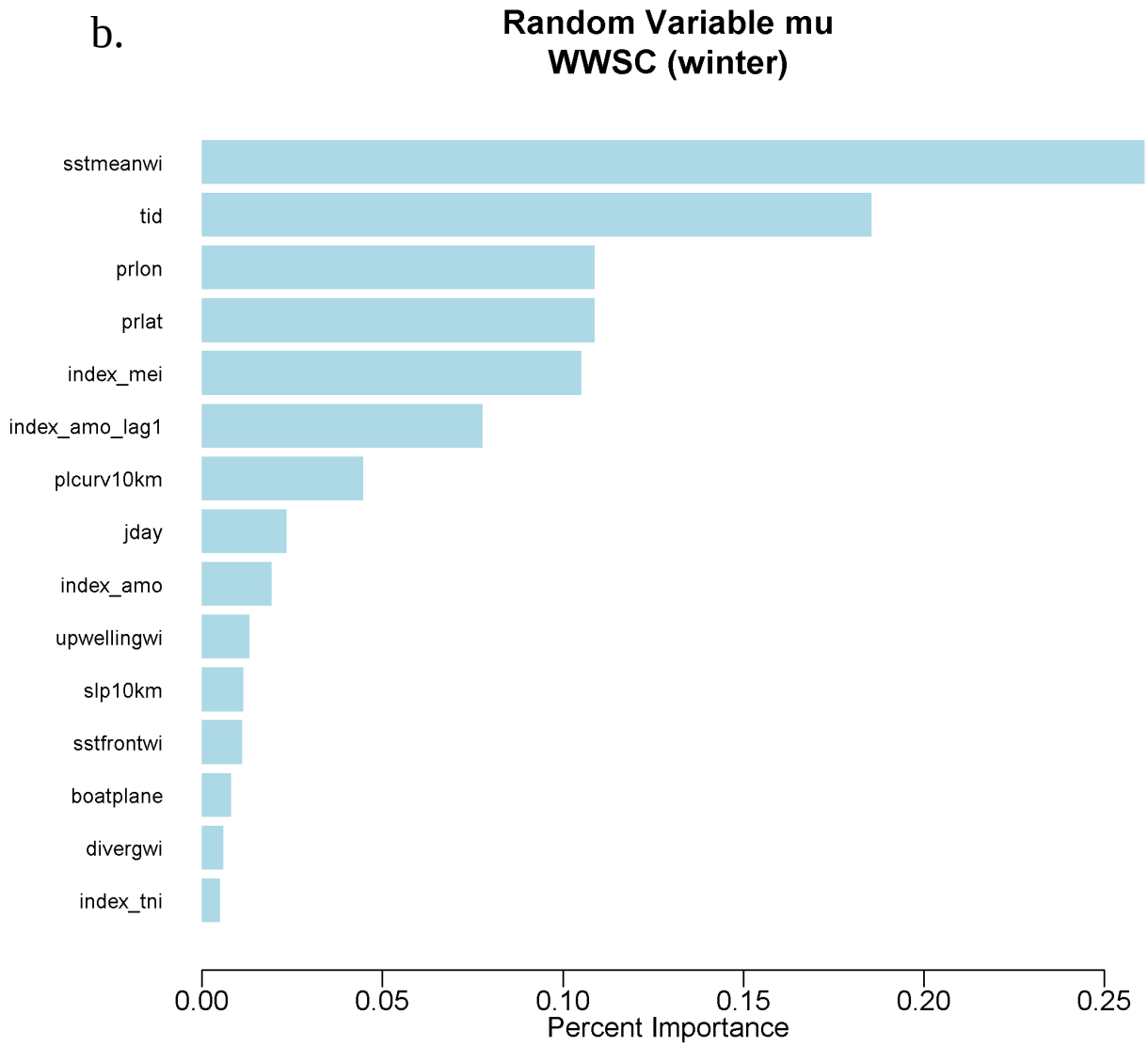

Figure 9.4. Continued.

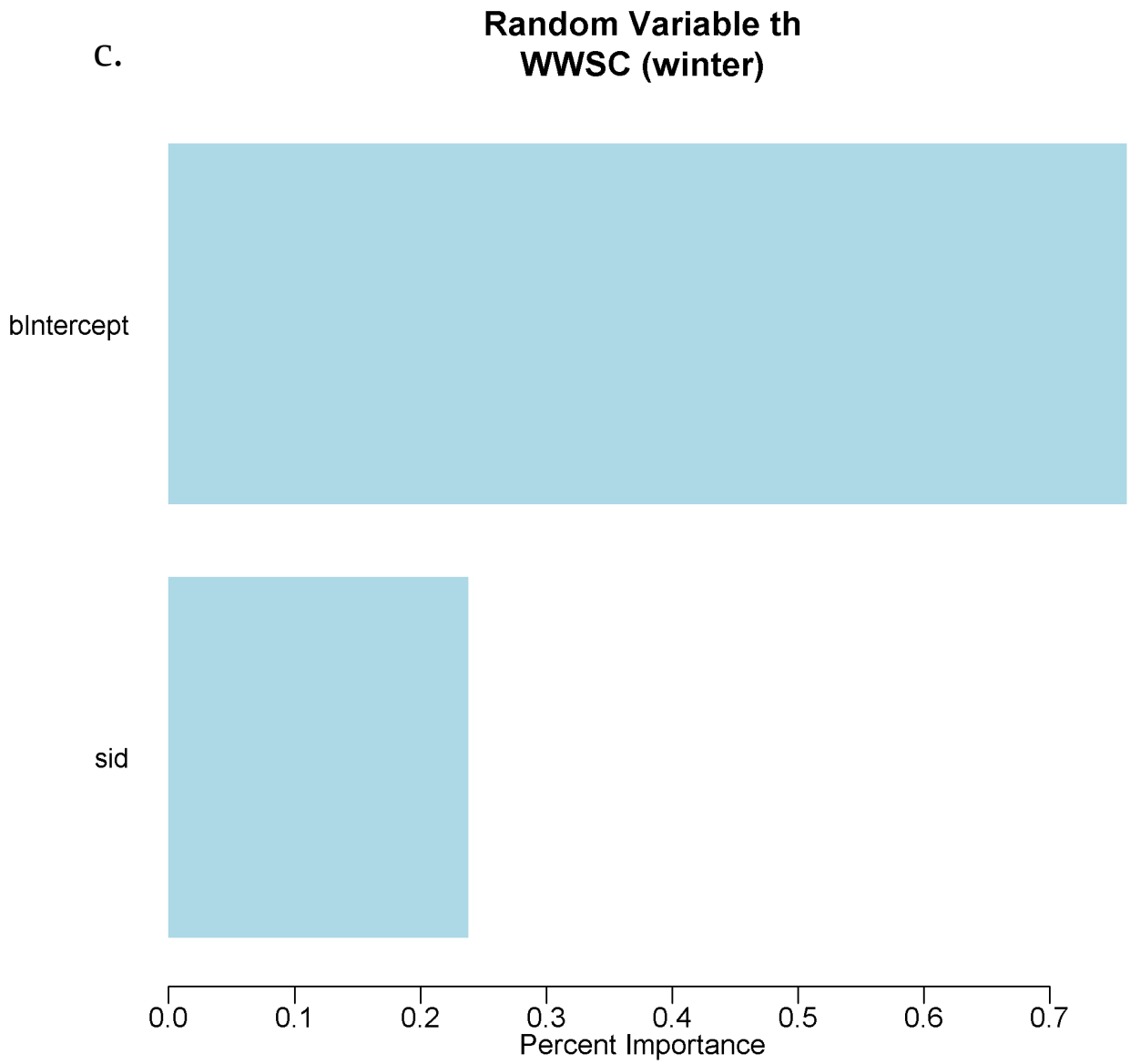

Figure 9.4. Continued.

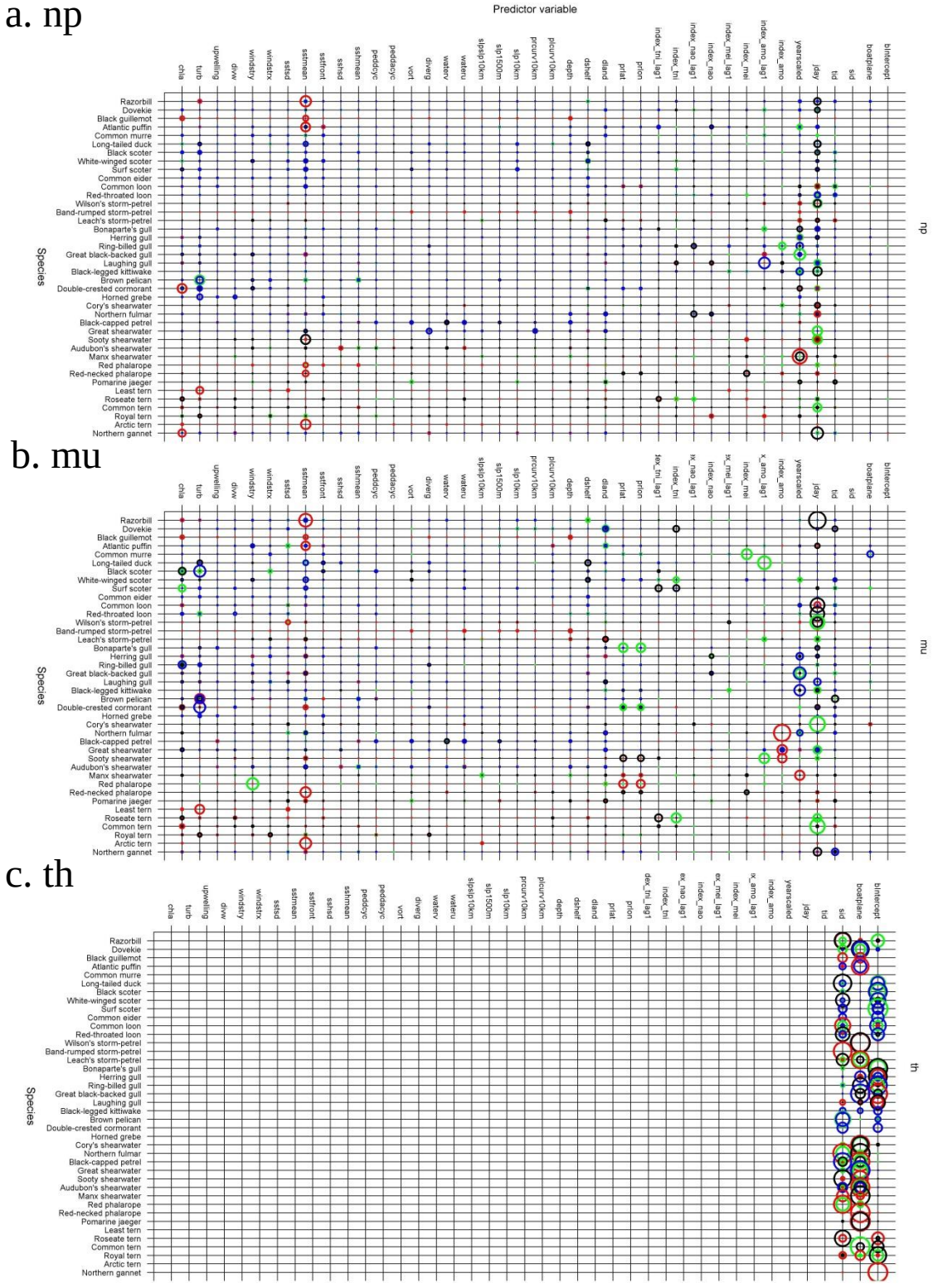

Figure 10. Summary of variable importance across all variables, species, and seasons modeled. a) np component; b) mu component; c) theta component. For complete set of variable importance plots, see Appendix H.

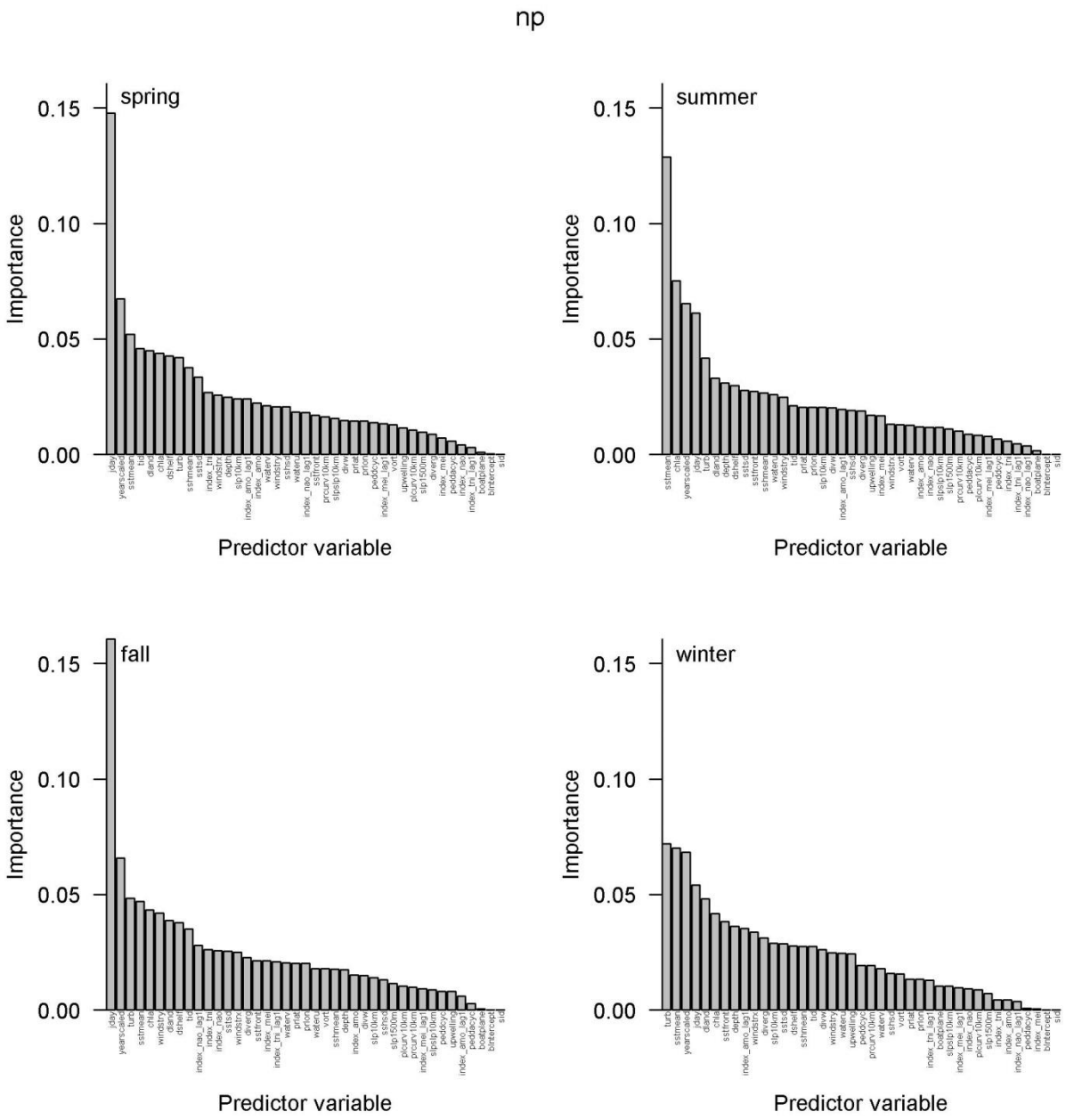

Figure 11. Variable importance for np model component: average importance of each variable calculated over all final selected models in each season. Note that average importance values have been sorted in descending order for each season, so that the order of variables along the x-axis varies from season to season. Also note that the species modeled in each season, and therefore the species included in the average for each seasonal panel of this plot, vary as shown in Table 2. For complete set of variable importance plots, see Appendix H.

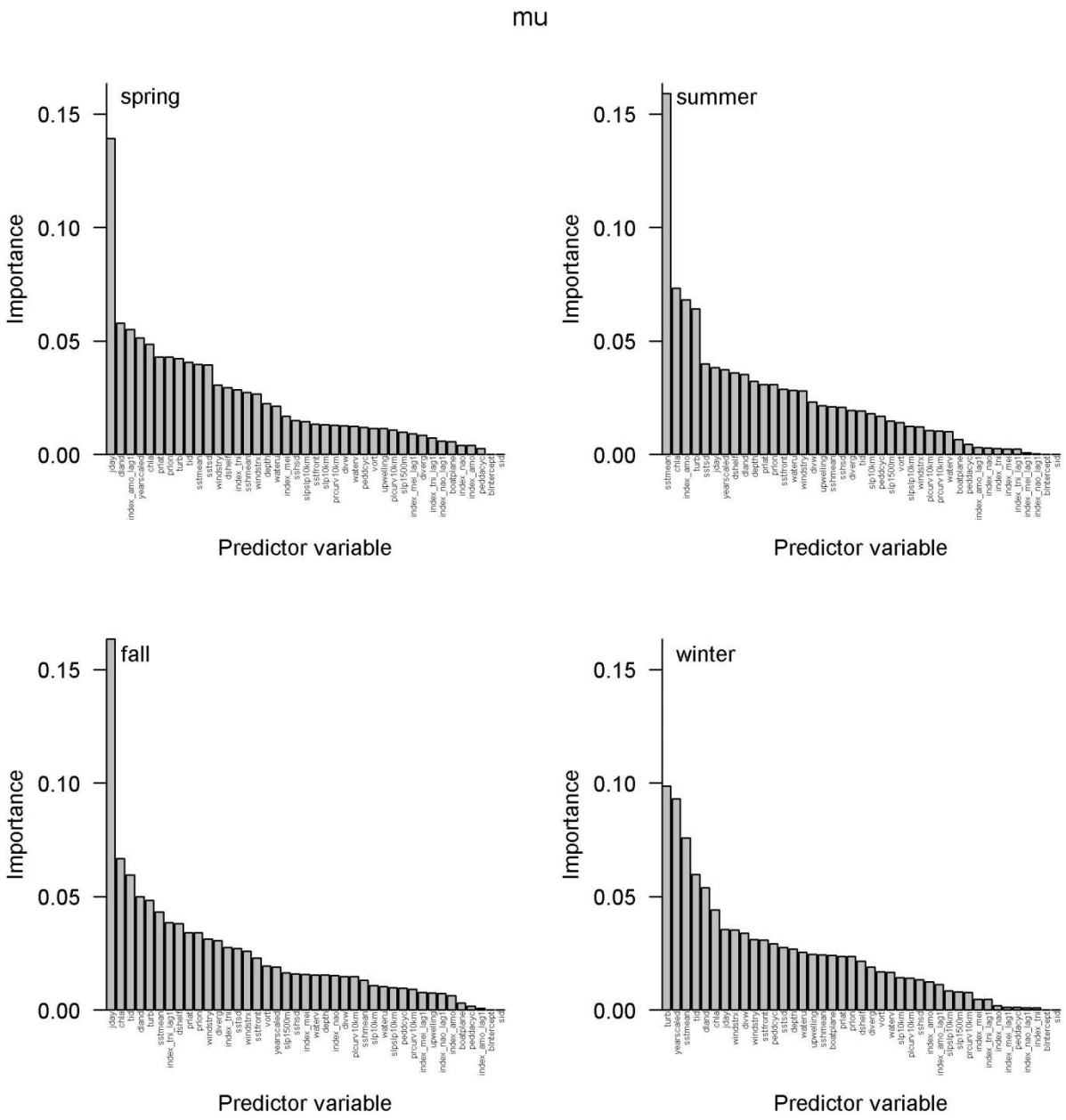

Figure 12. Variable importance for mu model component: average importance of each variable calculated over all final selected models in each season. Note that average importance values have been sorted in descending order for each season, so that the order of variables along the x-axis varies from season to season. Also note that the species modeled in each season, and therefore the species included in the average for each seasonal panel of this plot, vary as shown in Table 2. For complete set of variable importance plots, see Appendix H.

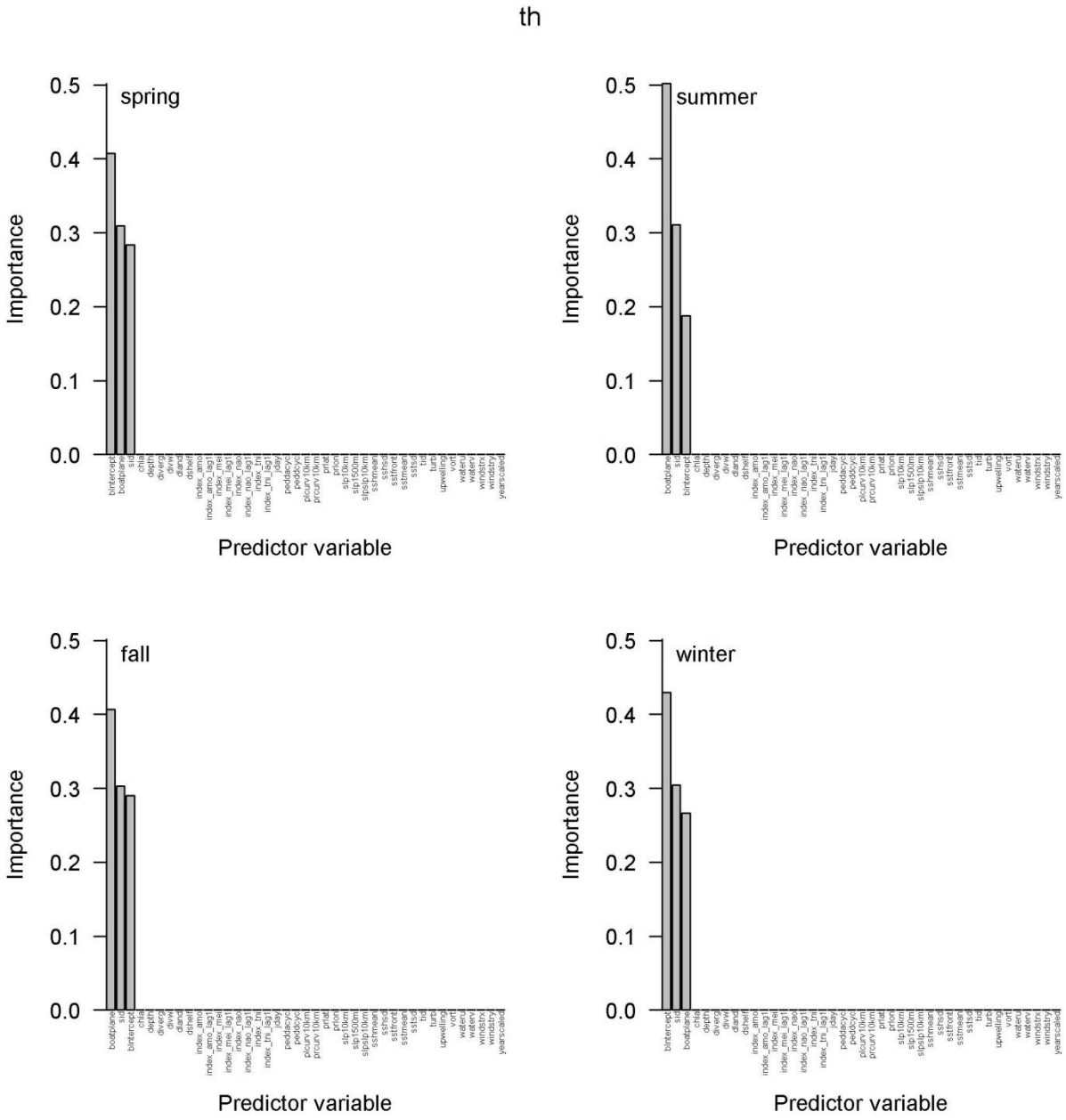

Figure 13. Variable importance for theta (th) model component: average importance of each variable calculated over all final selected models in each season. Note that average importance values have been sorted in descending order for each season, so that the order of variables along the x-axis varies from season to season. Also note that the species modeled in each season, and therefore the species included in the average for each seasonal panel of this plot, vary as shown in Table 2. Only species for which the ZINB model (Model 8) was selected are included in the average for the theta component (see Table 10 for the selected model for each species/season combination). Predictors used in the theta ensemble were limited to survey variables (sid, boatplane) and an intercept. For complete set of variable importance plots, see Appendix H.

a. selected bootstrap marginal plots from *np* model component

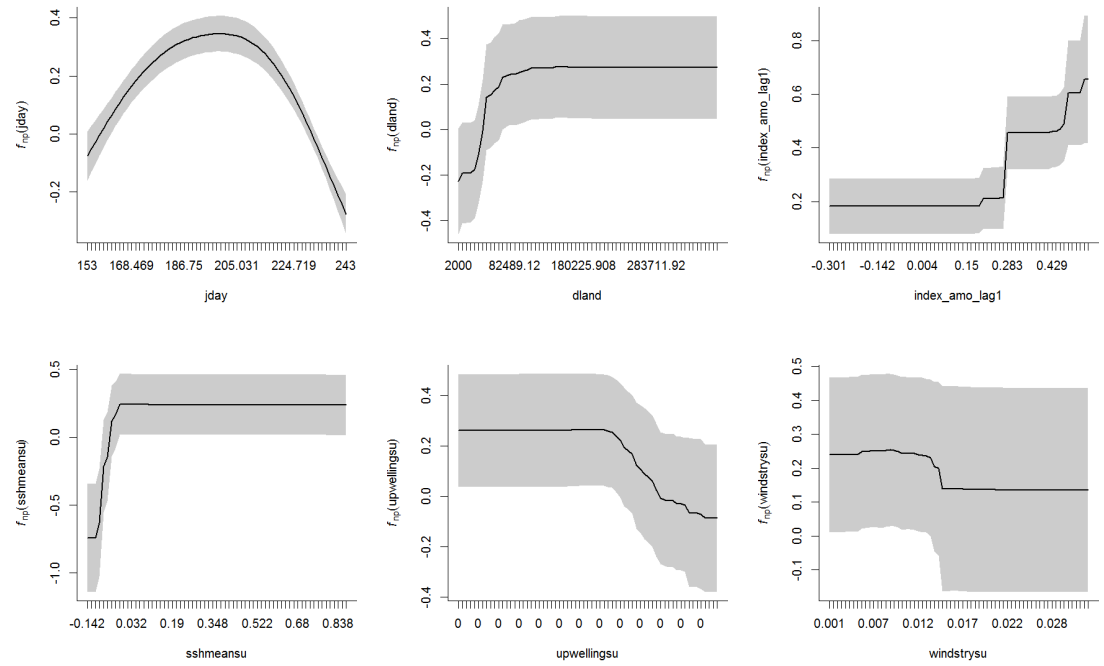

b. selected bootstrap marginal plots from *mu* model component

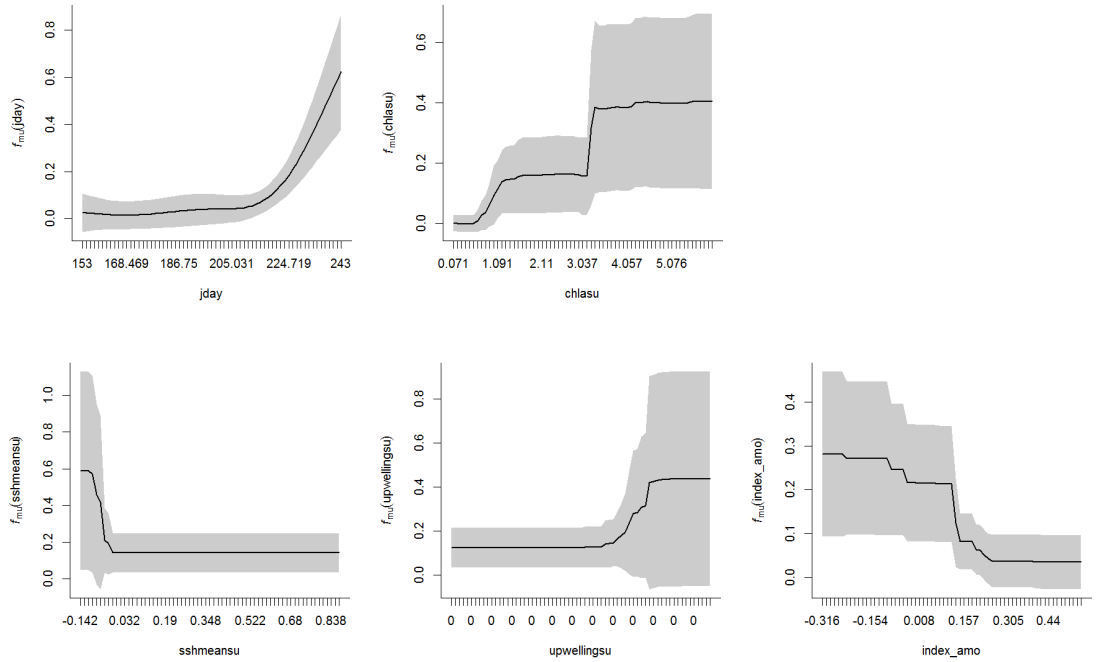

Figure 14.1. Selected bootstrap marginal plots for example model 7 (COTE/summer). Solid line is bootstrap mean and grey shading indicates +/- 1 bootstrap standard deviation. a) np component of model; b) mu component of model. Full sets of marginal plots in Appendix I.

a. selected bootstrap marginal plots from *np* model component

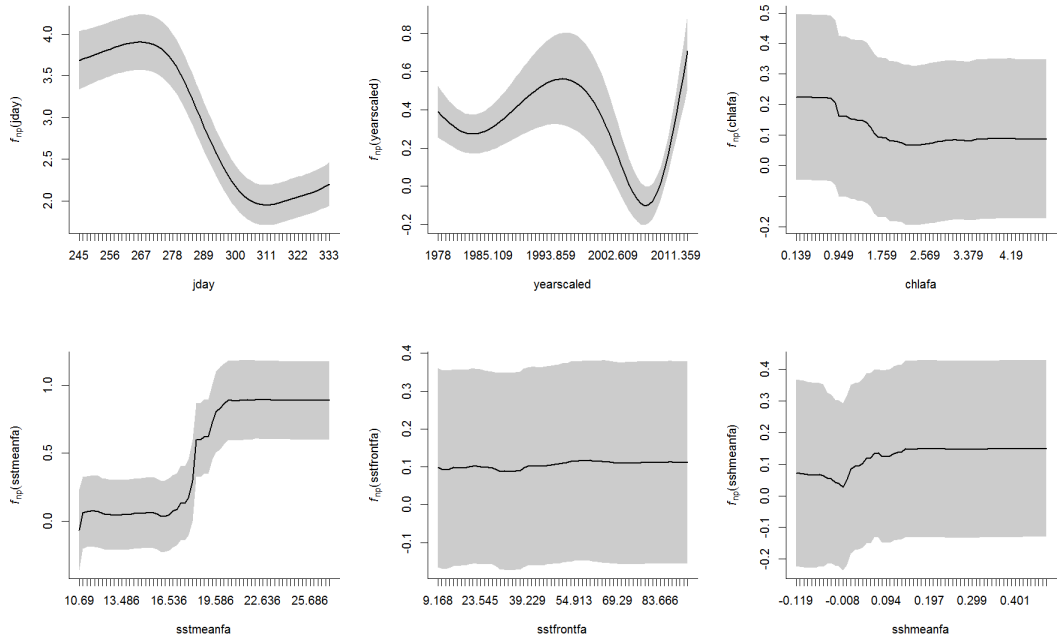

b. selected bootstrap marginal plots from *mu* model component

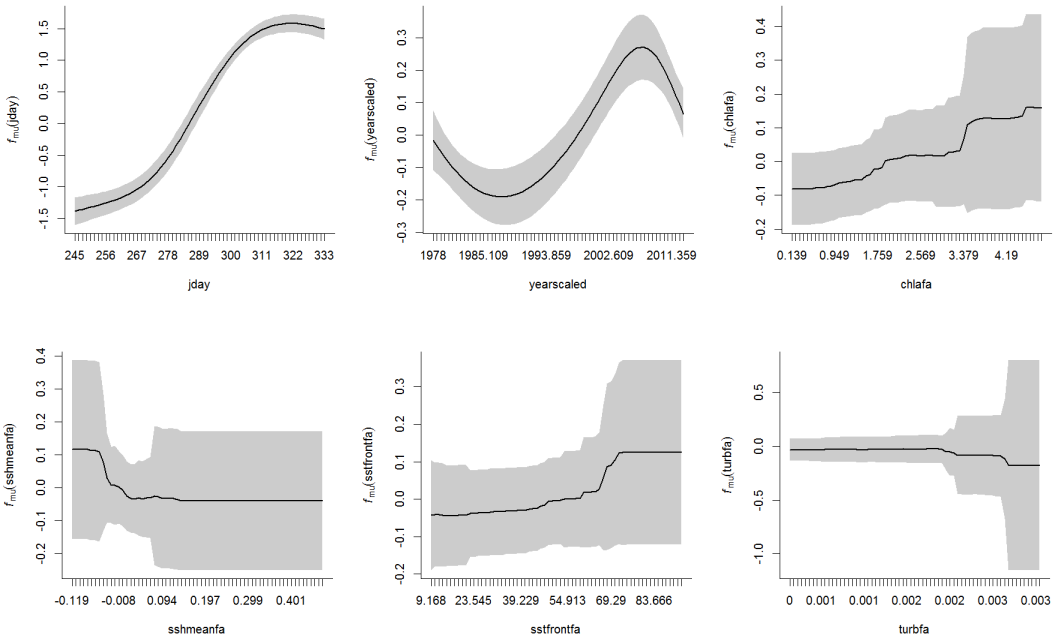

Figure 14.2. Selected bootstrap marginal plots for example model 7 (NOGA/fall). Solid line is bootstrap mean and grey shading indicates +/- 1 bootstrap standard deviation. a) np component of model; b) mu component of model. Full sets of marginal plots in Appendix I.

a. selected bootstrap marginal plots from *np* model component

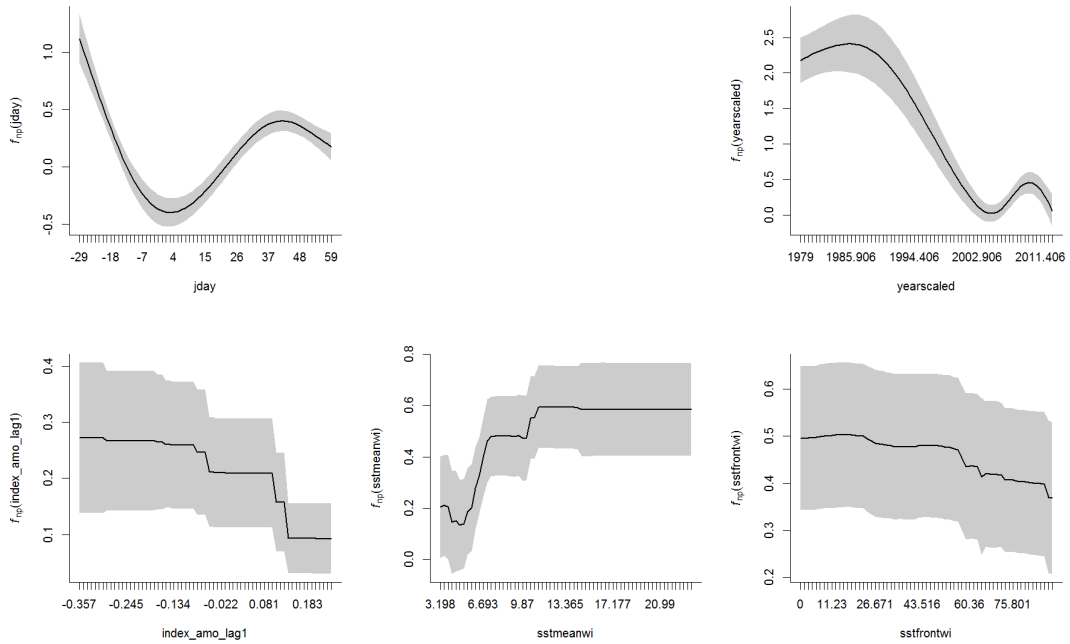

b. selected bootstrap marginal plots from *mu* model component

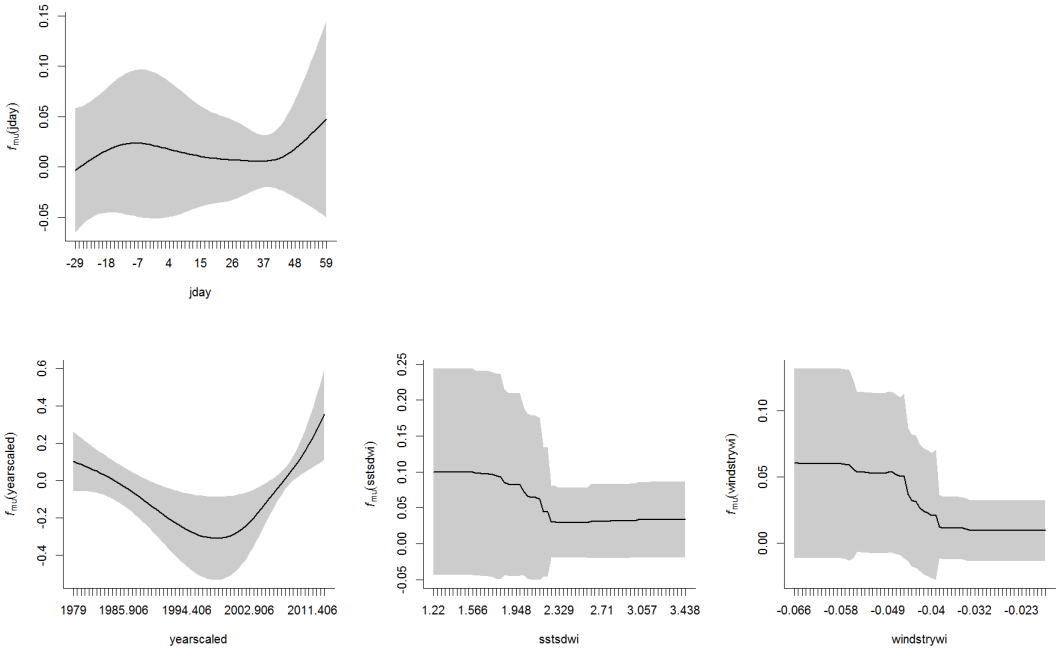

Figure 14.3. Selected bootstrap marginal plots for example model 7 (RAZO/winter). Solid line is bootstrap mean and grey shading indicates +/- 1 bootstrap standard deviation. a) np component of model b) mu component of model. Full sets of marginal plots in Appendix I.

a. selected bootstrap marginal plots from *np* model component

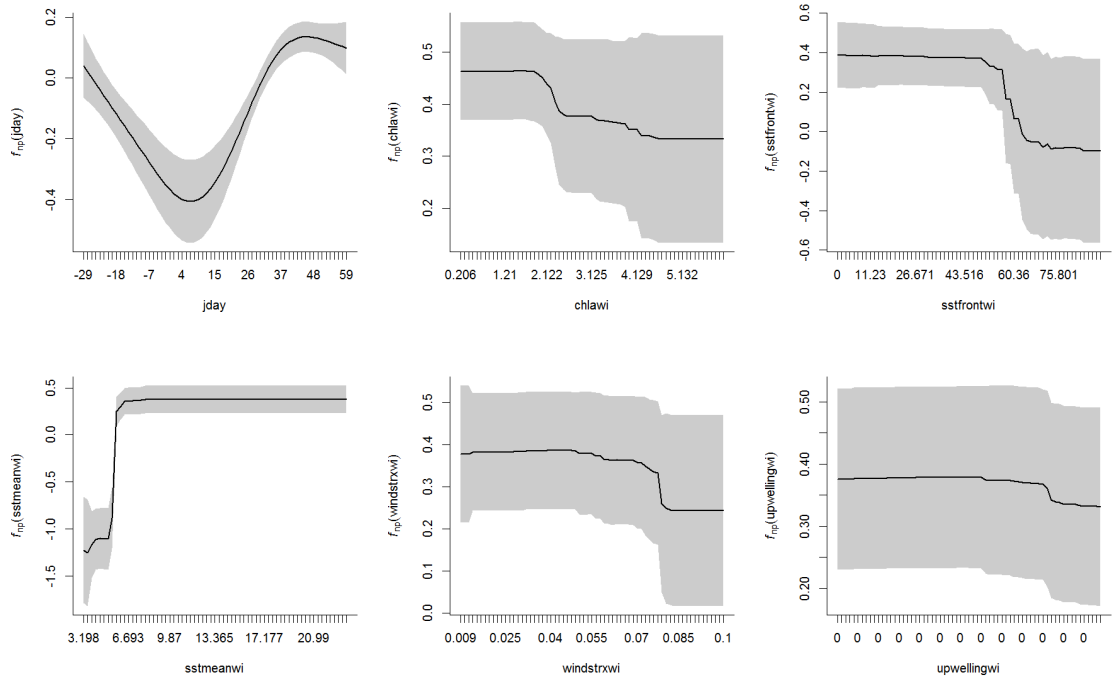

b. selected bootstrap marginal plots from *mu* model component

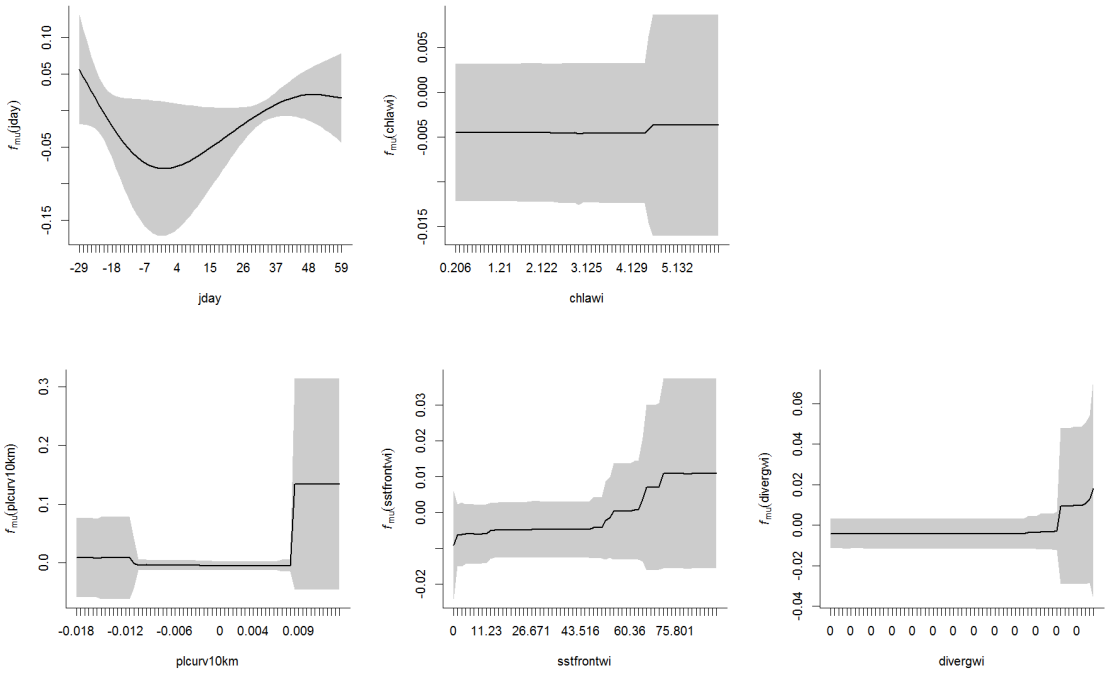

Figure 14.4. Selected bootstrap marginal plots for example model 8 (WWSC/winter). Solid line is bootstrap mean and grey shading indicates +/- 1 bootstrap standard deviation. a) np component of model; b) mu component of model. Full sets of marginal plots in Appendix I.

a. selected two-way interaction plots from *np* model component

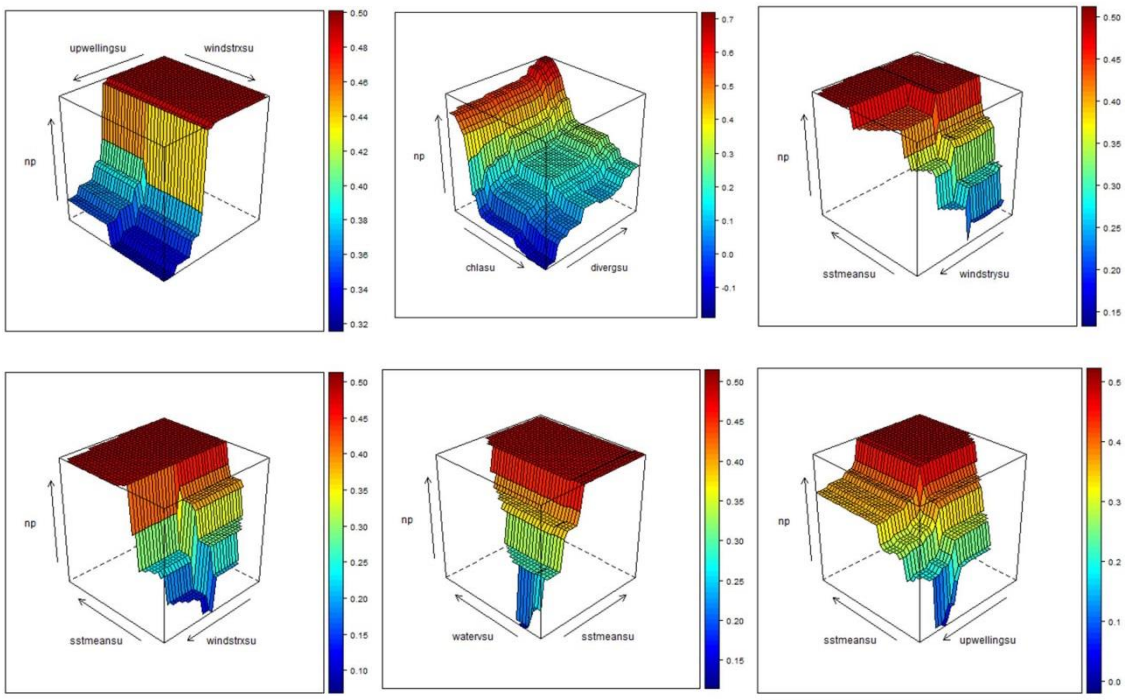

b. selected two-way interaction plots from *mu* model component

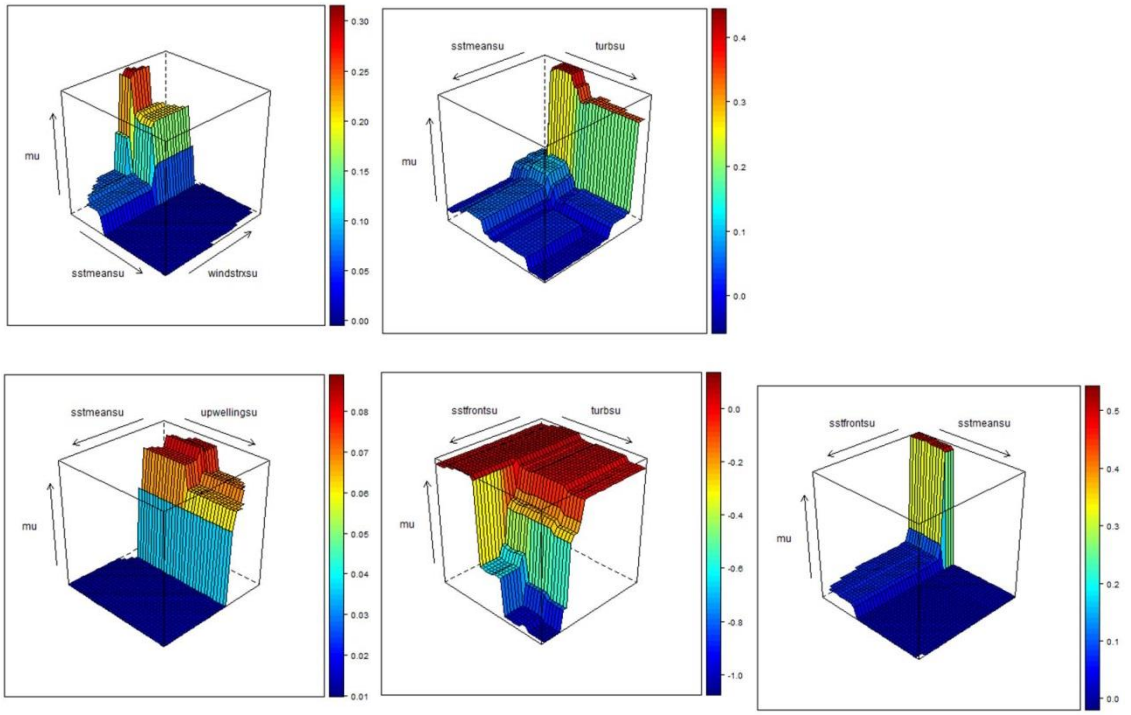

Figure 15.1. Selected two-way interaction plots for example model 7 (COTE/summer). a) np component of model; b) mu component of model. Full sets of two-way interaction plots in Appendix J.

a. selected bootstrap marginal plots from *np* model component

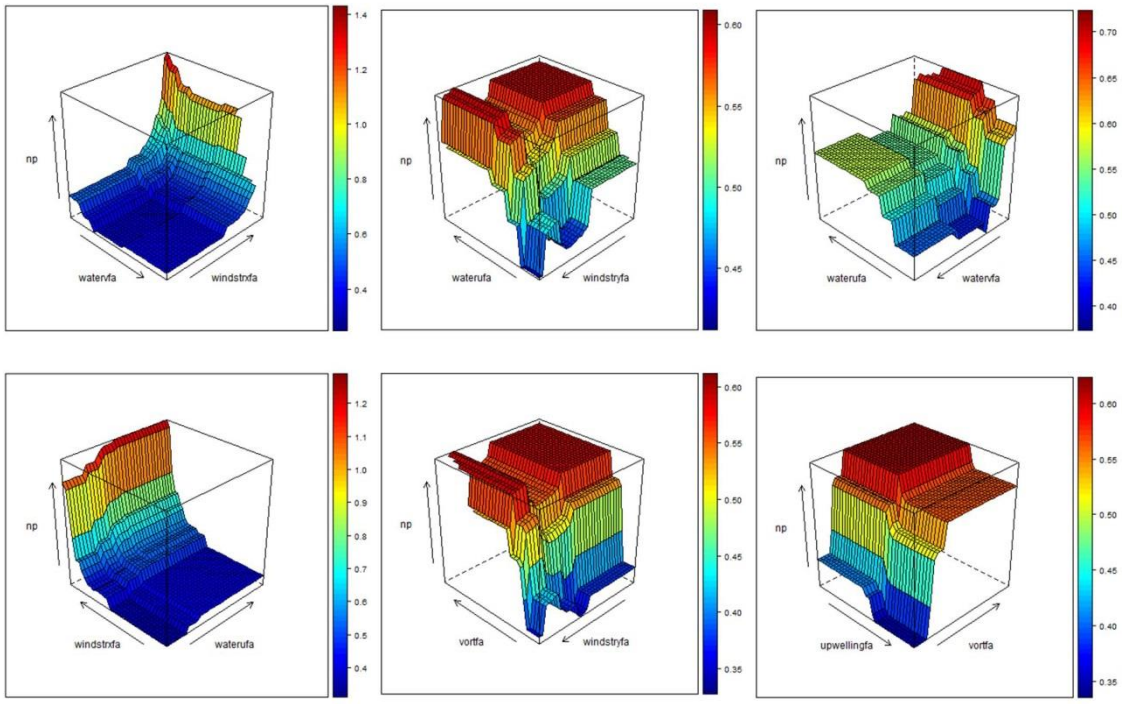

b. selected bootstrap marginal plots from *mu* model component

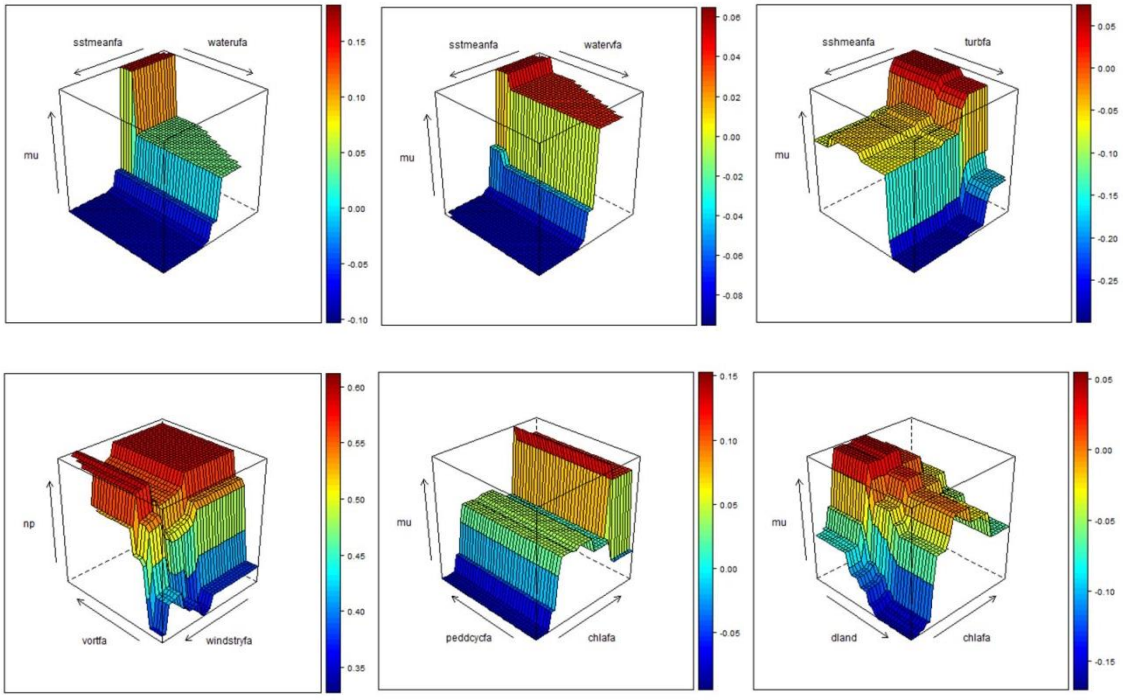

Figure 15.2. Selected two-way interaction plots for example model 7 (NOGA/fall). a) np component of model; b) mu component of model. Full sets of two-way interaction plots in Appendix J.

a. selected bootstrap marginal plots from *np* model

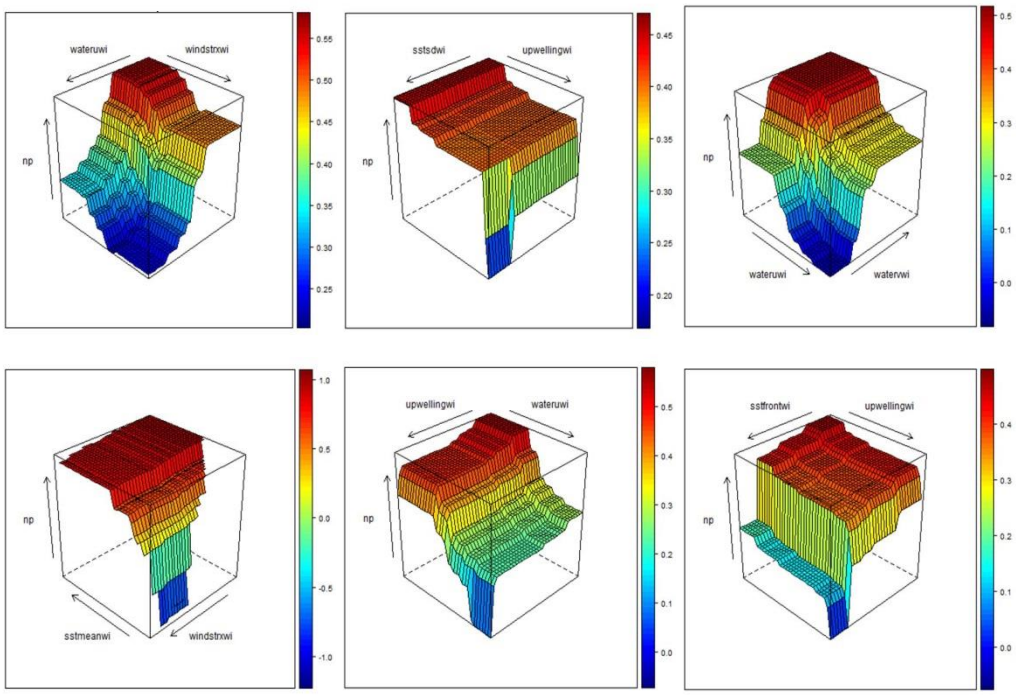

b. selected bootstrap marginal plots from *mu* model

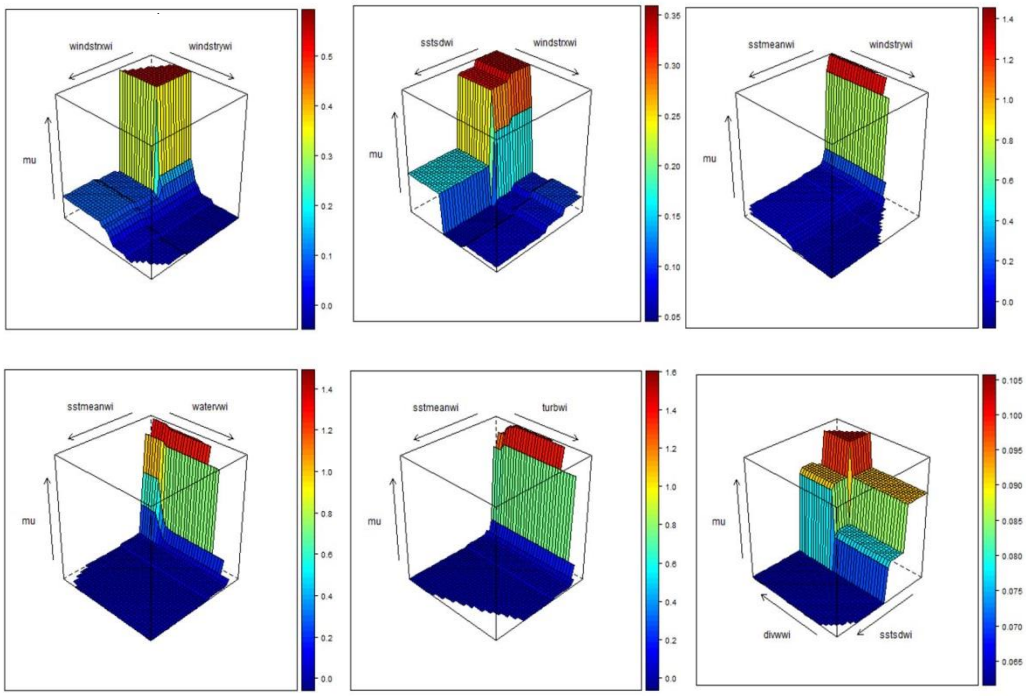

Figure 15.3. Selected two-way interaction plots for example model 7 (RAZO/winter) . a) np component of model; b) mu component of model. Full sets of two-way interaction plots in Appendix J.

a. selected bootstrap marginal plots from *np* model component

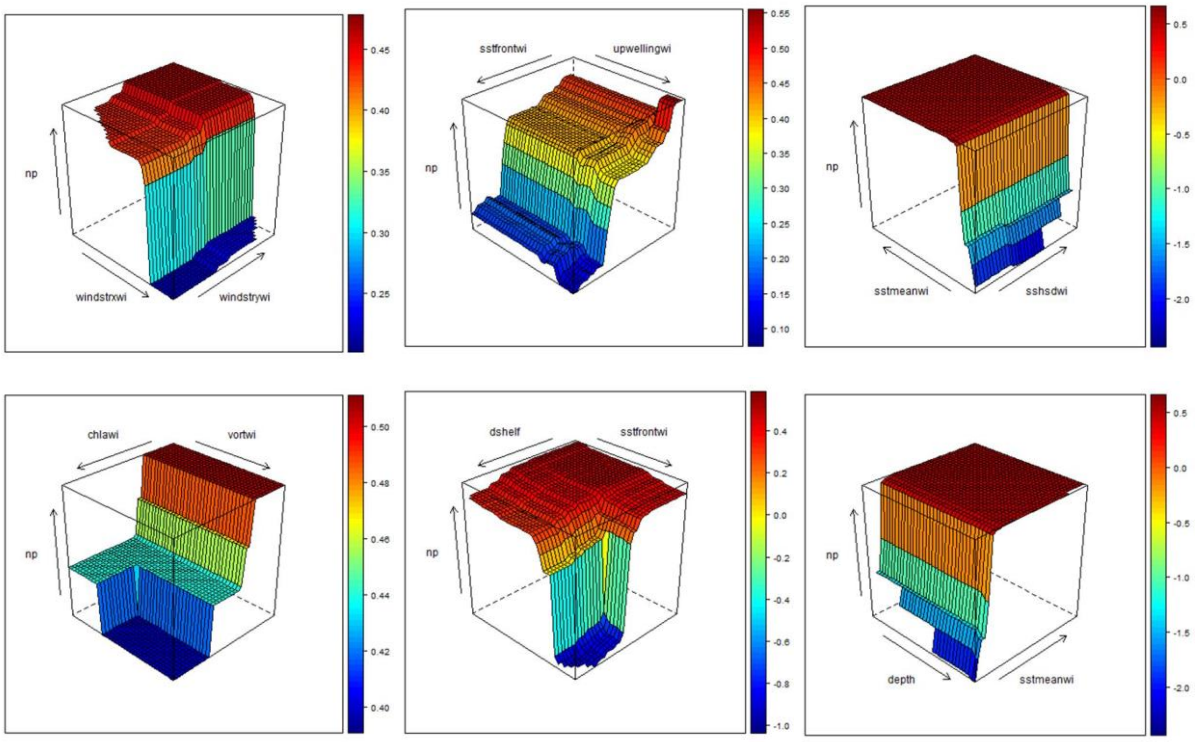

b. selected bootstrap marginal plots from *mu* model component

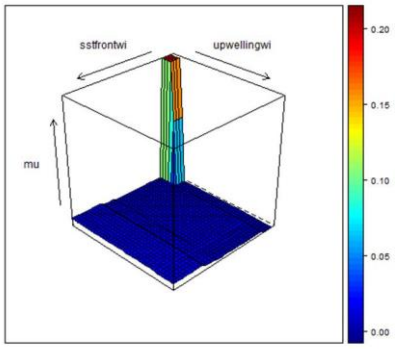

Figure 15.4. Selected two-way interaction plots for example model 8 (WWSC/winter). a) np component of model; b) mu component of model. Full sets of two-way interaction plots in Appendix J.

a. occupancy-full model mean

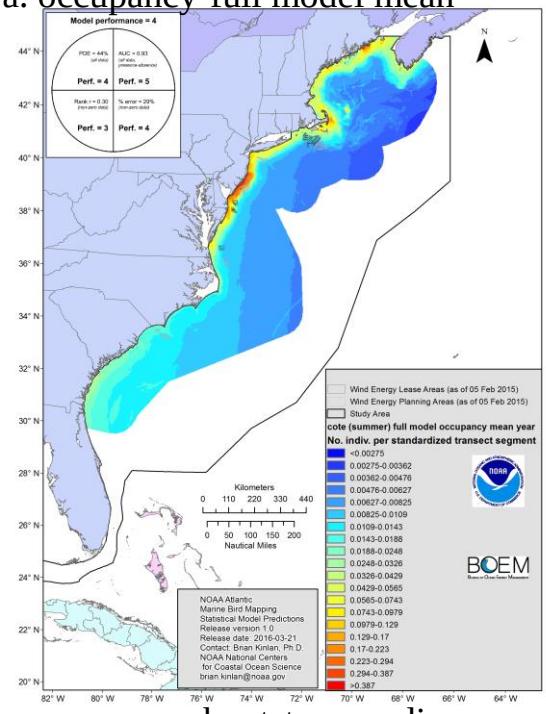

b. occupancy-bootstrap mean

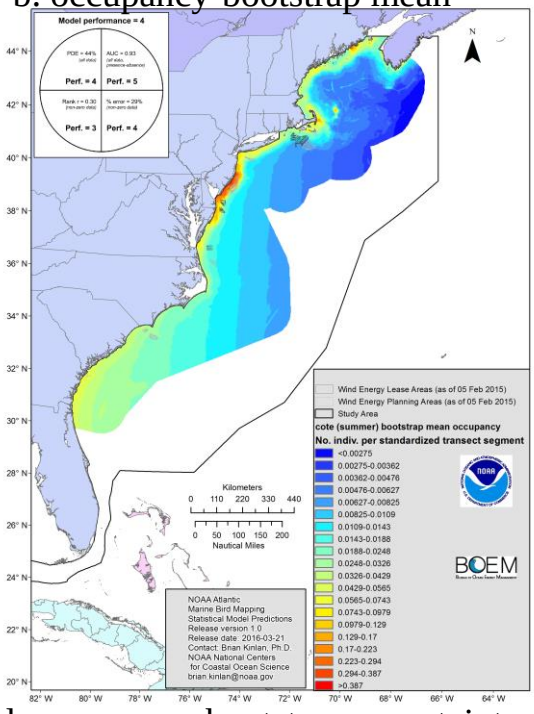

c. occupancy-bootstrap median

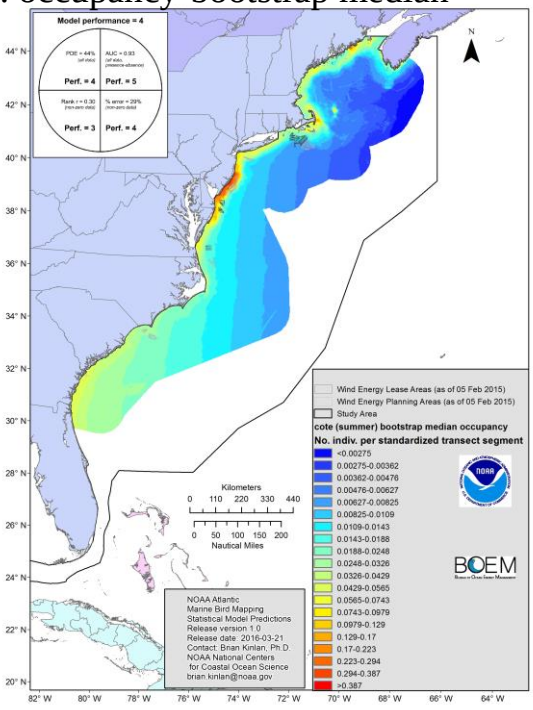

d. occupancy-bootstrap uncertainty (CI90)

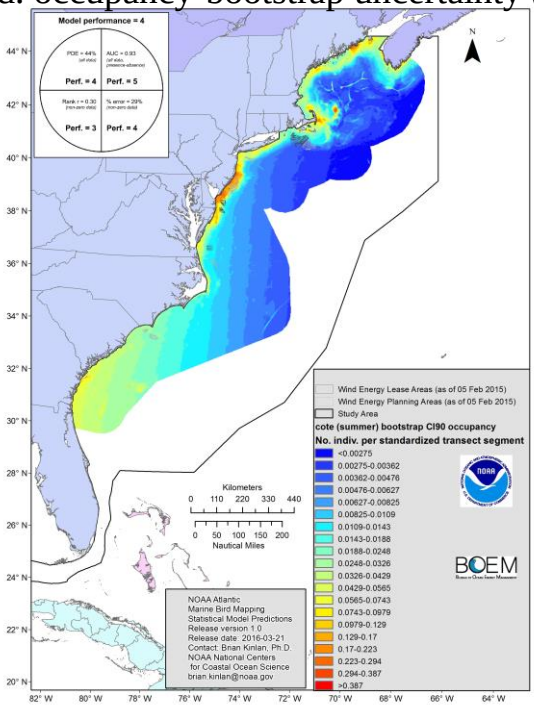

Figure 16.1 ABCD. Relative occupancy prediction maps for example model 7 (COTE/summer) from full model (a) and bootstrap (b,c) with bootstrap uncertainty map (d). For complete set of prediction and uncertainty maps, see Appendix K.

e. abundance-full model mean

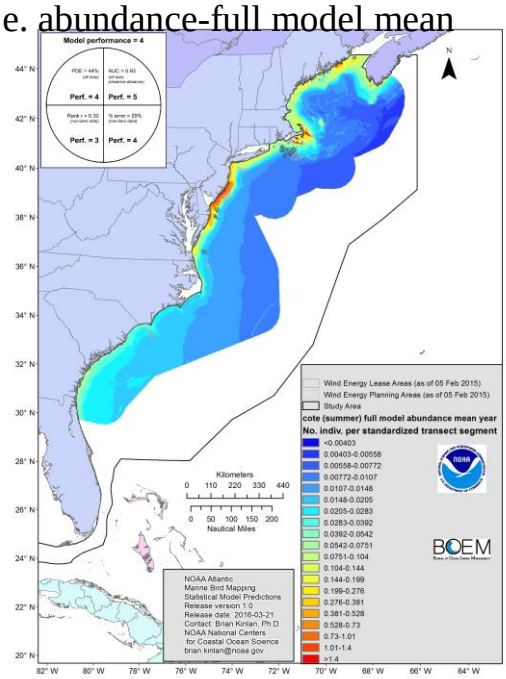

f. abundance-bootstrap mean

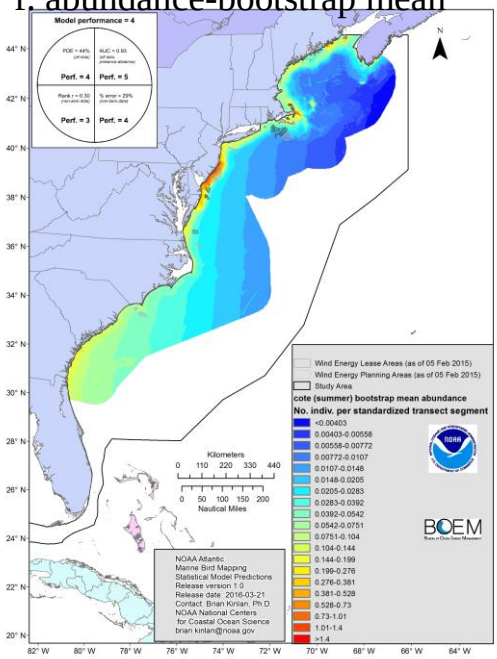

g. abundance-bootstrap median

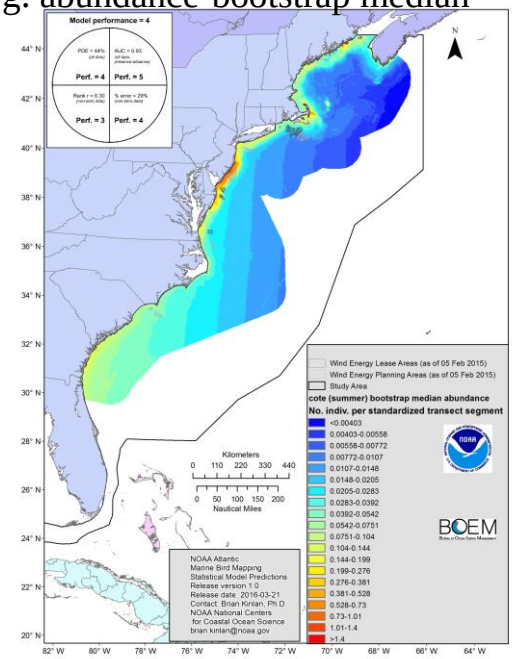

h. abundance-bootstrap uncertainty (CI90)

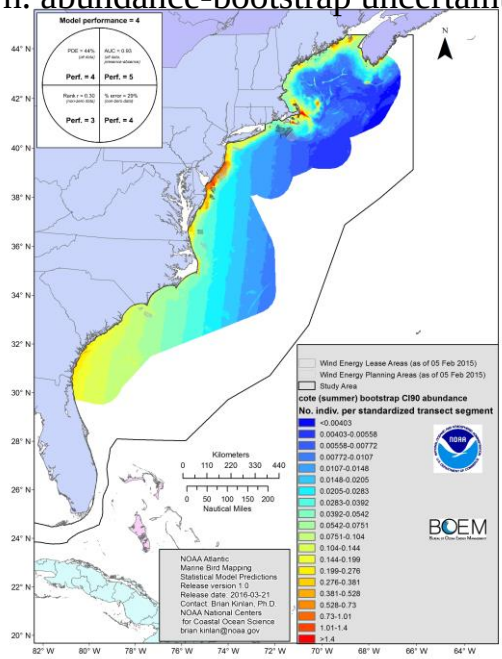

Figure 16.1 EFGH. Relative abundance prediction maps for example model 7 (COTE/summer) from full model (e) and bootstrap (f,g) with bootstrap uncertainty map (h). For complete set of prediction and uncertainty maps, see Appendix K.

i. average count per 10 x 10 km grid cell

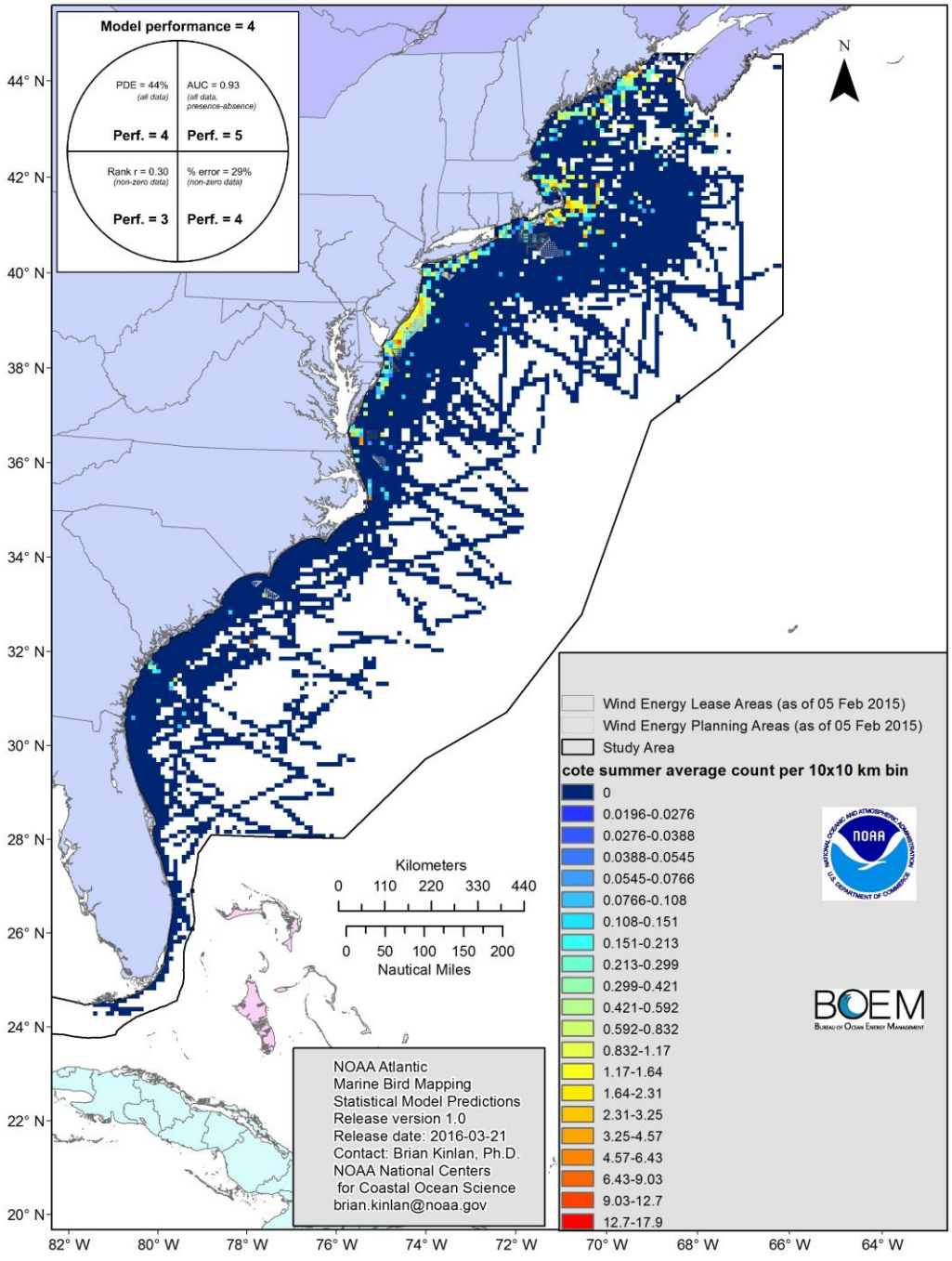

Figure 16.1 I. Average count per 10 x 10 km grid cell (COTE/summer).

a. occupancy-full model mean

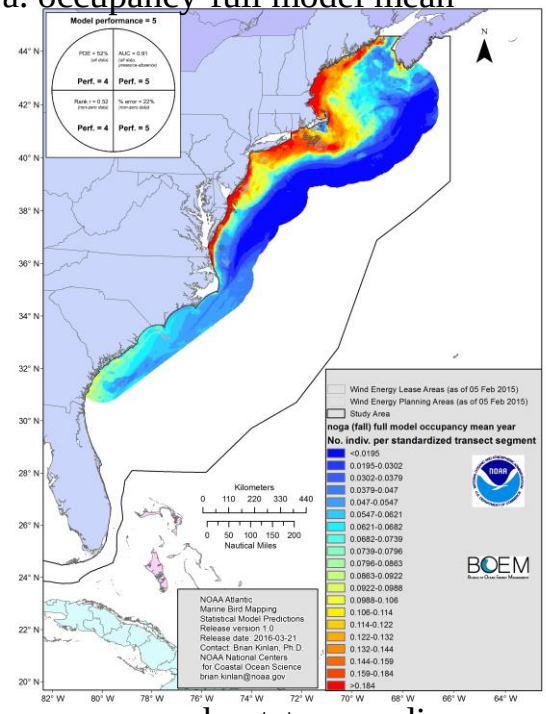

b. occupancy-bootstrap mean

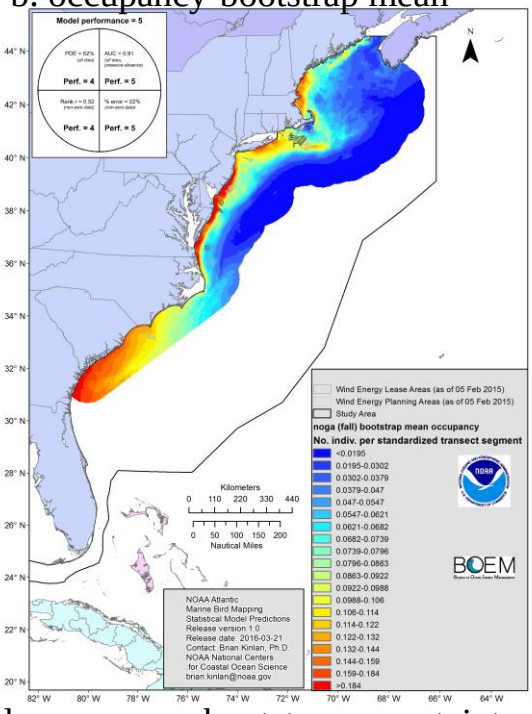

c. occupancy-bootstrap median

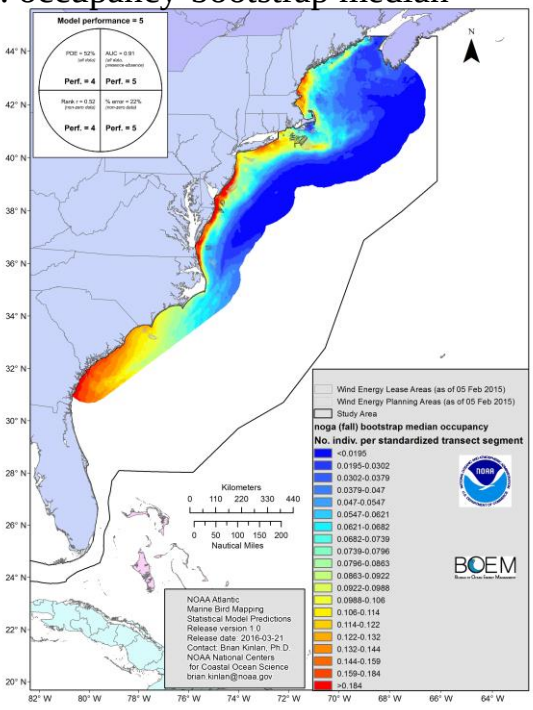

d. occupancy-bootstrap uncertainty (CI90)

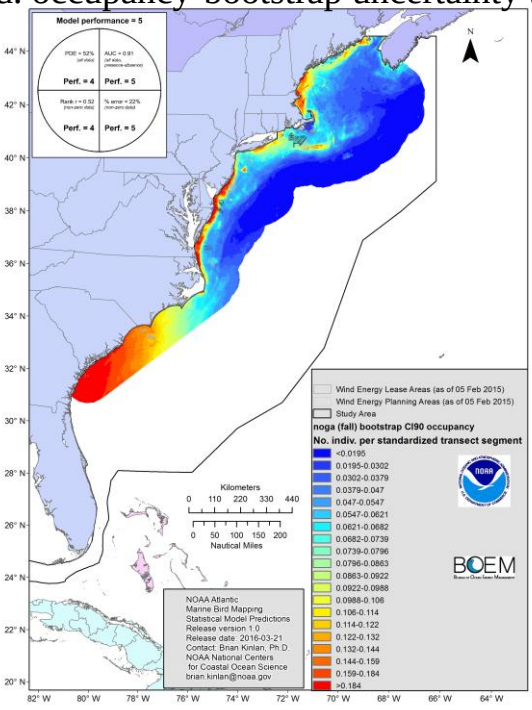

Figure 16.2 ABCD. Relative occupancy prediction maps for example model 7 (NOGA/fall) from full model (a) and bootstrap (b,c) with bootstrap uncertainty map (d). For complete set of prediction and uncertainty maps, see Appendix K.

e. abundance-full model mean

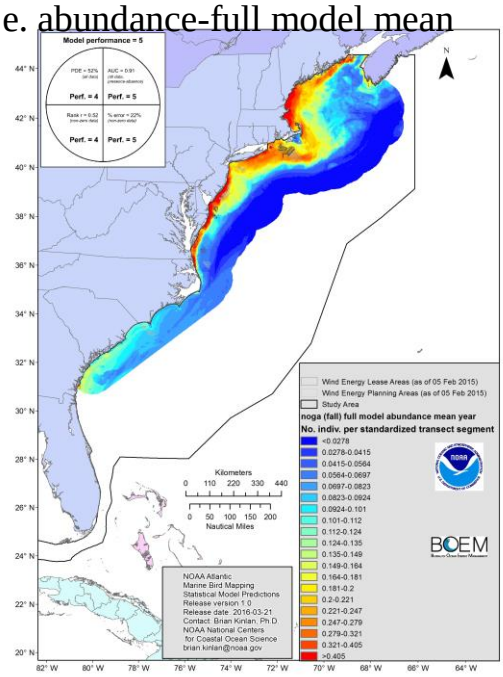

f. abundance-bootstrap mean

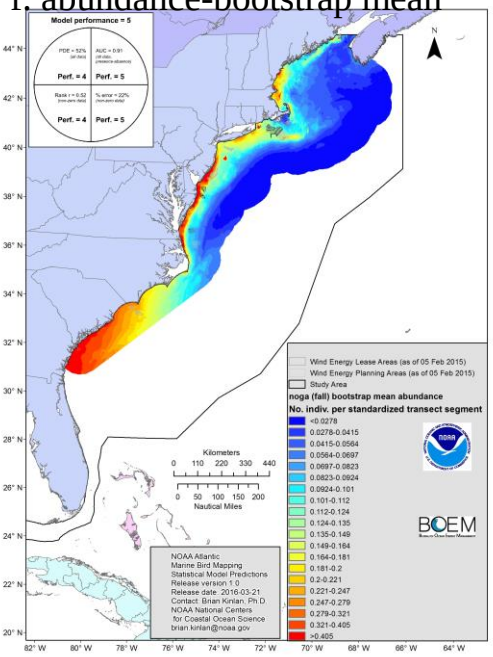

g. abundance-bootstrap median

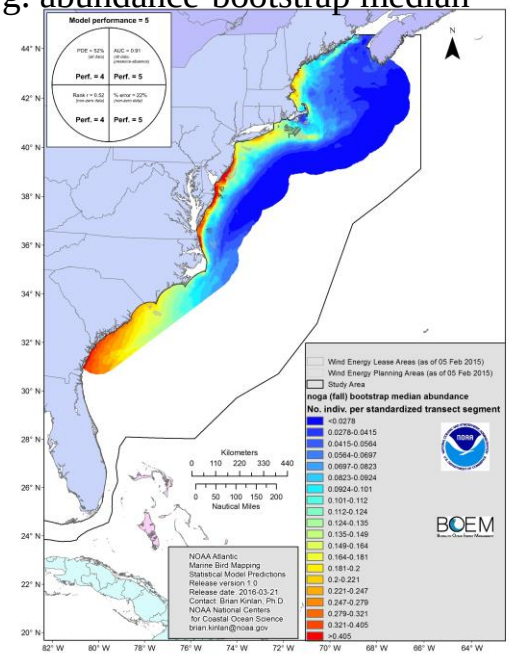

h. abundance-bootstrap uncertainty (CI90)

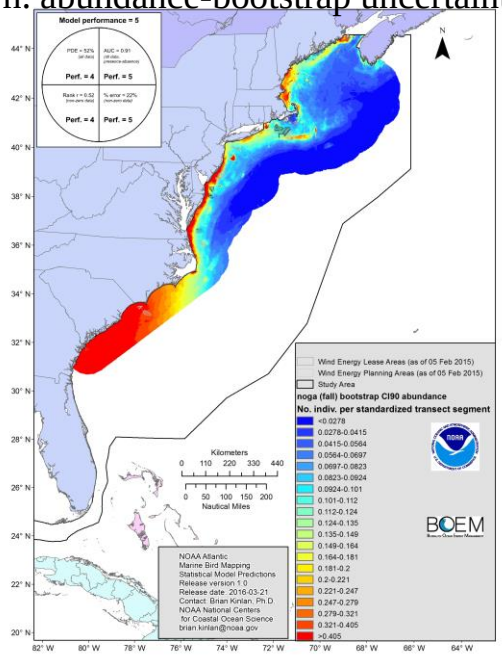

Figure 16.2 EFGH. Relative abundance prediction maps for example model 7 (NOGA/fall) from full model (e) and bootstrap (f,g) with bootstrap uncertainty map (h). For complete set of prediction and uncertainty maps, see Appendix K.

i. average count per 10 x 10 km grid cell

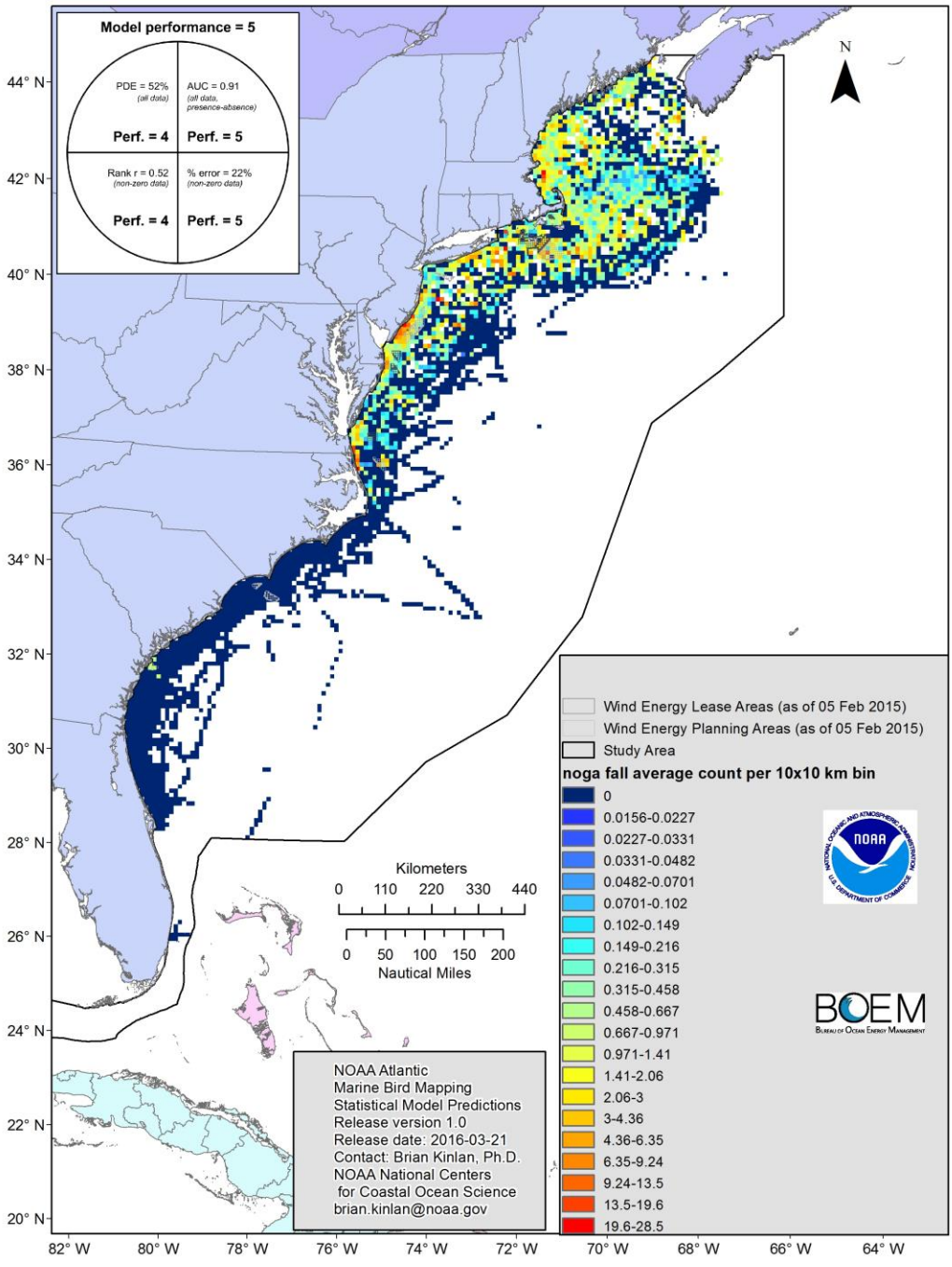

Figure 16.2 I. Average count per 10 x 10 km grid cell (NOGA/fall).

a. occupancy-full model mean

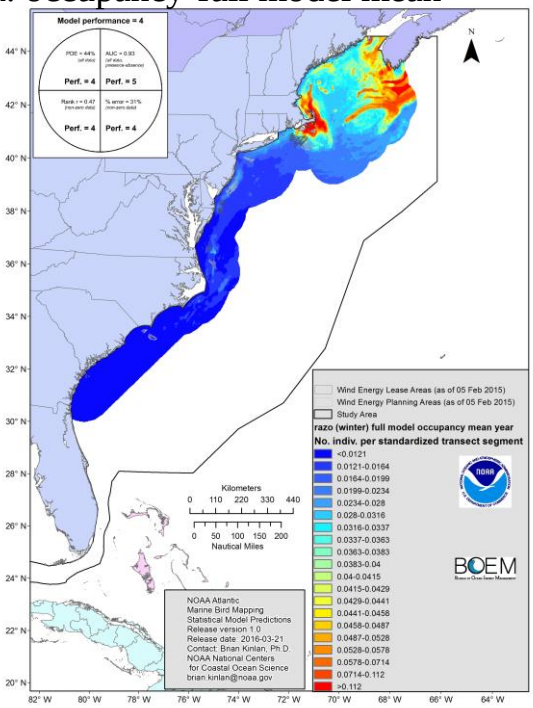

b. occupancy-bootstrap mean

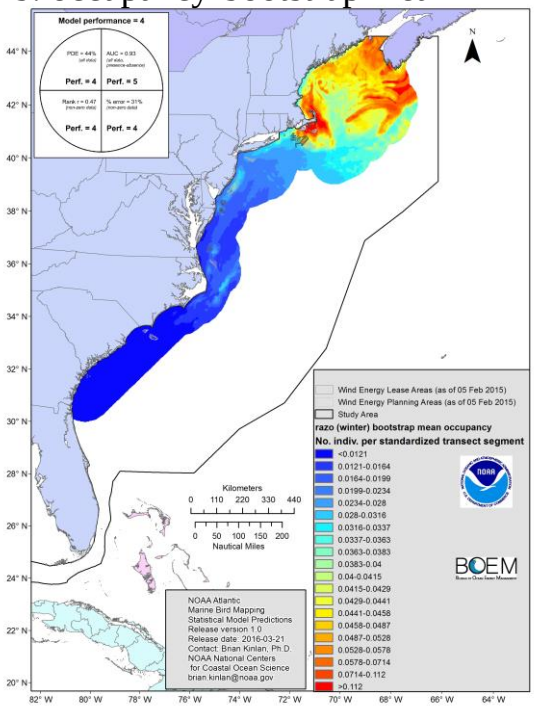

c. occupancy-bootstrap median

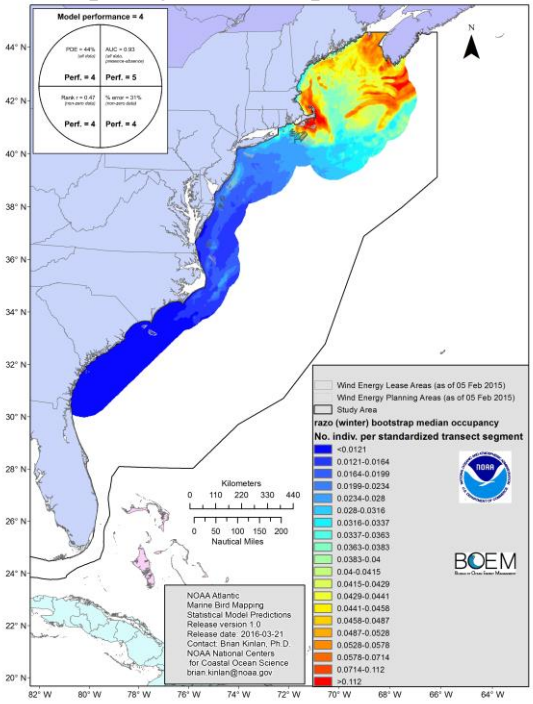

d. occupancy-bootstrap uncertainty (CI90)

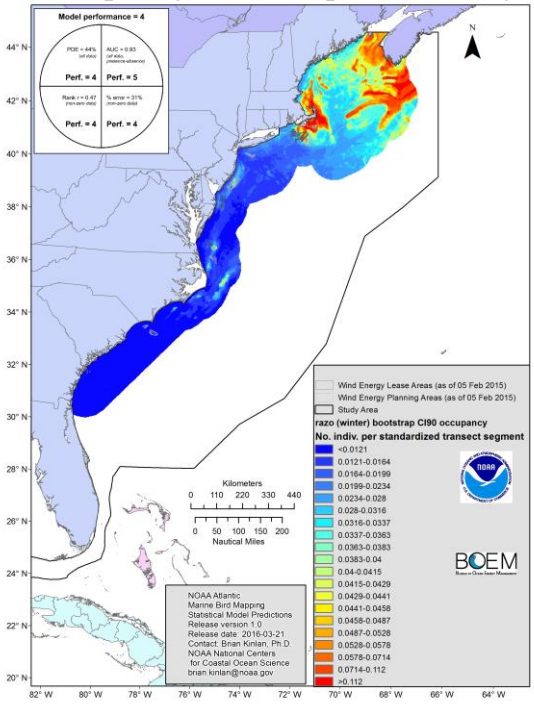

Figure 16.3 ABCD. Relative occupancy prediction maps for example model 7 (RAZO/winter) from full model (a) and bootstrap (b,c) with bootstrap uncertainty map (d). For complete set of prediction and uncertainty maps, see Appendix K.

e. abundance-full model mean

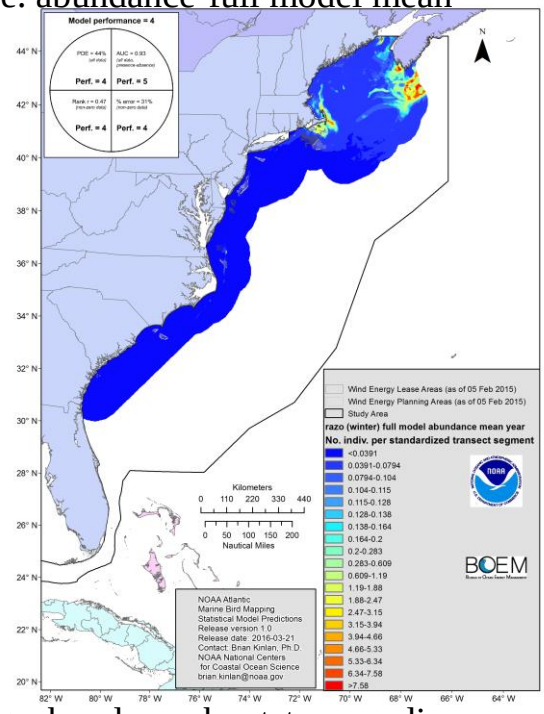

f. abundance-bootstrap mean

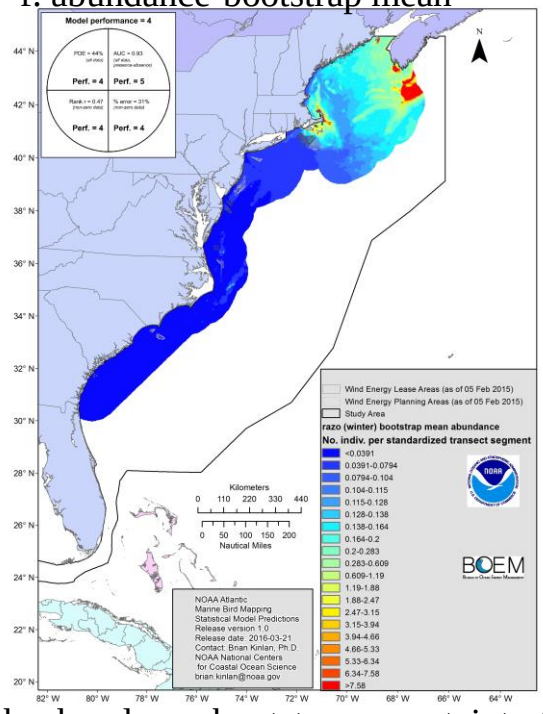

g. abundance-bootstrap median

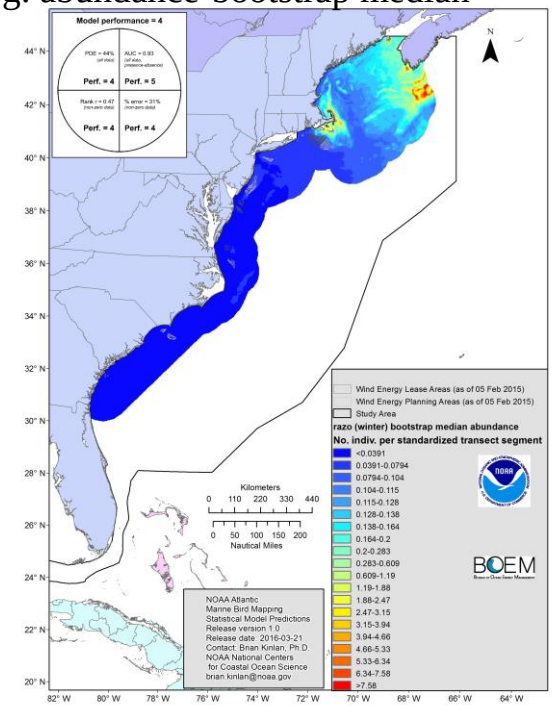

h. abundance-bootstrap uncertainty (CI90)

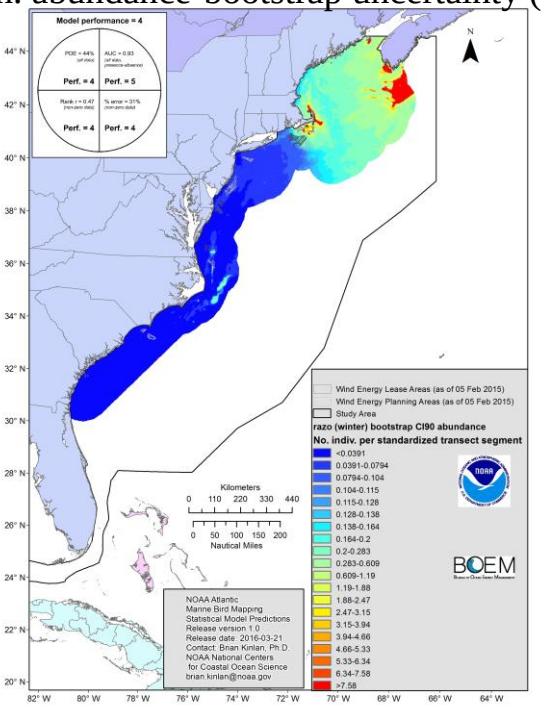

Figure 16.3 EFGH. Relative abundance prediction maps for example model 7 (RAZO/winter) from full model (e) and bootstrap (f,g) with bootstrap uncertainty map (h). For complete set of prediction and uncertainty maps, see Appendix K.

i. average count per 10 x 10 km grid cell

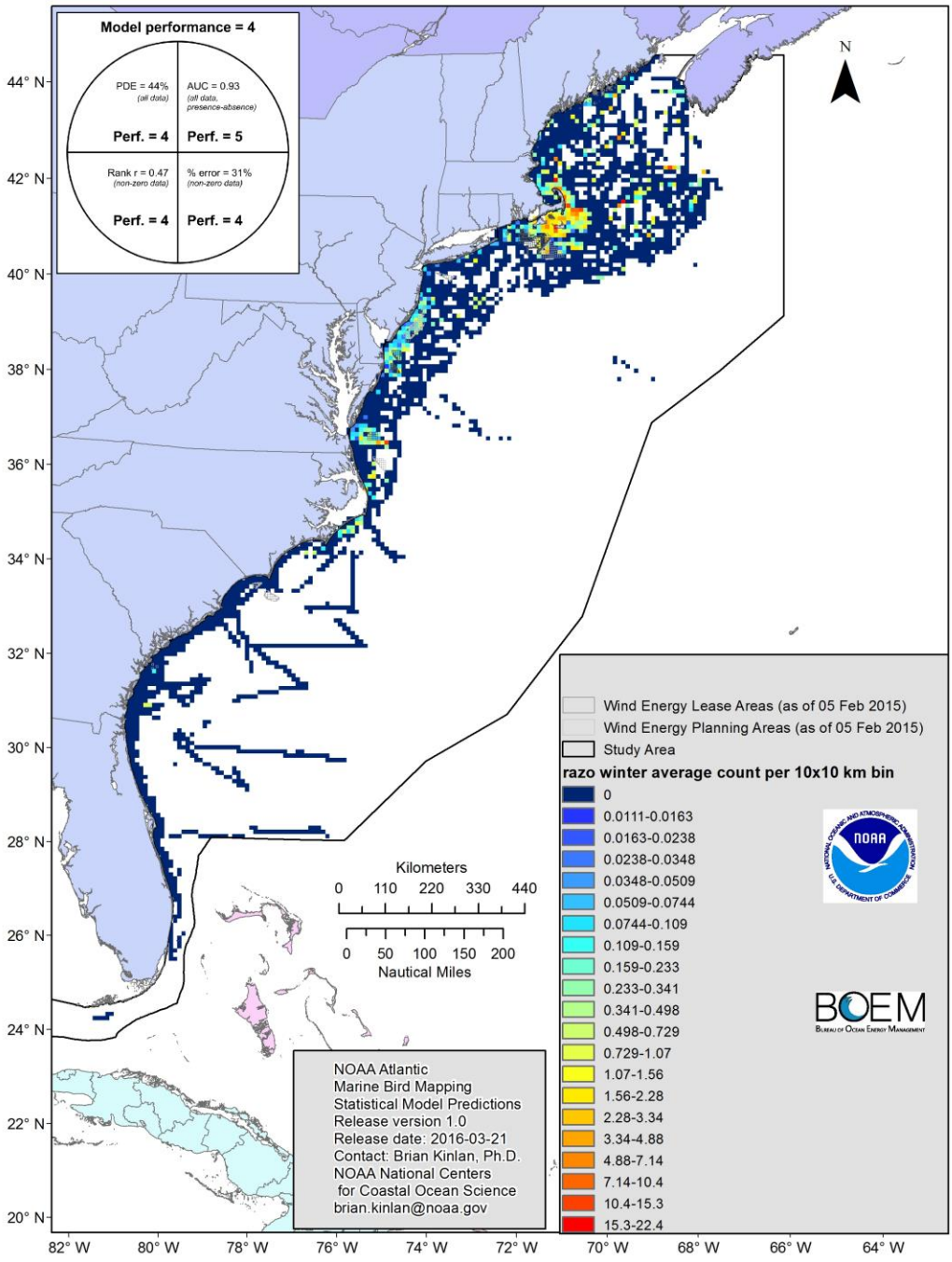

Figure 16.3 I. Average count per 10 x 10 km grid cell (RAZO/winter).

a. occupancy-full model mean

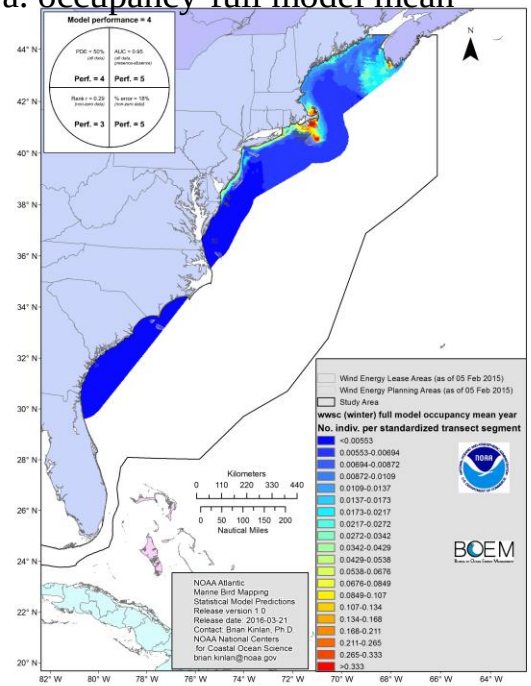

b. occupancy-bootstrap mean

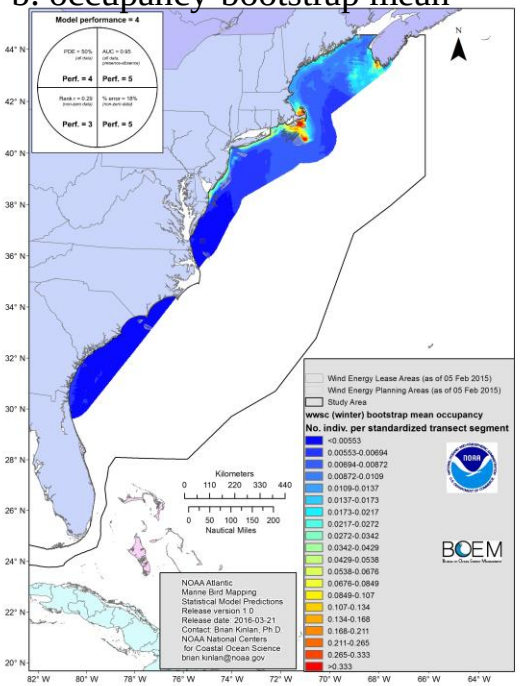

c. occupancy-bootstrap median

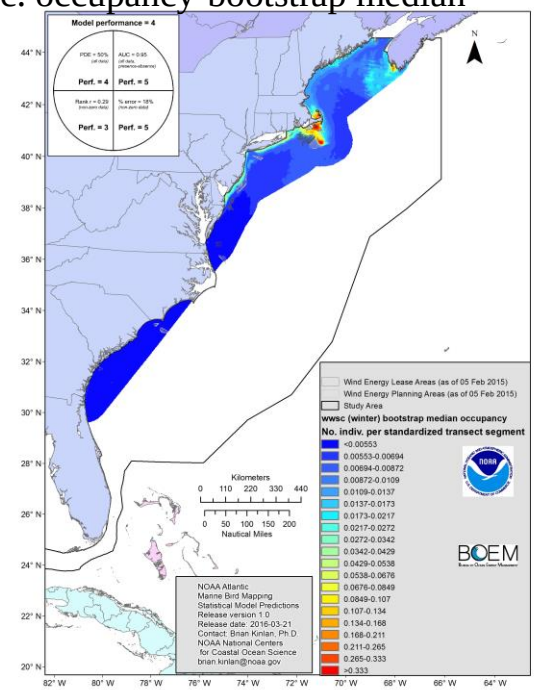

d. occupancy-bootstrap uncertainty (CI90)

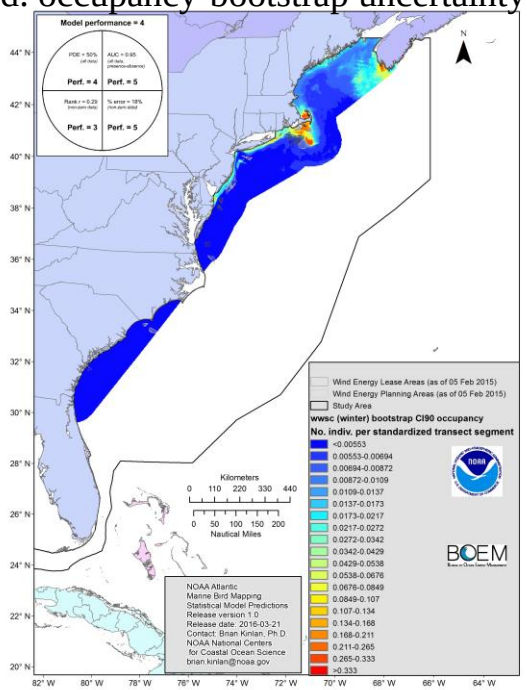

Figure 16.4 ABCD. Relative occupancy prediction maps for example model 8 (WWSC/winter) from full model (a) and bootstrap (b,c) with bootstrap uncertainty map (d). For complete set of prediction and uncertainty maps, see Appendix K.

e. abundance-full model mean

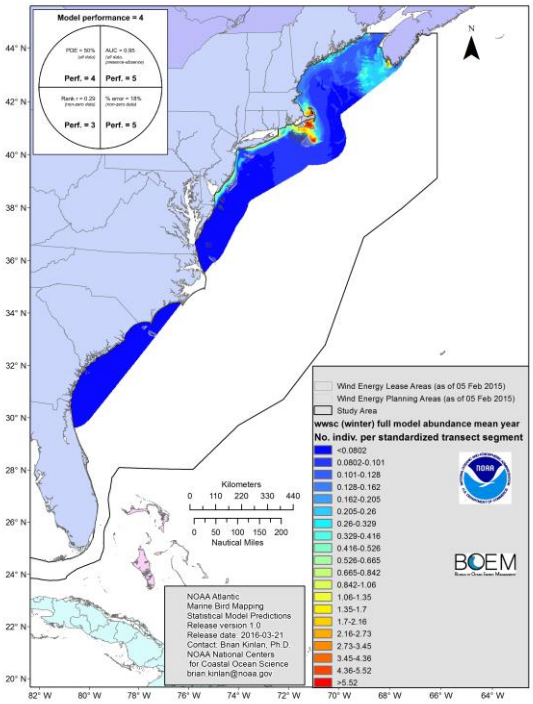

f. abundance-bootstrap mean

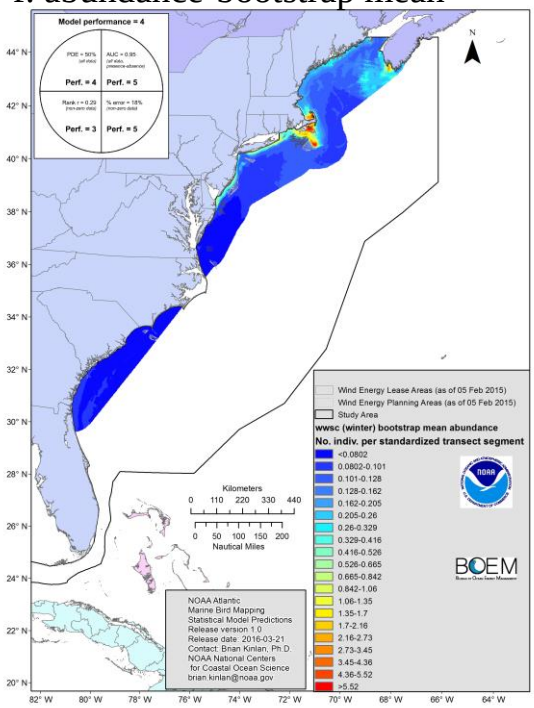

g. abundance-bootstrap median

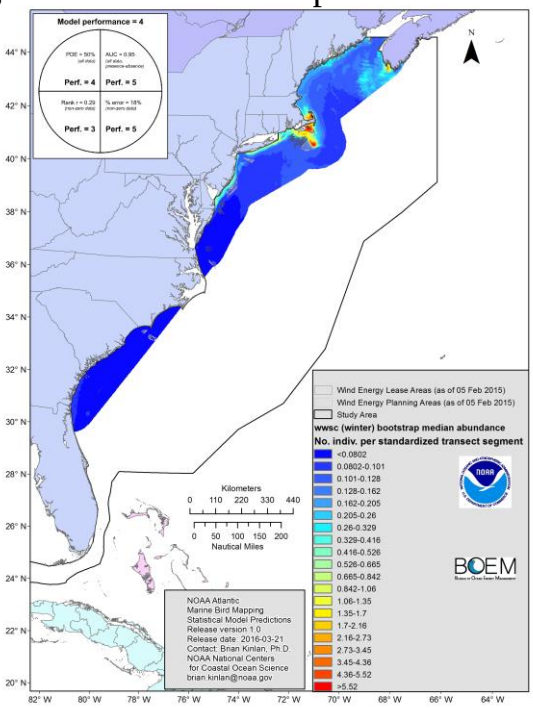

h. abundance-bootstrap uncertainty (CI90)

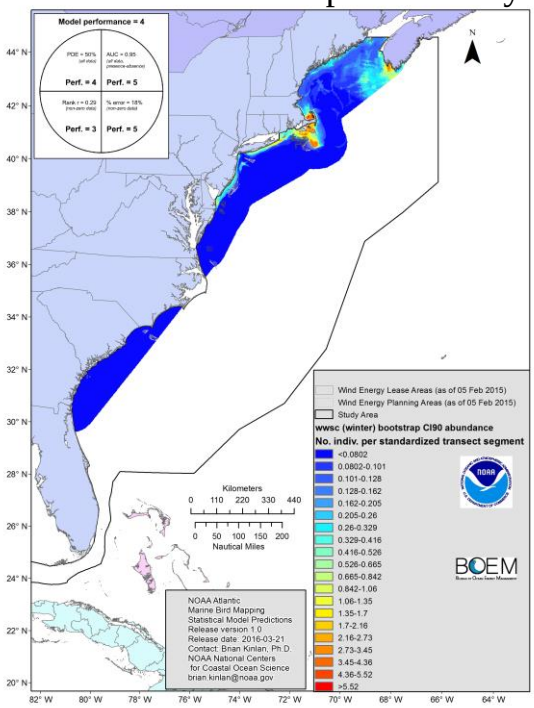

Figure 16.4 EFGH. Relative abundance prediction maps for example model 8 (WWSC/winter) from full model (e) and bootstrap (f,g) with bootstrap uncertainty map (h). For complete set of prediction and uncertainty maps, see Appendix K.

i. average count per 10 x 10 km grid cell

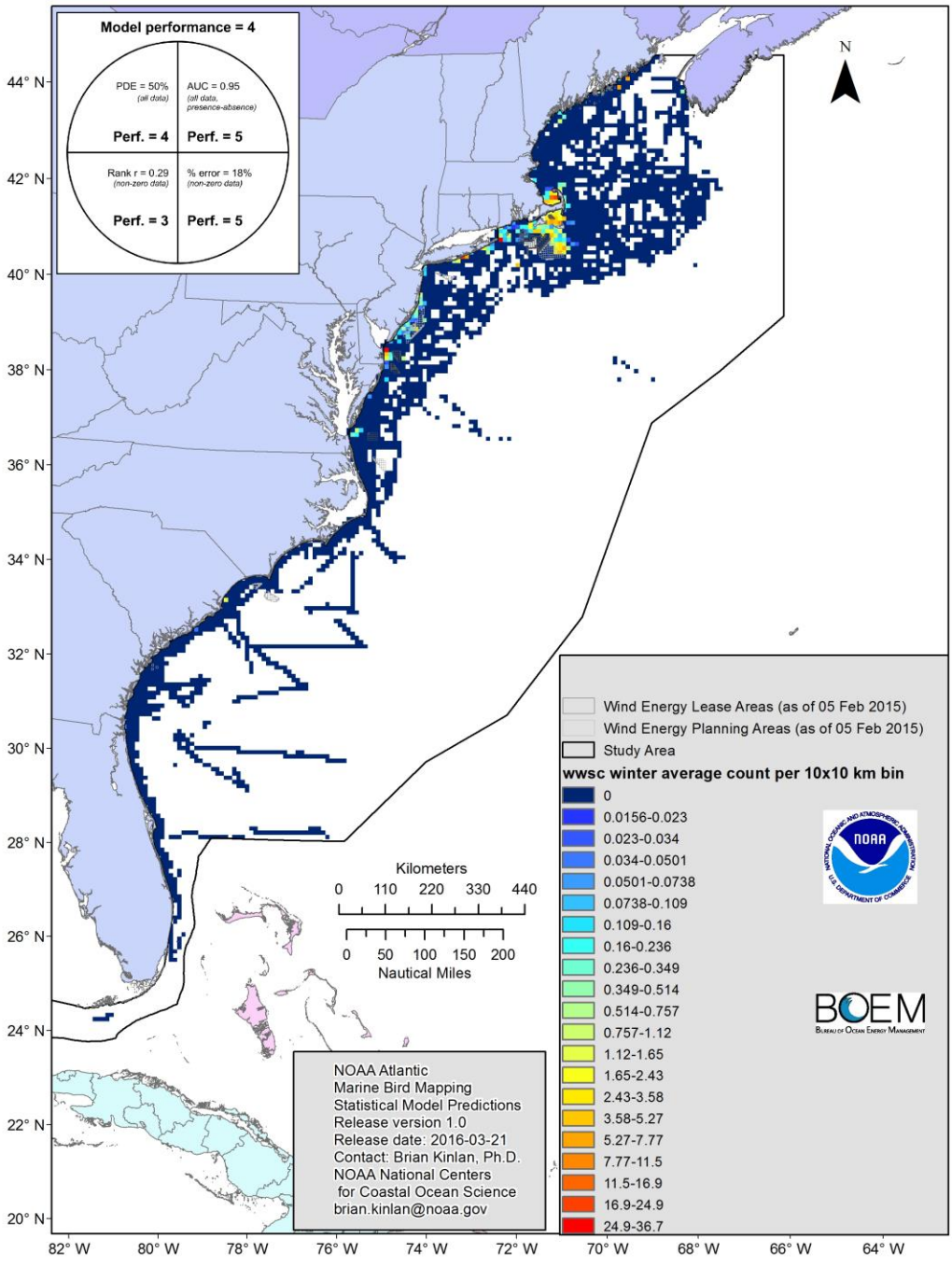

Figure 16.4 I. Average count per 10 x 10 km grid cell (WWSC/winter).

a. Annual average occupancy

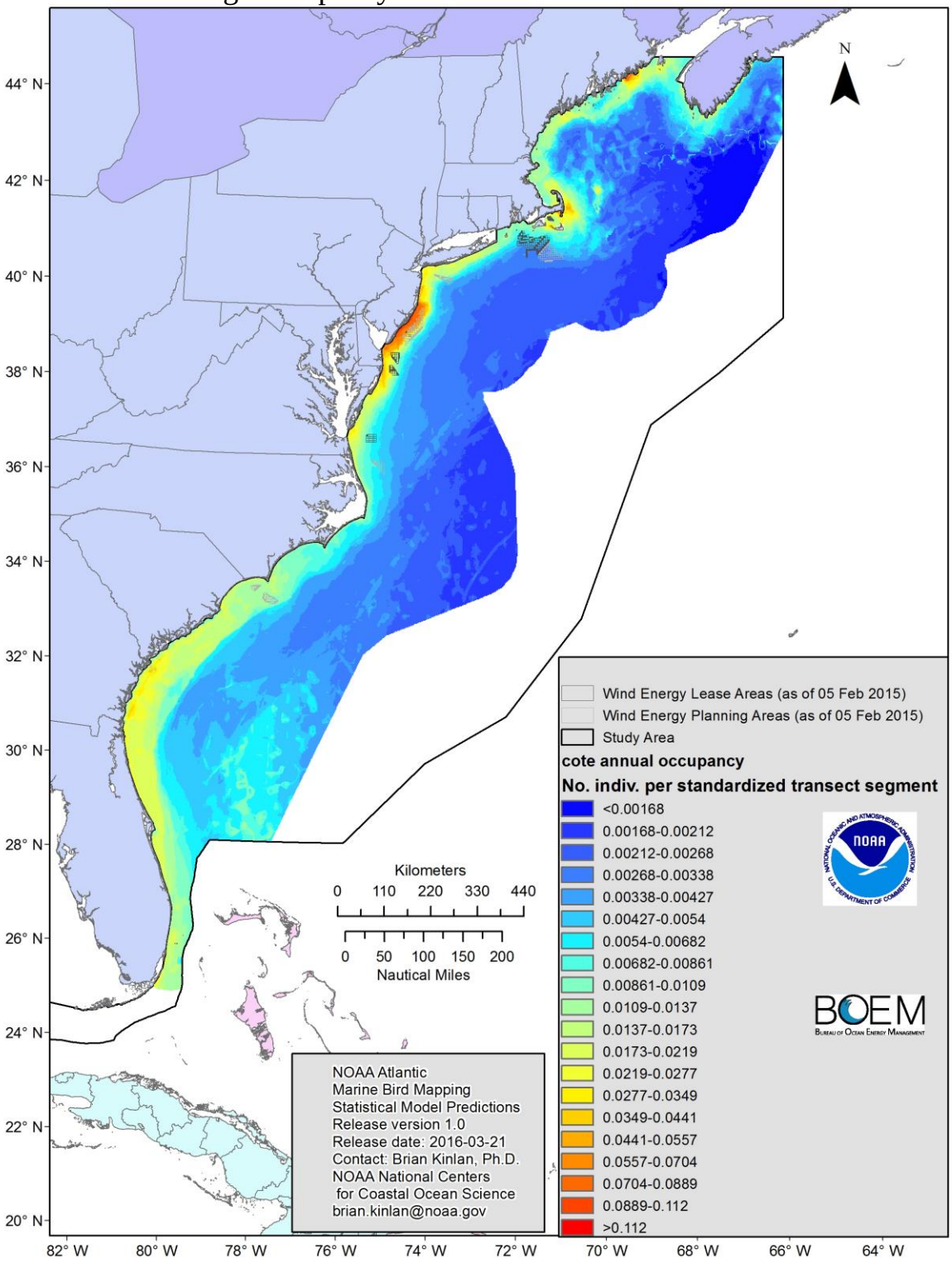

Figure 17.1A. Annual average relative occupancy prediction for example species 1 (COTE). For complete set of annual prediction maps, see Appendix L.

b. Annual average abundance

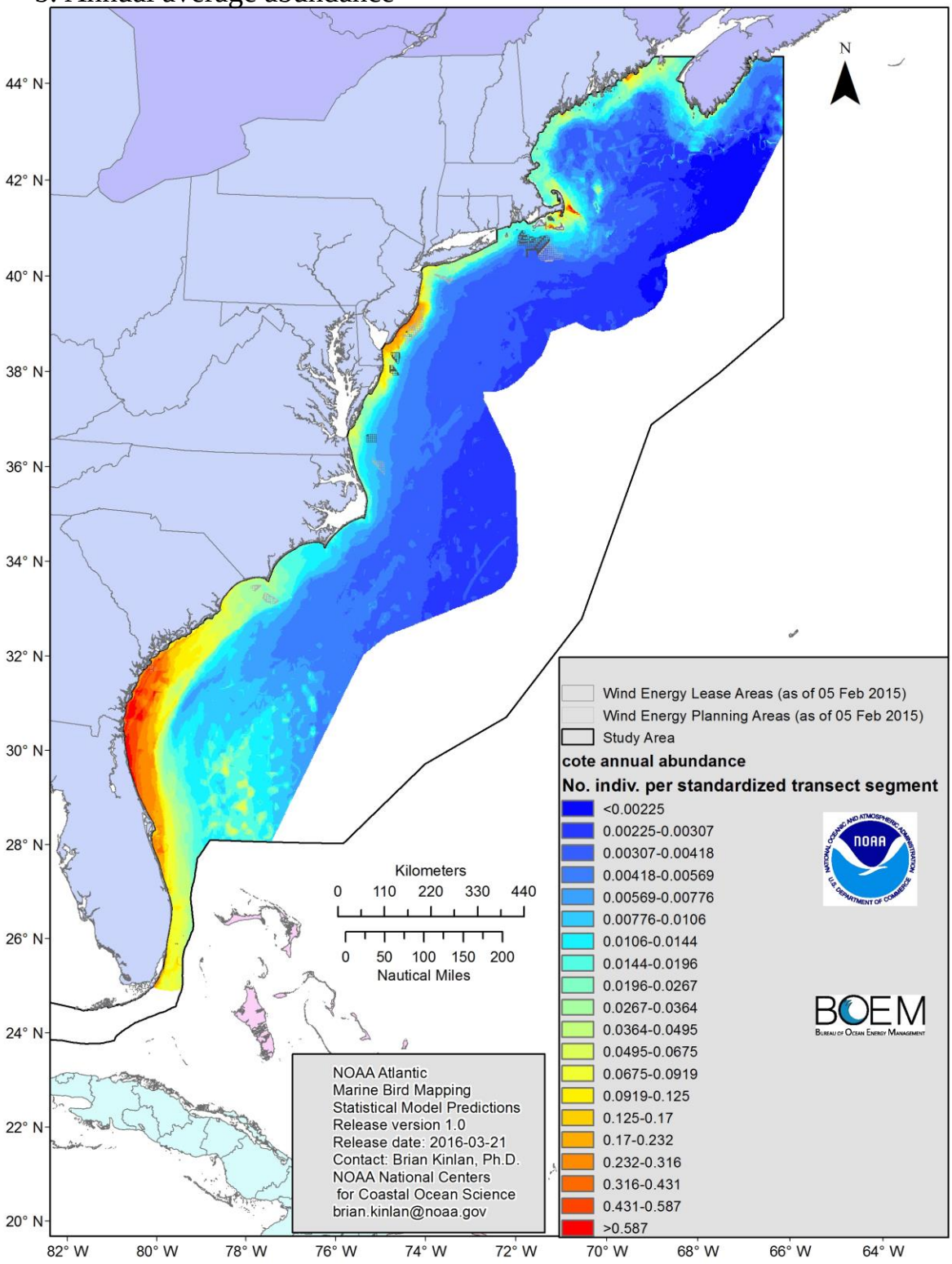

Figure 17.1B. Annual average relative abundance prediction for example species 1 (COTE). For complete set of annual prediction maps, see Appendix L.

a. Annual average occupancy

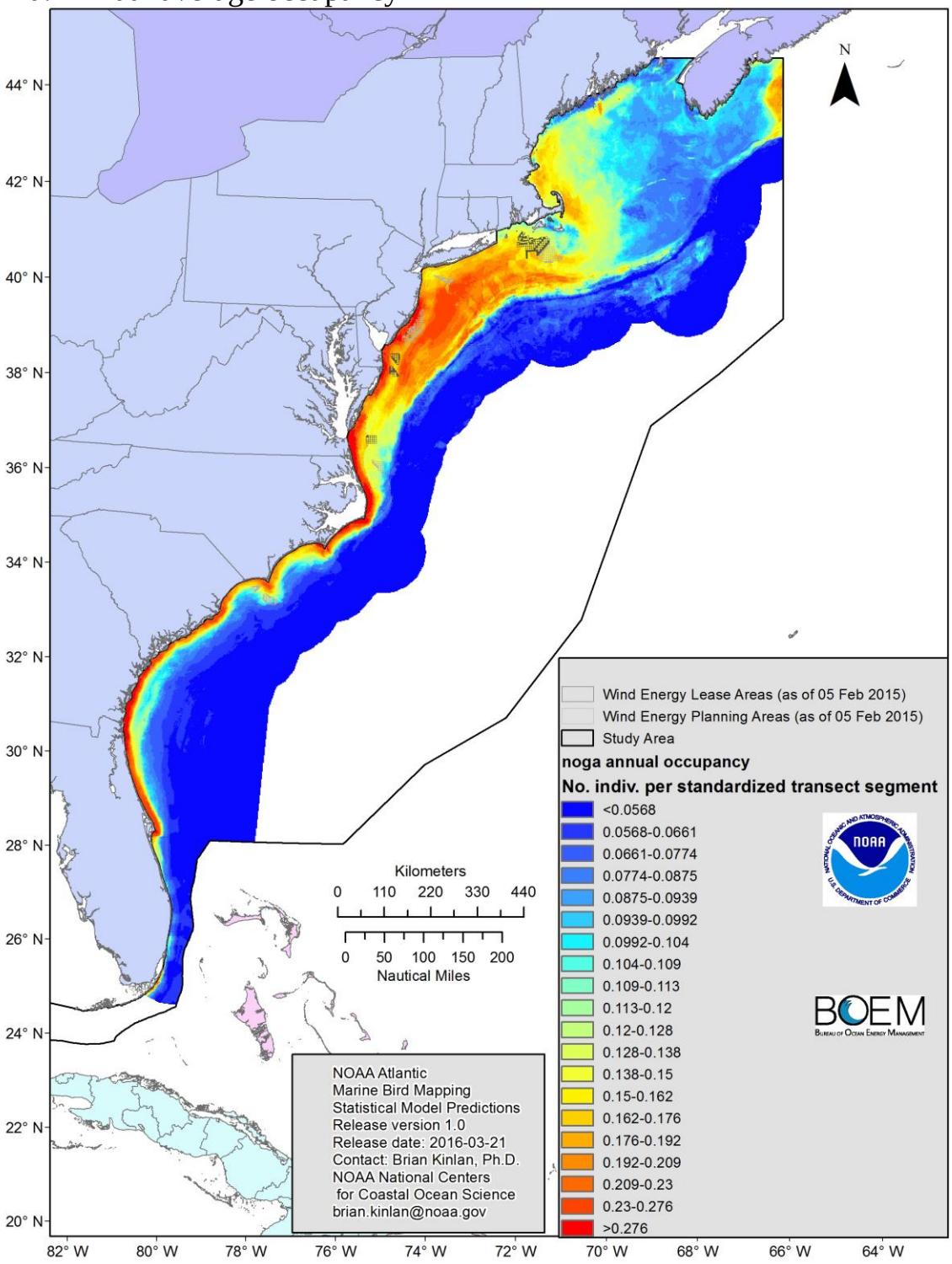

Figure 17.2A. Annual average relative occupancy prediction for example species 2 (NOGA). For complete set of annual prediction maps, see Appendix L.

b. Annual average abundance

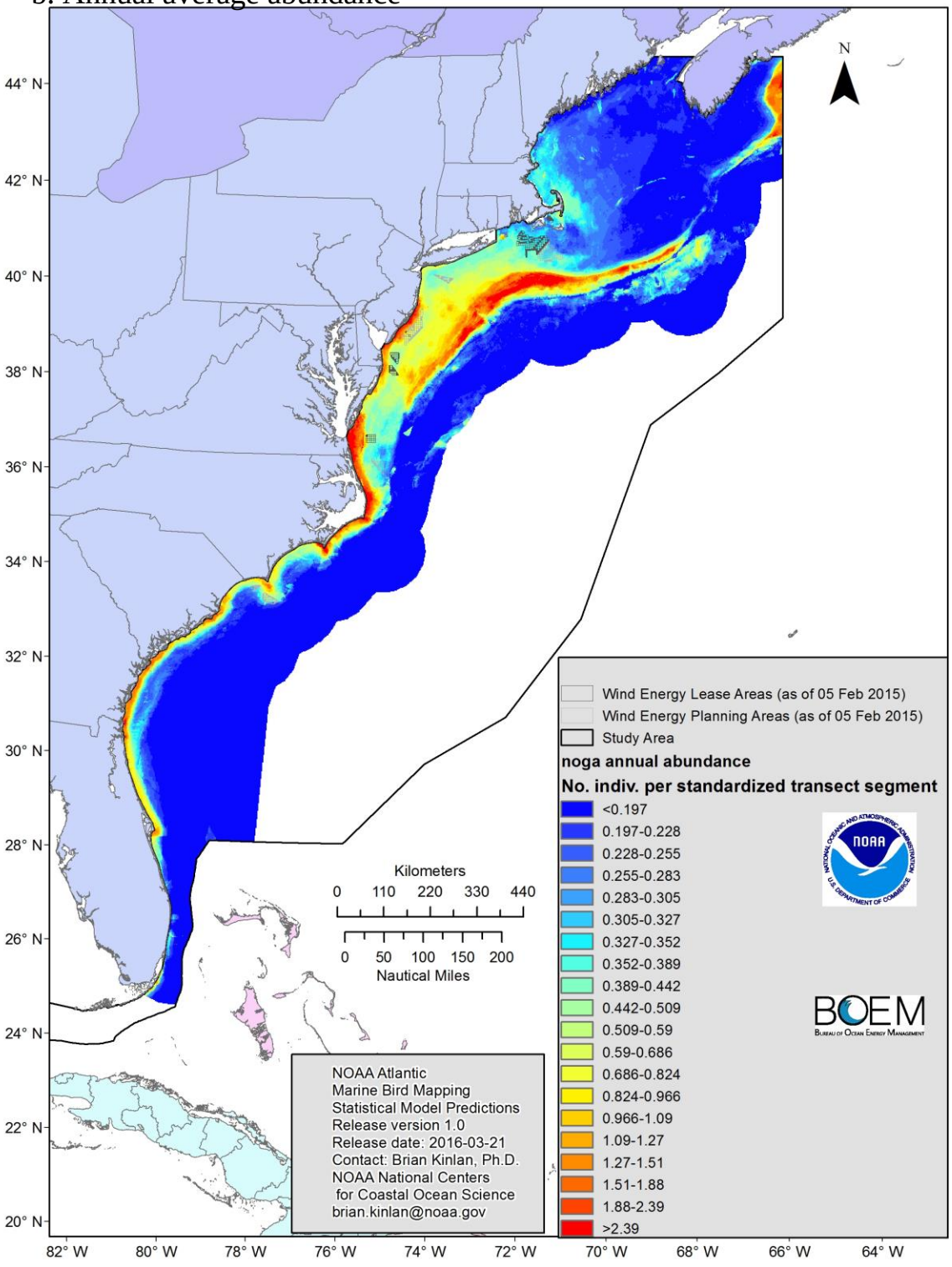

Figure 17.2B. Annual average relative abundance prediction for example species 2 (NOGA). For complete set of annual prediction maps, see Appendix L.

a. Annual average occupancy

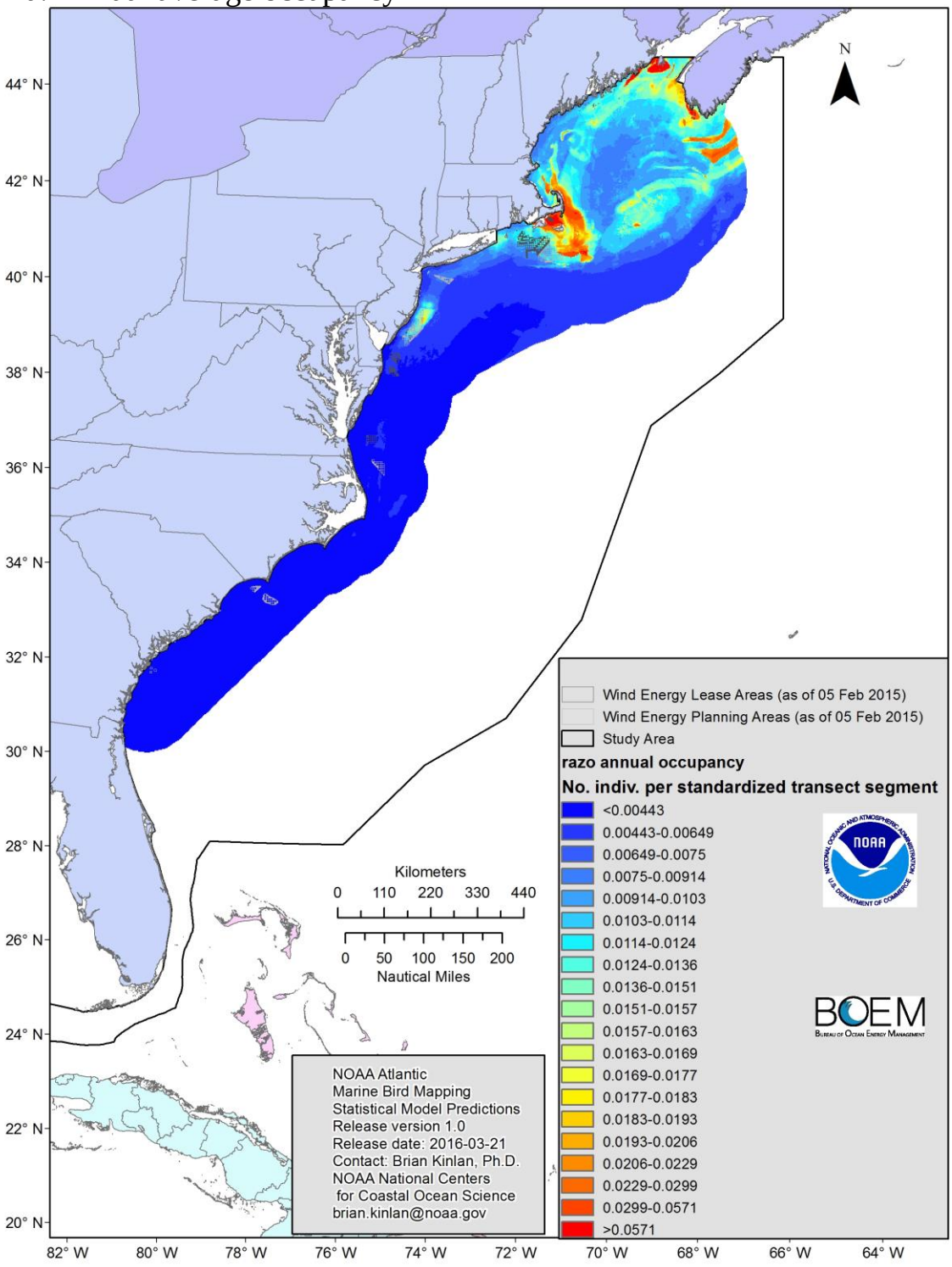

Figure 17.3A. Annual average relative occupancy prediction for example species 3 (RAZO). For complete set of annual prediction maps, see Appendix L.

b. Annual average abundance

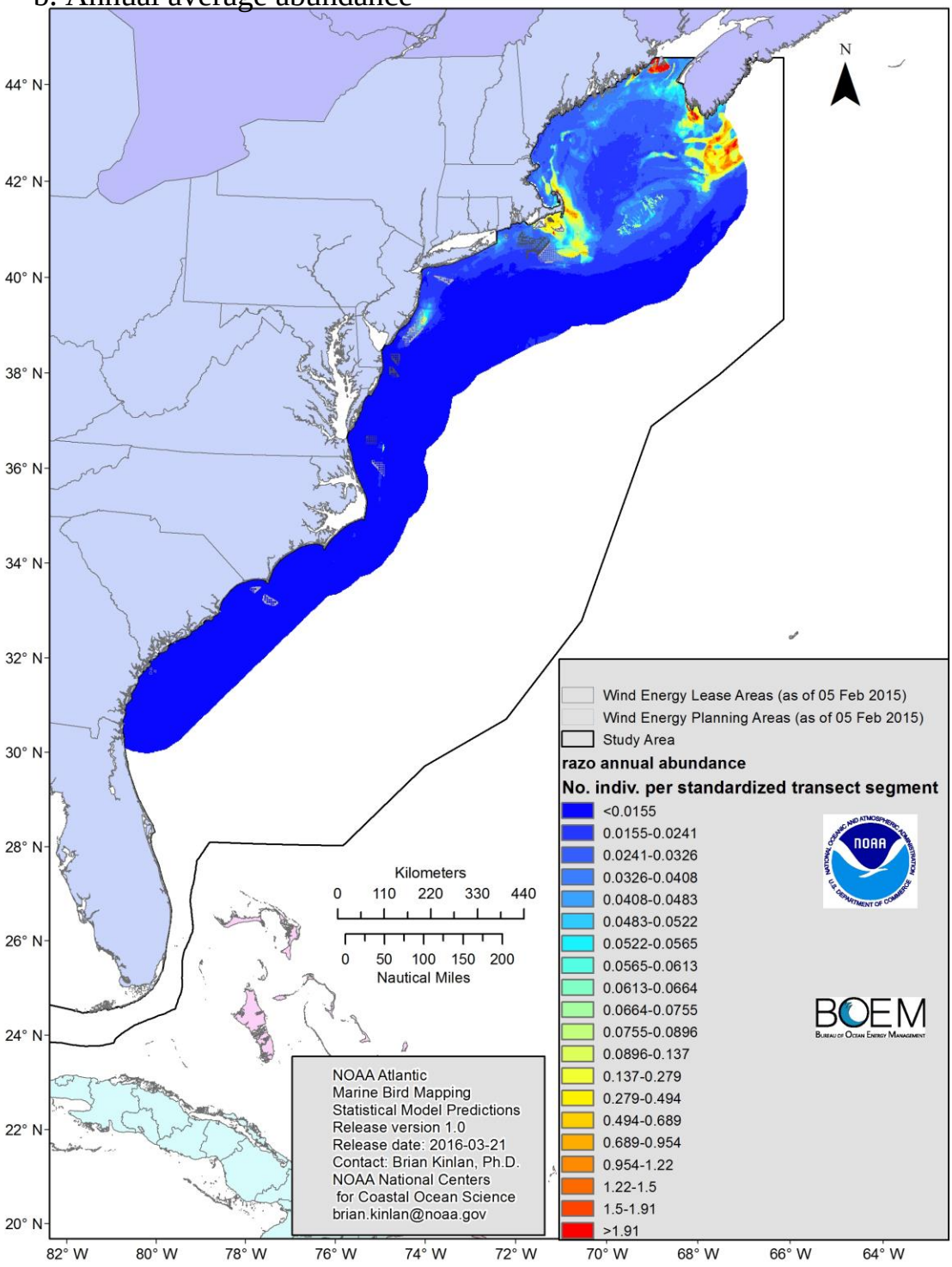

Figure 17.3B. Annual average relative abundance prediction for example species 3 (RAZO). For complete set of annual prediction maps, see Appendix L.

a. Annual average occupancy

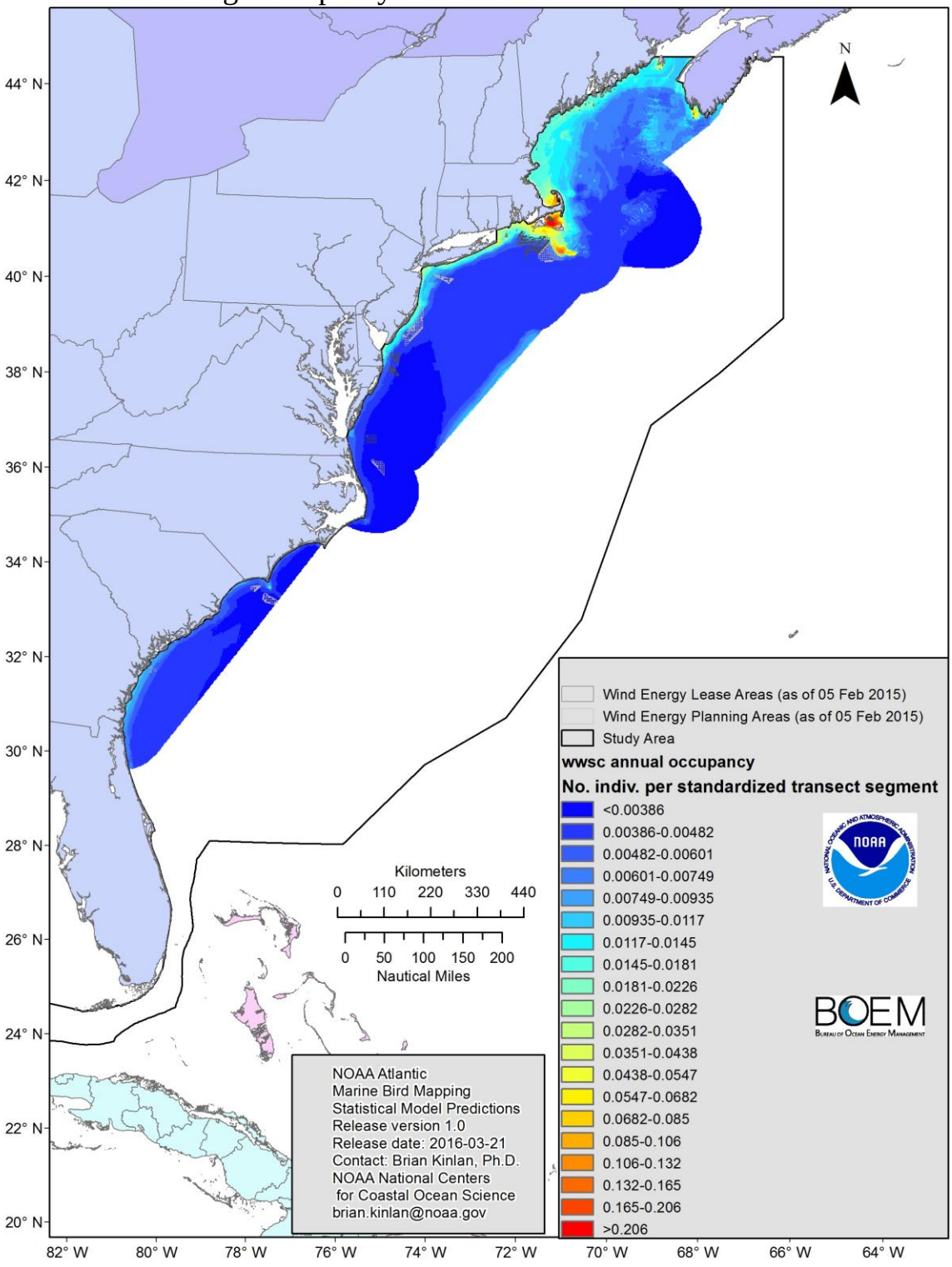

Figure 17.4A. Annual average relative occupancy prediction for example species 4 (WWSC). For complete set of annual prediction maps, see Appendix L.

b. Annual average abundance

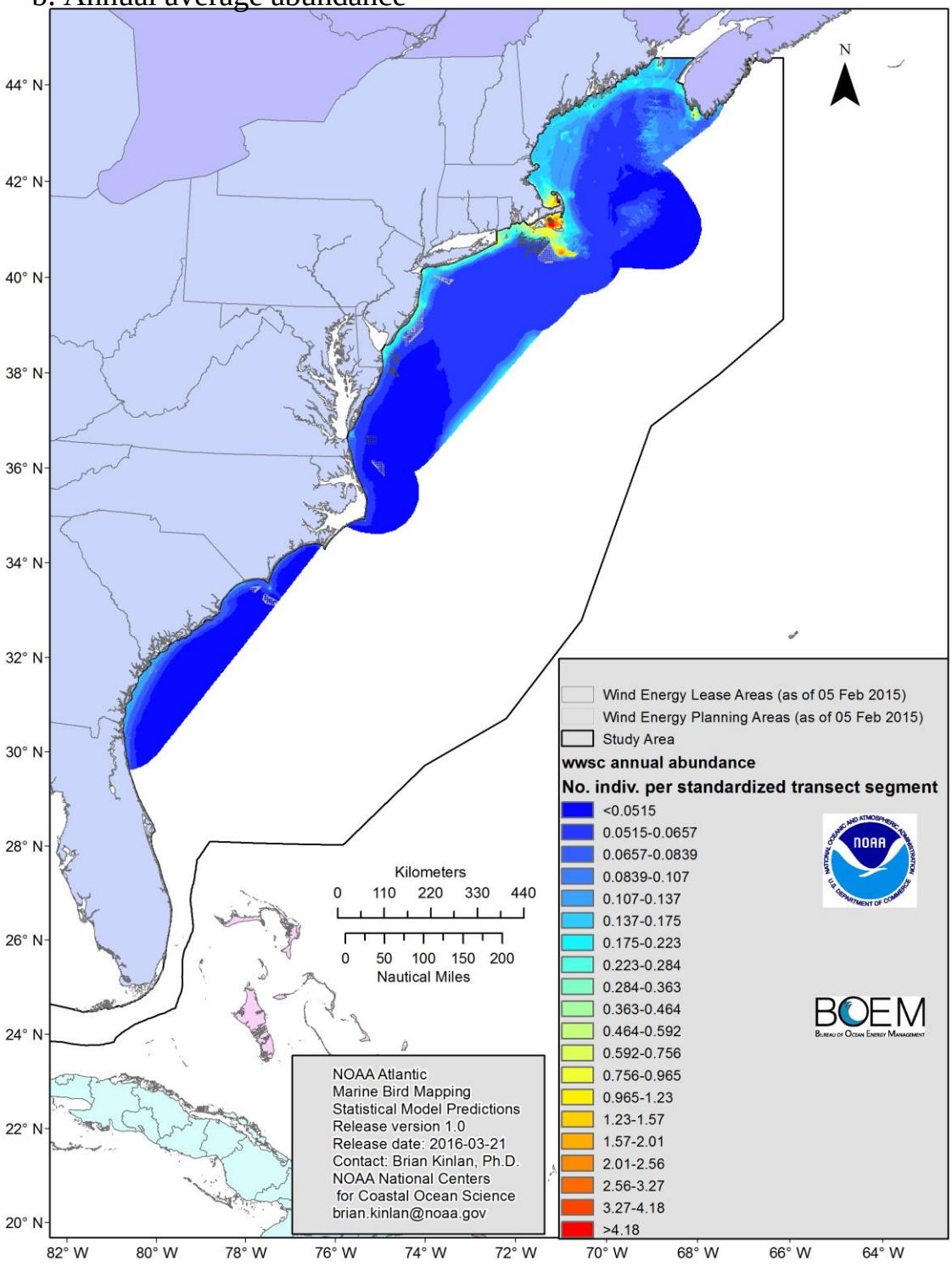

Figure 17.4B. Annual average relative abundance prediction for example species 4 (WWSC/winter). For complete set of annual prediction maps, see Appendix L.

a. Annual average occupancy - Nearshore Group

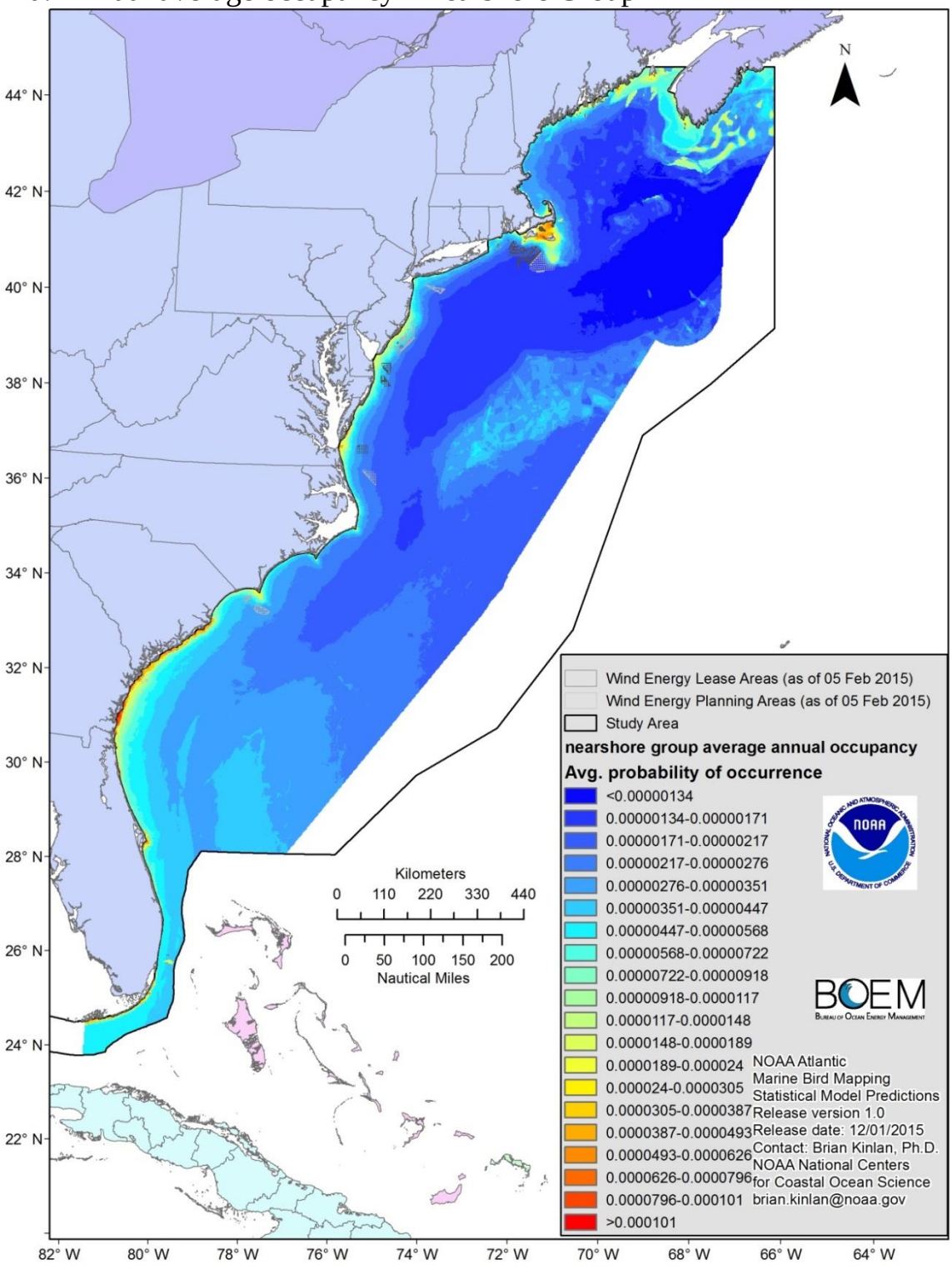

Figure 18A. Annual average relative occupancy prediction for group 1 (nearshore species). For complete set of group prediction maps, see Appendix M. For group definitions, see Table 12.

b. Annual average abundance – Nearshore Group

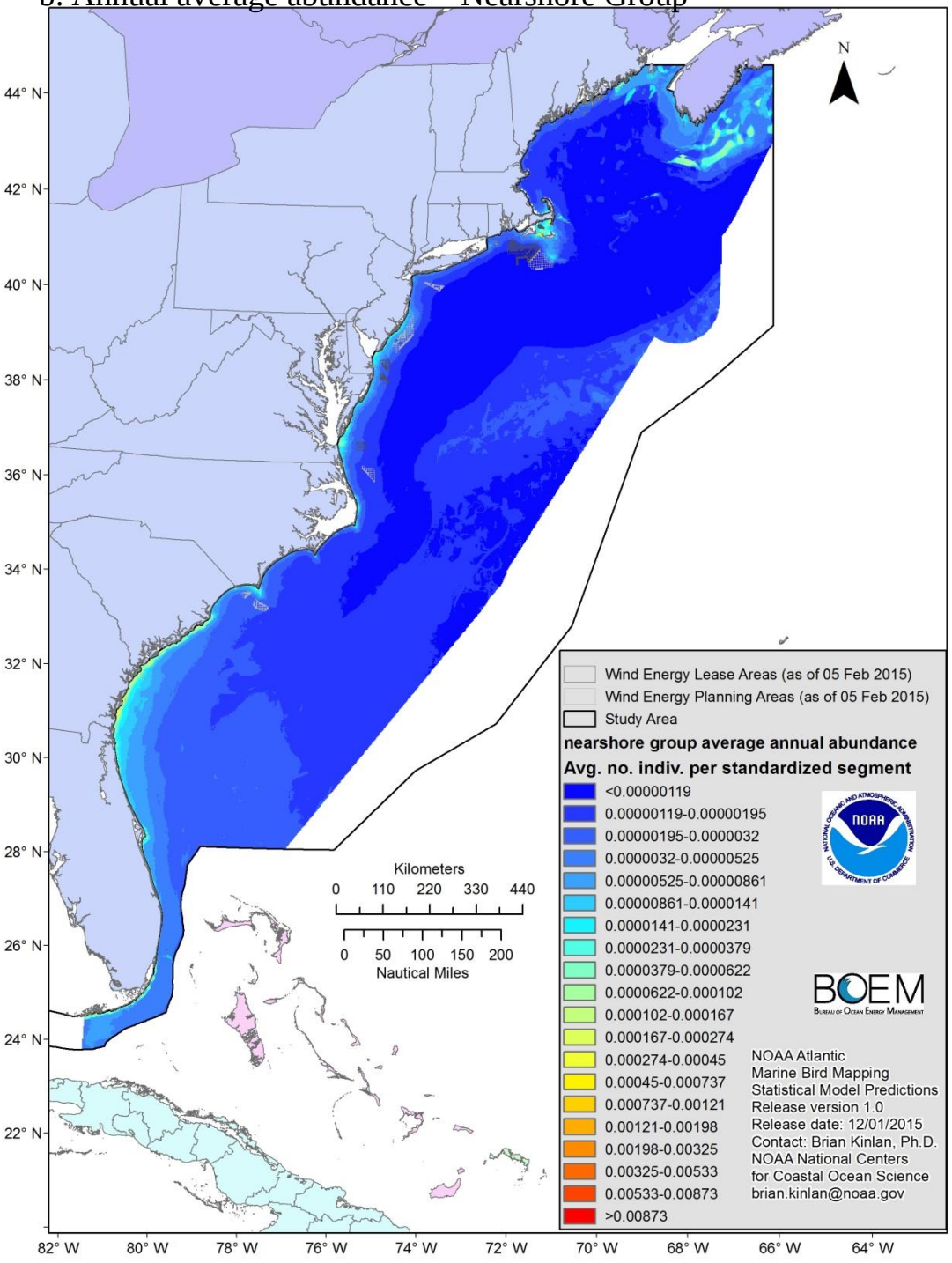

Figure 18B. Annual average relative abundance prediction for group 1 (nearshore species). For complete set of group prediction maps, see Appendix M. For group definitions, see Table 12.

a. Annual average occupancy - Pelagic Group

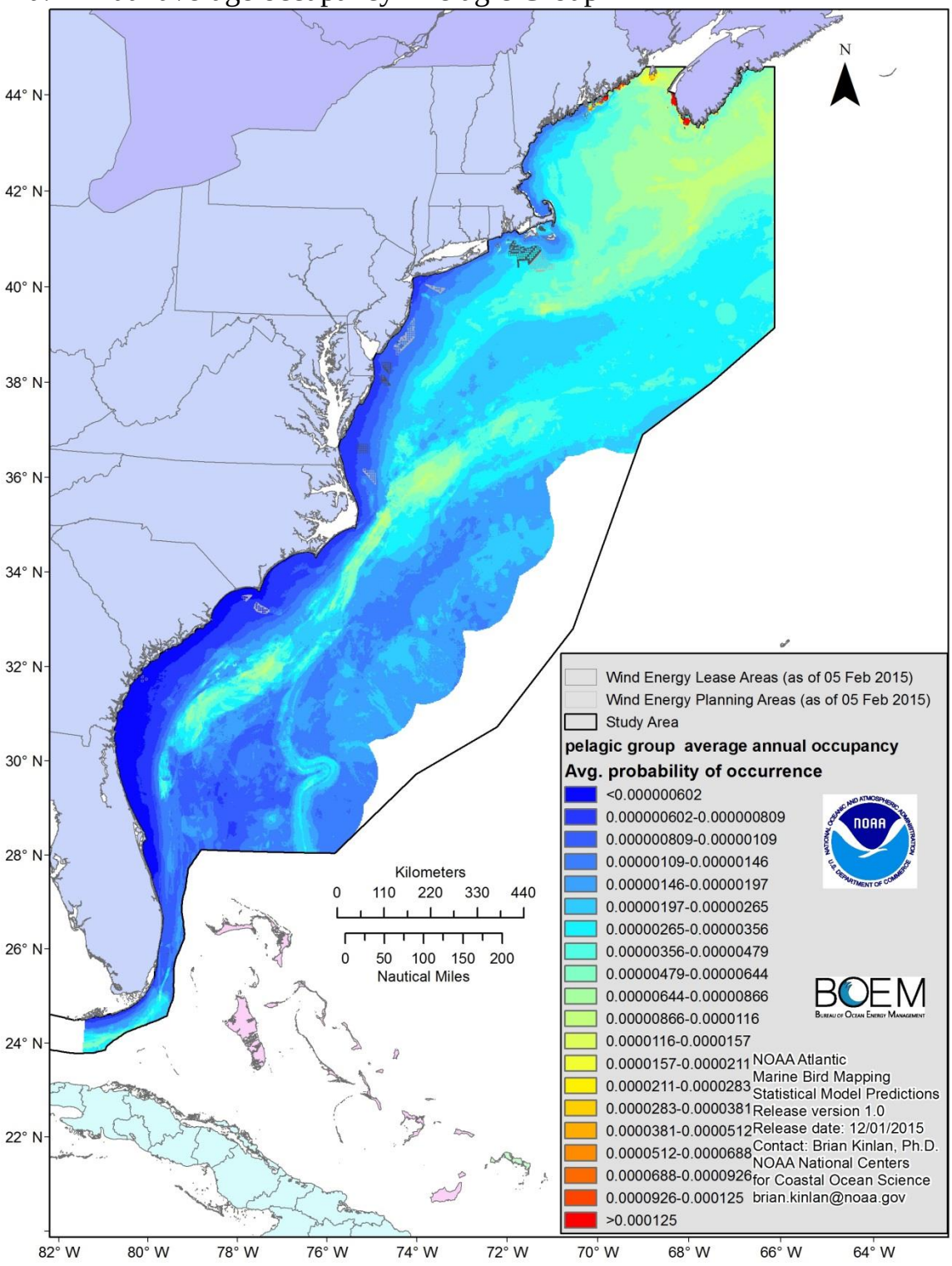

Figure 19A. Annual average relative occupancy prediction for group 2 (pelagic species). For complete set of group prediction maps, see Appendix M. For group definitions, see Table 12.

b. Annual average abundance – Pelagic Group

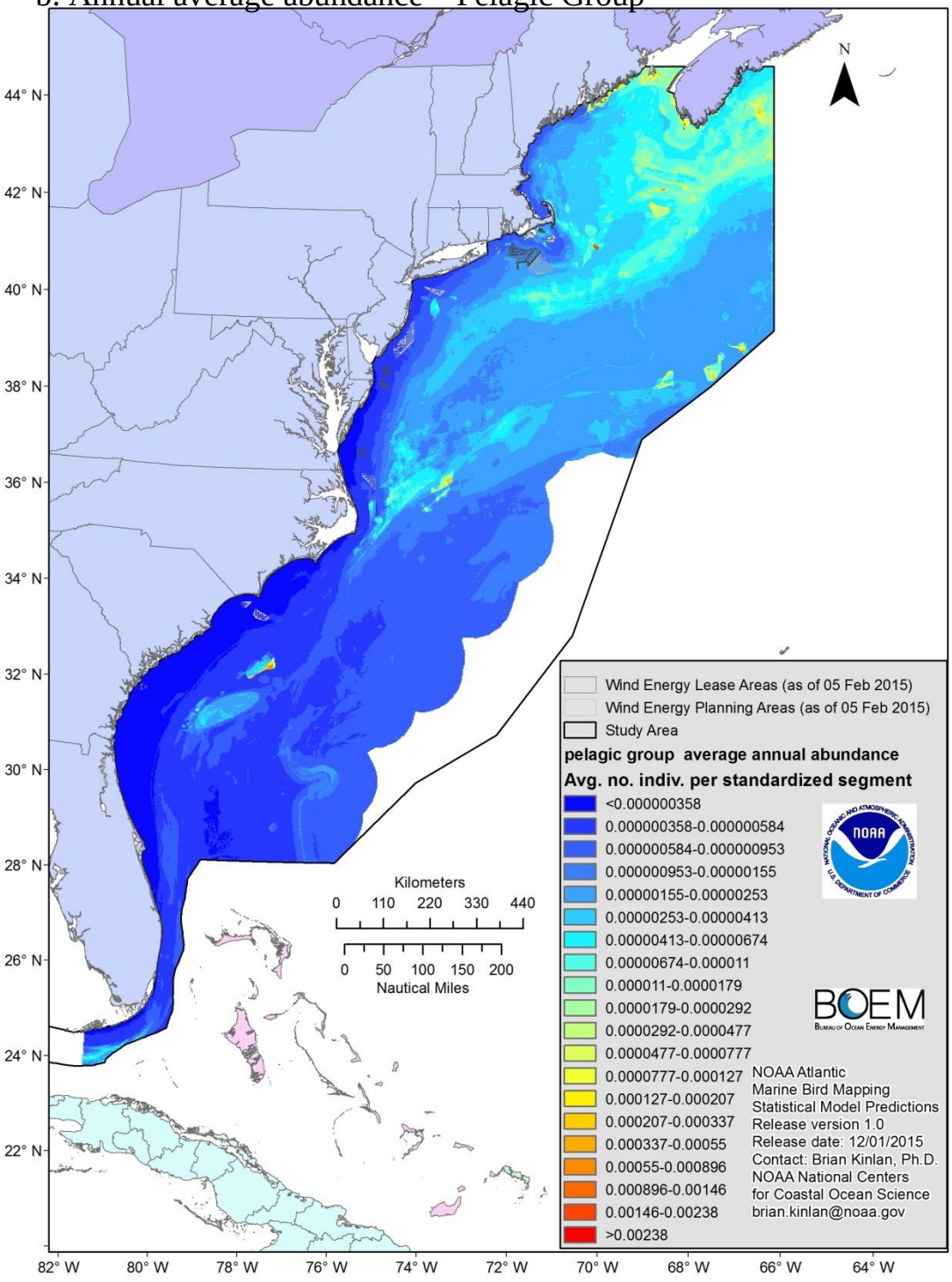

Figure 19B. Annual average relative abundance prediction for group 2 (pelagic species). For complete set of group prediction maps, see Appendix M. For group definitions, see Table 12.

a. Annual average occupancy – Gulls and Gannets Group

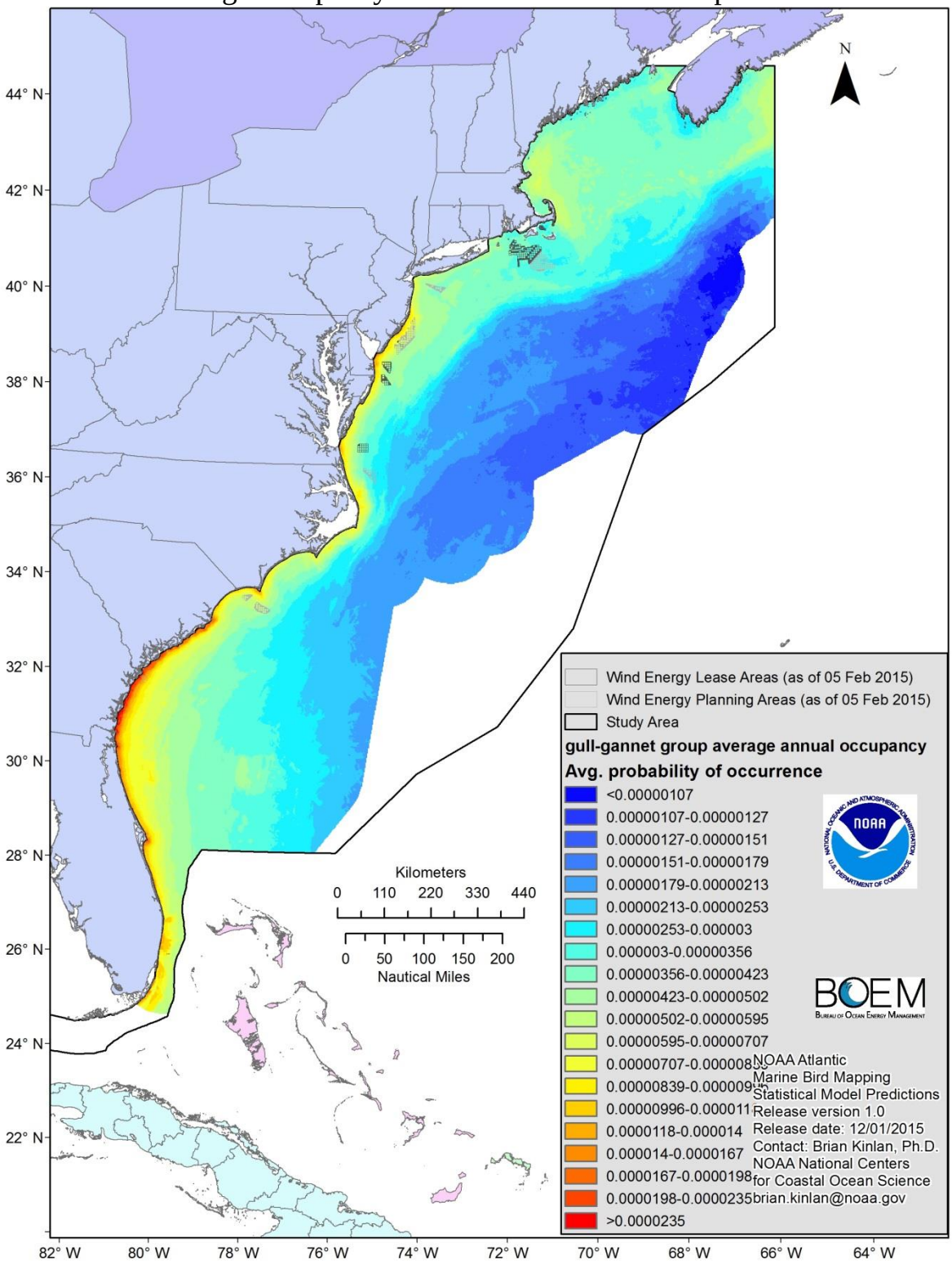

Figure 20A. Annual average relative occupancy prediction for group 3 (gulls and gannets). For complete set of group prediction maps, see Appendix M. For group definitions, see Table 12.

b. Annual average abundance – Gulls and Gannets Group

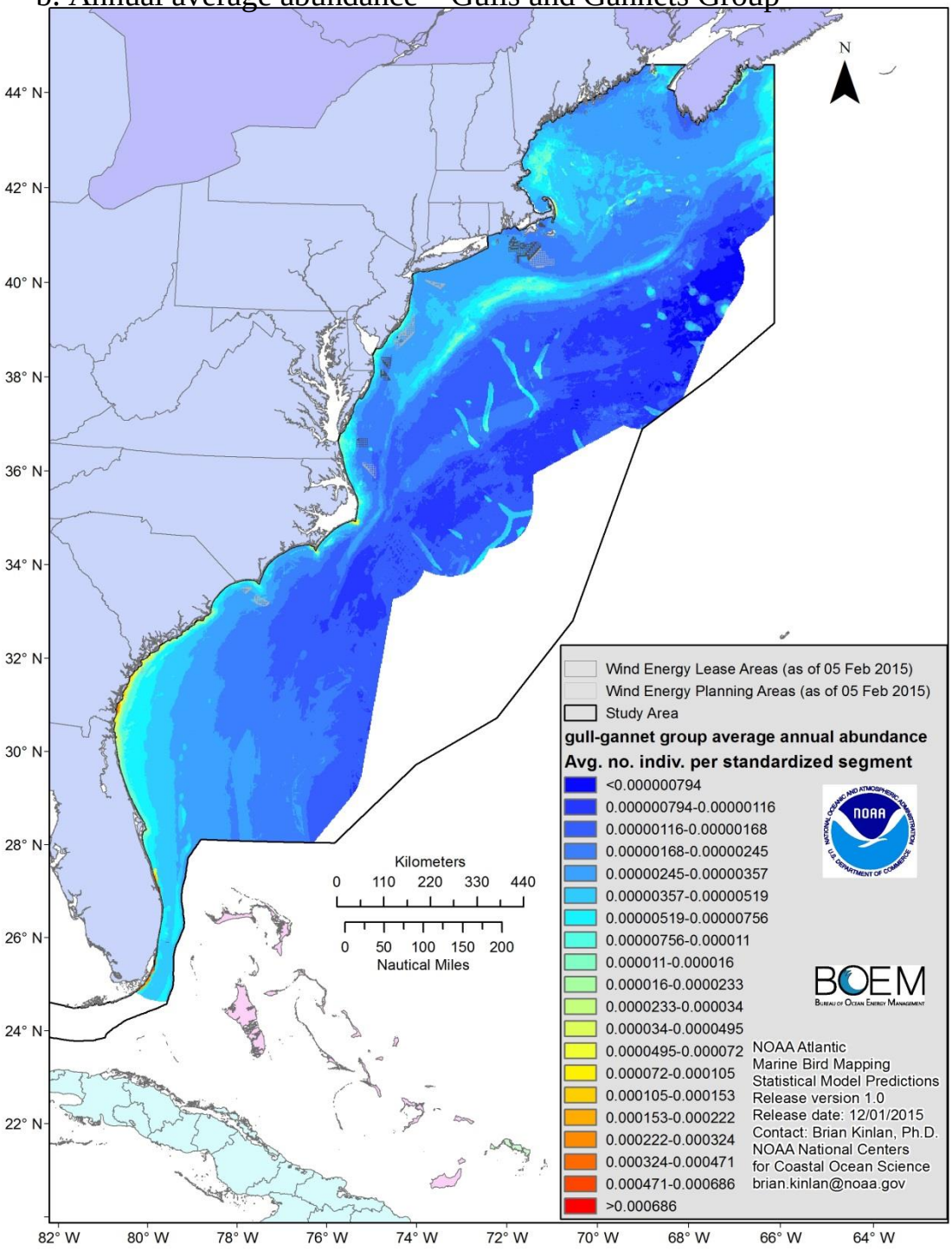

Figure 20B. Annual average relative abundance prediction for group 3 (gulls and gannets). For complete set of group prediction maps, see Appendix M. For group definitions, see Table 12.

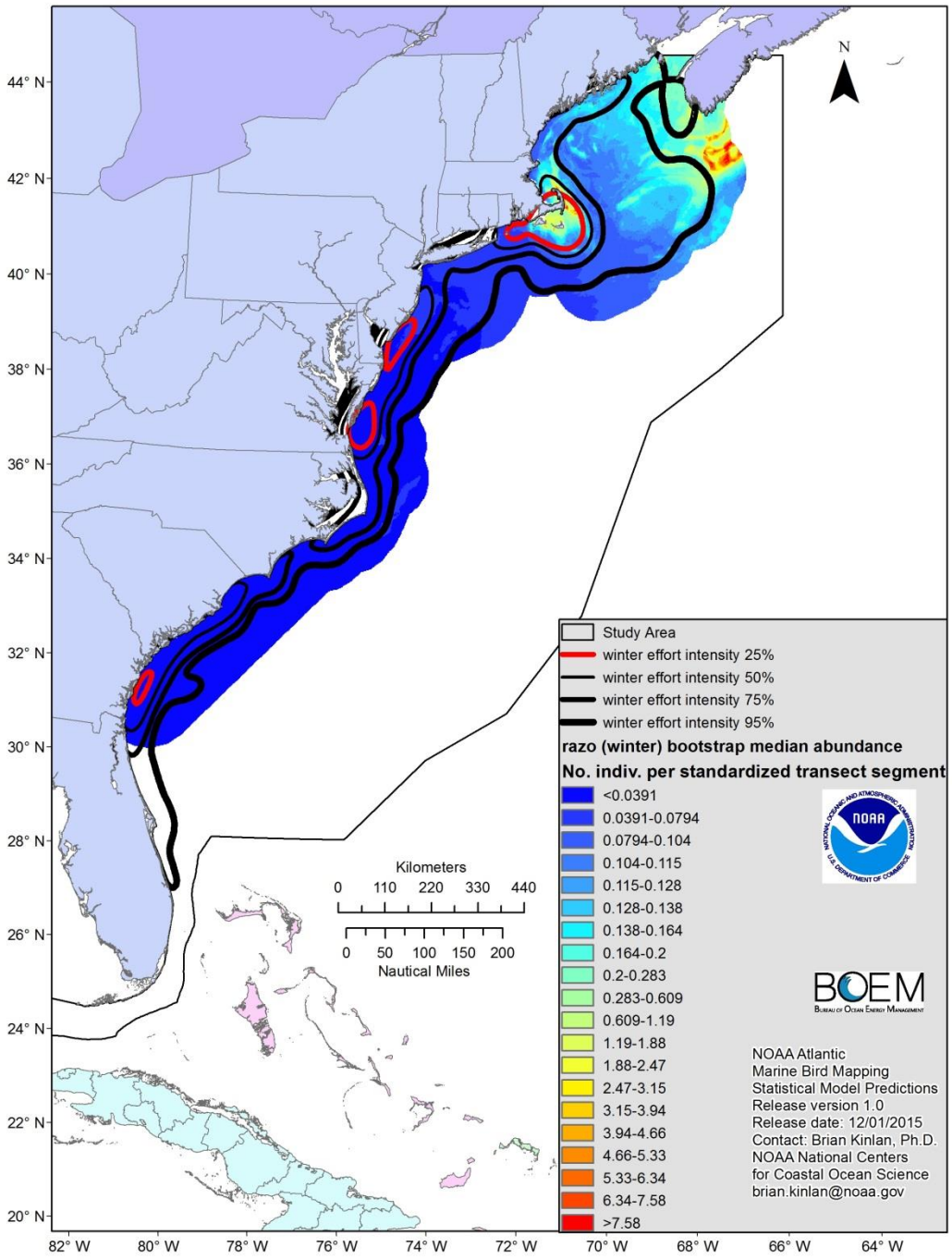

Figure 21. Intensity of winter survey effort and predicted bootstrap median relative abundance of RAZO in winter.

The Department of the Interior Mission

As the Nation's principal conservation agency, the Department of the Interior has responsibility for most of our nationally owned public lands and natural resources. This includes fostering sound use of our land and water resources; protecting our fish, wildlife, and biological diversity; preserving the environmental and cultural values of our national parks and historical places; and providing for the enjoyment of life through outdoor recreation. The Department assesses our energy and mineral resources and works to ensure that their development is in the best interests of all our people by encouraging stewardship and citizen participation in their care. The Department also has a major responsibility for American Indian reservation communities and for people who live in island territories under US administration.

BOEM
Bureau of Ocean Energy Management

The Bureau of Ocean Energy Management

As a bureau of the Department of the Interior, the Bureau of Ocean Energy (BOEM) primary responsibilities are to manage the mineral resources located on the Nation's Outer Continental Shelf (OCS) in an environmentally sound and safe manner.

The BOEM Environmental Studies Program

The mission of the Environmental Studies Program (ESP) is to provide the information needed to predict, assess, and manage impacts from offshore energy and marine mineral exploration, development, and production activities on human, marine, and coastal environments.